STUDIES ON EPISOMAL MAINTENANCE AND VIRAL MicroRNAS OF KAPOSI'S SARCOMA-ASSOCIATED HERPESVIRUS

By

REBECCA LYNN SKALSKY

A DISSERTATION PRESENTED TO THE GRADUATE SCHOOL
OF THE UNIVERSITY OF FLORIDA IN PARTIAL FULFILLMENT
OF THE REQUIREMENTS FOR THE DEGREE OF
DOCTOR OF PHILOSOPHY

UNIVERSITY OF FLORIDA
2007

To my family, in particular, my parents, my sister, my husband Nate, and our two sources of constant amusement, Keakers and Bali.

ACKNOWLEDGEMENTS

I would like to acknowledge all the people who contributed to this work and helped guide me in the laboratory.

First, thanks to all the current and former members of the Renne lab: Dr. Jianhong Hu, Dr. Soo-Jin Han, Dr. Mark Samols, Karlie Plaisance, Isaac Boss, Kevin Neal, Dr. Feng-Qi An, Ann Maldonado, and Tyler Beals for all of their help over the years in making the lab a great working environment. I would particularly like to thank Dr. Jianhong Hu and Dr. Mark Samols for collaborating with me on a number of projects, endless discussions, and for help editing parts of this dissertation.

Thanks to the members of my committee: Dr. David Bloom, Dr.Philip Laipis, and Dr. Sankar Swaminathan for their helpful suggestions. Thanks also to the Training Grant in Cancer Biology for supporting me while at the University of Florida and the Training Grant in Cell Biology for supporting me while at Case Western Reserve University.

I want to say a special thank you to my husband, Nathan Skalsky, for his constant support of me in the pursuit of my studies and understanding when sometimes they have to be achieved at distances.

Finally, thank you to my advisor, Dr. Rolf Renne, for his mentoring, patience, encouragement, always keeping an open office door, and helping turn me into a critical-thinking scientist.

TABLE OF CONTENTS

page

LIST OF TABLES

LIST OF FIGURES

LIST OF ABBREVIATIONS

Ago	argonaute protein
AIDS	acquired immune deficiency syndrome
ALV	avian leukosis virus
APC	anaphase promoting complex
ATP	adenosine tri-phosphate
BAC	bacterial artificial chromosomes
BACH-1	Btb and Cnc homolog 1
BCBL	body cavity based lymphoma
BCLAF1	Bcl-2 associated transcription factor 1
BCL2L11	Bcl-2-like 11
BCL6B	B-cell CLL/lymphoma 6, member B
BIC	B cell integration cluster
Bp	base pair
BPV-1	bovine papillomavirus type 1
CBS	chromosome binding site
Cdk	cyclin dependent kinase
cDNA	cloned DNA
CV	cross validation
DNA	deoxyribonucleic acid
DS	dyad symmetry
dsRNA	double-stranded RNA
EBV	Epstein-Barr virus

EBNA-1	Epstein-Barr virus nuclear antigen
FISH	fluorescent *in situ* hybridization
FITC	fluorescein
FLIP	FLICE interacting protein
FR	family of repeats
GFP	green fluorescence protein
HAART	highly active anti-retroviral treatment
HCMV	human cytomegalovirus
HHV-8	human herpesvirus 8
HIV	human immunodeficiency virus
HVS	herpesvirus Saimiri
HSV	herpes simplex virus
IRES	internal ribosomal entry site
ITM2A	integral membrane protein 2A
KLAR	KSHV latency associated region
KS	Kaposi's sarcoma
KSHV	Kaposi's sarcoma-associated herpesvirus
LAMP	latency-associated membrane protein
LANA	latency-associated nuclear antigen
LAT	latency-associated transcript
LBS	LANA binding site
LDOC1	leucine zipper, downregulated in cancer 1
MAF	musculoaponeurotic fibrosarcoma oncogene homolog

MALAT1	metastasis associated lung adenocarcinoma transcript 1
MCD	multicentric Castleman's disease
MCM	mini-chromosome maintenance protein
MDV	Mareck’s disease virus
MeCP2	methyl CpG binding protein 2
MHV68	murine herpesvirus 68
MIFC	multispectral imaging flow cytometry
miRNA	microRNA
mRNA	messenger RNA
NaB	sodium butyrate
nt	nucleotide
ORC	origin recognition complex
ORF	open reading frame
PCR	polymerase chain reaction
PEL	primary effusion lymphoma
PRG1	plasticity related gene 1
Pre-IC	pre-initiation complex
Pre-RC	pre-replication complex
qRT-PCR	quantitative real time PCR
RE	replication element
RFP	red fluorescent protein
RISC	RNA-induced silencing complex
rLCV	rhesus lymphocryptovirus

RNA	ribonucleic acid
RNAi	interfering RNA
RRV	rhesus rhadinovirus
siRNA	small inhibitory RNA
SPP1	osteopontin
SV40	simian virus 40
TGF-β	transforming growth factor beta
THBS1	thrombospondin 1
TIVE	telomerase-immortalized vein endothelial
TIVE-LTC	TIVE long term clone
TM6SF1	transmembrane 6 superfamily member 1
TPA	tetradecanoyl phorbol acetate
TR	terminal repeats
URR	unique regulatory region
UTR	untranslated region
vGPCR	viral G-protein coupled receptor
vIL-6	viral interleukin 6
VIP	variable ITAM-containing protein

Abstract of Dissertation Presented to the Graduate School
of the University of Florida in Partial Fulfillment of the
Requirements for the Degree of Doctor of Philosophy

STUDIES ON EPISOMAL MAINTENANCE AND VIRAL MicroRNAs OF KAPOSI'S SARCOMA-ASSOCIATED HERPESVIRUS

By

Rebecca Lynn Skalsky

August 2007

Advisor: Rolf Renne
Major: Medical Sciences--Immunology and Microbiology

Kaposi's sarcoma-associated herpesvirus (KSHV) is associated with Kaposi's sarcoma (KS) and two lymphoproliferative diseases, primary effusion lymphoma (PEL), and multicentric Castleman's disease (MCD). KSHV establishes long-term latent infection within dividing cells. Important for viral latency are proteins and small RNAs expressed from the KSHV latency-associated region (KLAR). The latency-associated nuclear antigen (LANA), encoded by ORF73 within KLAR, facilitates maintenance of latent viral episomes. LANA binds sites within the viral terminal repeats (TR) and recruits origin recognition complex proteins, thus mediating latent DNA replication. Additionally, LANA acts as a molecular linker to tether episomes to mitotic chromosomes. Using KSHV GFP-expressing replicons in short-term maintenance assays, we determined that early events mediated by LANA greatly contribute to the efficiency by which episomes are established. Additionally, we uncoupled replication and partitioning elements within TR and formally demonstrated that LANA binding sites (LBS1/2) within TR act as a *cis*-partitioning element for KSHV.

Also expressed from KLAR are KSHV microRNAs. MiRNAs post-transcriptionally silence gene expression by binding 3'UTRs of target messenger RNAs. We found that KSHV miR-K12-11 has sequence homology to miR-155, an oncogenic miRNA highly expressed in B

cell lymphomas and solid tumors. To determine whether these two miRNAs could regulate a common set of cellular genes, potentially contributing to tumorigenesis, we used a combination of bioinformatics tools, Affymetrix-based microarray analysis, and reporter assays. We identified 64 genes significantly downregulated in response to both miRNAs. Reporter assays confirmed several of these genes and further showed that BACH-1, a transcriptional repressor involved in stress response, can be targeted by both miR-155 and miR-K12-11. We mapped the miRNA binding sites within the BACH-1 3'UTR using site-directed mutagenesis and found that both miRNAs preferentially used a specific target site. The identification of these overlapping miRNA targets is an important first step in elucidating the roles of these potentially oncogenic miRNAs in KSHV pathogenesis. Together, the data presented here indicate that genes expressed from KLAR are critical to not only the establishment and maintenance of viral latency but also may contribute to the neoplastic state of KSHV-infected cells by post-transcriptionally regulating cellular gene expression via viral miRNAs.

CHAPTER 1
INTRODUCTION

Kaposi's Sarcoma

Kaposi's sarcoma (KS) was first described in 1872 as "idiopathic multiple pigmented sarcomas" by Austro-Hungarian dermatologist Moritz Kaposi working at the University of Vienna (Kaposi 1872). Highly vascular in form, multifocal KS lesions are characterized by neoangiogenesis and proliferating spindle cells amidst infiltrating inflammatory cells. Lesions occur in several morphological variants as well as clinical variants, including (i) classic or indolent KS, (ii) endemic KS, (iii) iatrogenic KS, and (iv) AIDS-related KS (Boshoff and Weiss 2002; Schwartz et al. 2003).

Classic KS occurs predominantly in elderly males of south European or Middle Eastern decent, and although disfiguring, is usually not life-threatening. Endemic KS is prevalent in regions of sub-Saharan Africa, is more aggressive, and the lymphadenopathic form, when presented in children, often results in death (Ziegler et al. 1997). Iatrogenic KS made its first debut in 1969 in a renal transplant patient, and in the United States, KS currently remains one of the most common neoplasms associated with immunosuppressive therapy and organ-transplants with a 40%-60% mortality rate (Boshoff and Weiss 2002). Immunosuppression is an important cofactor in KS tumorigenesis and to date, the disease is the most common AIDS-related cancer, reaching epidemic proportions in certain regions of sub-Saharan Africa (Campbell et al. 2003). At the onset of the AIDS epidemic in the early 1980s, over 40% of American men with AIDS developed KS. AIDS-related KS often disseminates to the lungs and other internal organs (Cotter and Robertson 2002). Widespread use of highly active anti-retroviral therapy (HAART) has led to a decline in KS occurrences since restoration of the immune system often leads to a regression in KS tumors (Boshoff and Chang 2001); however, despite such treatments, KS

malignancies continue to be one of the leading causes of mortality in HIV patients (Cheung et al. 2005).

KSHV Is The Etiological Agent Of KS And Lymphoproliferative Diseases

Following the description of KS in the late 19th century, researchers began looking for a causative agent of this disease. In the 1920s through 1960s, epidemiologists working in Africa believed KS to be caused by an infectious agent. In 1972, Giraldo et al found herpesvirus-like particles, presumed to be human cytomegalovirus at the time, in short-term KS cultures (Giraldo et al. 1972). Finally, in 1994, Chang et al. identified Kaposi's sarcoma-associated herpesvirus (KSHV) in AIDS-KS biopsies using representational difference analysis (RDA) by comparing DNA sequences from a KS sample to healthy skin of the same patient (Chang et al. 1994). Sequencing and phylogenetic analysis of KSHV placed this virus in the γ-herpesvirus family (Neipel et al.1997; Russo et al. 1996) along with human Epstein-Barr virus (EBV/HHV-4), murine γ-herpesvirus 68 (MHV68) and primate herpesviruses including herpesvirus saimiri (HVS) and rhesus rhadinovirus (RRV) (Desrosiers et al. 1997). Based on the sequences of several conserved proteins, KSHV is most closely related to HVS, a γ-2-herpesvirus, and thus is within the rhadinovirus subfamily.

KSHV, like other γ-herpesviruses, is lymphotrophic, and has been linked not only to KS, but also lymphoproliferative diseases including primary effusion lymphoma (PEL), a type of non-Hodgkin's lymphoma also known as body cavity based lymphoma (BCBL) (Cesarman et al. 1995a) and multicentric Castleman's disease (MCD) (Soulier et al. 1995). PEL cells have a distinct phenotype from other B cells, and are thought to be in a transitory state between antigen-selected, germinal center (GC) B cells and terminally differentiated plasma cells. PEL cells lack expression of most mature B-cell associated genes, but have rearranged immunoglobulin (Ig)

genes as well as somatic point mutations within rearranged Ig variable genes, indicating that transit has occurred through the GC of lymphoid organs (Fais et al. 1999; Matolcsy et al. 1998). Thus, the PEL phenotype is termed plasmablastic- intermediate to immunoblasts and plasma cells (Klein et al. 2003). PEL can be co-infected with EBV and often, but not always, associated with advanced AIDS (Arvanitakis et al. 1996). The KSHV load in PEL is approximately 50-100 viral copies per cell and is almost always higher than that of KS tissues (Schulz 1998). Patients diagnosed with PEL have a very poor prognosis with a median survival time of 6-12 months following diagnosis, even with combination chemotherapy and radiation therapy (Nador et al. 1996). Since the identification of KSHV, *in situ* hybridization studies have shown that not only is the viral DNA found in KS tumors and PEL, but that the majority of these cells are latently infected (Boshoff et al. 1995; Boshoff and Weiss 1997; Staskus et al. 1997), providing further evidence that this virus is the causative agent of these malignancies.

MCD is a rare, lymphoproliferative disorder which can affect multiple organs and is characterized by severe lymph node enlargement and atypical clonal B cells in a microenvironment of excess IL-6 (Leger-Ravet et al. 1991; Soulier et al. 1995; Staskus et al. 1999). KSHV-positive MCD is of the plasma cell variant (Dupin et al. 2000), and similar to PEL, has a strong association with HIV infection (Oksenhendler et al. 1996). In contrast to KS and PEL, MCD pathogenesis is thought to involve not only latent viral proteins but also several lytic gene products, namely vIL-6, the viral IL-6 homolog, which is a cytokine known to stimulate cell proliferation (Staskus et al. 1999). As such, KSHV gene products may contribute to MCD pathogenesis via paracrine signaling. vIL-6 has also been shown to block viral interferon response pathways in PEL cells, resulting in autocrine dependence of PEL cells on this viral cytokine (Chatterjee et al. 2002).

The KSHV Genome

The unique long coding region of KSHV is approximately 140 bp, and contains over 90 open reading frames, at least nine of which share functional homology to human genes and are thought to be the result of molecular piracy (Russo et al. 1996; Neipel et al. 1997). Fifteen ORFs are unique to KSHV (denoted K1 to K15) while the majority of ORFs are common amongst herpesviruses and have roles in viral replication and packaging during lytic infection (Fig. 1-1). The coding region is flanked by 35 to 45 copies of highly G+C rich terminal repeats (TR) (Lagunoff and Ganem 1997) which are proposed to facilitate genome circularization early after infection and function as an origin for latent DNA replication (Hu et al. 2002).

KSHV Life Cycle

Like all herpesviruses, KSHV exhibits a biphasic life cycle: lytic and latent. During lytic infection, viral gene expression is fully active and a virally-encoded DNA polymerase (ORF9) replicates the viral genome via a rolling circle mechanism (Chang 2001); linear double-stranded DNA genomes are then packaged into virions for egress, inevitably resulting in necrotic death of the host cell (Moore 2001). Two lytic replication origins have been described for KSHV, ori-Lyt(L), located between ORF K4.2 and K5, and ori-Lyt(R), located between ORF69 and vFLIP (AuCoin et al. 2002; Lin et al. 2003). Plasmids containing either of these two regions replicate in transient transfection assays in the presence of Rta/ORF50 and K-bZIP, the K8 gene product which has been found to associate with ori-Lyt and thus is thought to be a lytic origin binding protein (Lin et al. 2003; AuCoin et al. 2004). Recently, ori-Lyt(R) has been shown to be dispensable for lytic replication in the context of the viral genome following *de novo* infection, indicating that only ori-Lyt(L) is required (Xu et al. 2006).

The lytic cycle can be induced by treating latently infected cells, such as PEL-derived BCBL-1, with agents such as phorbal esters (TPA) (Renne et al. 1996) or chromatin-modifying

agents like sodium butyrate (NaB) (Miller et al. 1997), a histone deacetylase inhibitor. Lytic infection is regulated by the viral transactivator, Rta, encoded by ORF50, which is both necessary and sufficient for the switch from latency to lytic replication (Lukac et al. 1998; Sun et al. 1998). Demethylation of the ORF50 promoter is an important step in reactivation from latency (Chen et al. 2001). Rta is a sequence-specific DNA binding protein which transactivates numerous viral promoters including those of immediate early and early genes during lytic infection, and autoregulates its own promoter (Lukac et al. 1998; Lukac et al. 2001; Song et al. 2002).

In latent infection, predominantly thought to be the default pathway for γ-herpesviruses after *de novo* infection, only a subset of viral genes are expressed, and the circular viral genomes, termed episomes, persist within host cells without production of progeny virions. The latency-associated nuclear antigen (LANA) was the first latent gene product of KSHV to be identified in PEL-derived BCBL-1 cells. When incubated with sera from KS patients, these cells exhibited nuclear speckled staining patterns (Kedes et al. 1997). LANA is consistently detected in all KSHV associated malignancies as shown both by immunohistochemistry and *in situ* hybridization studies (Dittmer et al. 1998; Dupin et al. 1999), indicating this protein has important biological functions in KSHV biology. Additionally, the presence of LANA antibodies is used as the main serological tool for diagnosis of KSHV infection (Martin et al. 1998). This 222 to 234 kDa latent protein is encoded by ORF73, a gene located within the latency associated region.

The KSHV Latency-Associated Region (KLAR)

During latency, viral gene expression is restricted to a single genomic locale, the KSHV latency-associated region (KLAR). Located within this region are LANA (ORF73), vFLIP

(ORF71/K13), v-cyclin (ORF72), the kaposin locus (K12), and 12 different microRNA genes (miRNA) (Fig. 1-1 and 1-4). ORFs 73, 72, and 71 are transcribed from the constitutively active LTc promoter which gives rise to an alternatively spliced set of transcripts, a 5.4 kb polycistronic spliced mRNA from which LANA is translated and a 1.7 kb bicistronic mRNA for vFLIP and v-cyclin (Dittmer et al. 1998; Sarid et al. 1998; Talbot et al. 1999). vFLIP is synthesized from an internal ribosomal entry site (IRES) between ORF71 and ORF72 (Bieleski and Talbot 2001; Grundhoff and Ganem 2001; Bieleski et al. 2004). LANA, composed of 1003 to 1162 amino acids, is a multifunctional protein which interacts with cell cycle and transcriptional regulatory proteins such GSK3β, p53, and Rb (Friborg et al. 1999; Fujimuro et al. 2003; Radkov et al. 2000) and regulates several cellular and viral promoters, including its own (Krithivas et al. 2000; Lim et al. 2000; Knight et al. 2001). Additionally, LANA is absolutely required for latent viral DNA replication and episome maintenance (Ballestas et al. 1999; Hu et al. 2002; Ye et al. 2004). vFLIP is a FLICE-inhibitory protein which promotes cell survival by interfering with CD95/Fas signaling (Bertin et al. 1997). vFLIP can also regulate a number of proinflammatory cytokines and cell adhesion proteins via NF-kB and inhibit antigen presentation (Grossmann et al. 2006; Lagos et al. 2007). v-cyclin (ORF72) is a cyclin D homologue that promotes S phase entry by phosphorylating Rb (Dittmer et al. 1998; Kedes et al. 1997).

The kaposin locus is a very complex locus from which the kaposin family of proteins (A, B, and C) is expressed. K12 encodes the 60 amino acid protein kaposin A; adjacent upstream to K12 are DR1 and DR2, G+C rich repeats. Kaposin B and C initiate from alternate codons and include sequences of DR1 and DR2 (Sadler et al. 1999). Kaposin A has reported transforming activity (Muralidhar et al. 1998), while the kaposin B protein is involved in cytokine mRNA stabilization and can activate the p38/MAPK signaling pathway (McCormick and Ganem 2005),

thus contributing to immune modulation during KSHV infection. Thus, gene products expressed from KLAR have a substantial impact on the host cellular environment, particularly during latent infection.

A Molecular Basis For KSHV-induced Tumorigenesis

In addition to the viral proteins expressed from KLAR, a number of lytic genes also have potential roles in virally-induced oncogenesis, including the vIL-6 cytokine, vIRF3 which is an interferon regulatory factor with pro-survival activity (Moore et al. 1996), the vGPCR which induces cytokines and has angiogenic activity (Arvanitakis et al. 1997) and the mitogenic membrane-associated signaling proteins variable ITAM-containing protein (VIP) and latency associated membrane protein (LAMP) (Nicholas 2007).

This suggests that cell transformation is mediated both by the latent viral gene products that promote cell survival and proliferation as well as maintain the latent episomal state, but also paracrine signaling by viral cytokines and virally-induced cytokines during the early stages of KSHV infection. Indeed, while the majority of cells within KS tumors and PEL are latently infected, the tumor microenvironment likely consists of a mixture of lytically and latently infected cells, the combination of which may contribute to tumorigenesis (Grundhoff and Ganem 2004). Maintenance of viral latency, however, seems to be a requirement for endurance of the neoplastic state. SiRNA knock-down studies or drug inhibition of latent proteins such as LANA in PEL (Curreli et al. 2005; Godfrey et al. 2005), results in cell death, suggesting that ongoing viral gene expression is required for sustaining the transformed phenotype. It is within this context that understanding the establishment and maintenance of latency may contribute to new therapeutic strategies in the future.

Viral Episome Maintenance During Latent Infection

The current model of episome maintenance involves a strategy employed by various DNA tumor viruses in which newly synthesized viral genomes are tethered via viral proteins to host mitotic chromosomes during cell division, thus ensuring their faithful segregation to daughter cells and retention within the nucleus following cell division (Fig. 1-2). Episome maintenance is a two-step process, involving both the replication and segregation of viral genomes. One major focus of my research has been the development and use of a KSHV replicon model system to examine the relative efficiency by which these two processes contribute to the establishment of stable episome maintenance, described in Chapter 2. The following sections outline our current knowledge of viral episome maintenance with regards to (i) replication and (ii) segregation/partitioning.

EBV, a γ-herpesvirus associated with mononucleosis and Burkitt's lymphoma (Liebowitz and Kieff 1993), has been extensively characterized in regard to the mechanisms of latent episome persistence (Leight and Sugden 2000). EBV requires a single viral protein, Epstein-Barr virus nuclear antigen 1 (EBNA-1), for these processes (Yates et al. 1984; Yates et al. 1996). Genetic analysis of EBV demonstrated that a single genomic region, the 1.8 kb *oriP*, is necessary and sufficient for EBNA-1 mediated latent viral DNA replication (Yates et al. 1984; Yates et al. 1985). *oriP* contains two distinct cis-elements for episome maintenance. The 120 bp dyad symmetry (DS) of *oriP* functions as an origin of replication and contains two pairs of EBNA-1 binding sites (Harrison et al. 1994). In addition, 20 copies of 30 bp EBNA-1 binding sites compose the family of repeats (FR) and facilitate episome partitioning (Yates et al. 1984). EBNA-1 binds *oriP* via its C-terminal DNA binding domain (Yates et al. 1996) and interacts with chromosomes via domains within its amino-terminus (Marechal et al. 1999; Sears et al.

2003). Plasmids containing *oriP* are replicated once during S phase (Yates and Guan 1991) and stably maintained in EBNA-1 expressing cells when grown under antibiotic selection (Yates et al. 1985). Efficient plasmid maintenance requires the DS and at least seven copies of EBNA-1 binding sites from the FR, which can be substituted by three copies of DS, forming an array of EBNA-1 binding sites for tethering to mitotic chromosomes (Hebner et al. 2003; Wysokenski and Yates 1989).

In papillomaviruses such as bovine papillomavirus type 1 (BPV-1), two viral proteins are required for episome maintenance. The E1 protein has ATP-dependent helicase activity to separate viral DNA strands during replication and interacts with DNA polymerase alpha (Yang et al. 1993). The E2 protein supports DNA replication by binding to multiple sites in the upstream regulatory region (URR) and directs E1 to appropriate initiation sites (Piirsoo et al. 1996). Additionally, E2 associates with mitotic chromosomes to partition the viral DNA (Yang et al. 1993; Piirsoo et al. 1996; You et al. 2004). Hence, E2, like EBV EBNA-1, is a viral origin binding protein.

For KSHV, two viral components are known to be required for the two distinct steps (replication and partitioning) of the maintenance process: (i) LANA and (ii) *cis*-elements located within the TR (Ballestas et al. 1999; Ballestas and Kaye 2001; Hu et al. 2002). Ballestas et al. first showed using long-term maintenance assays that cosmids bearing a stretch of the KSHV genome containing the TR are maintained as episomes in LANA-expressing cells (Ballestas et al. 1999). LANA binds cooperatively to two adjacent sites (LBS1 and LBS2) within the viral TR (Garber et al. 2002) and facilitates replication of plasmids containing one or more 801 bp 83% G+C rich TR units (Hu et al. 2002; Lim et al. 2002). The LANA C-terminus contains a sequence-specific DNA binding domain that binds the TR (Garber et al. 2001), mediates LANA

dimerization (Schwam et al. 2000), and alone can confer partial replicative activity to TR plasmids (Hu et al. 2002). Thus, the minimal viral elements for episome maintenance and latent DNA replication are LANA and the TR while all other factors are provided by the host cell. LANA lacks any enzymatic activity, relying entirely on its partnering with cellular factors for its function. As such, LANA shares functional homology with the EBV EBNA-1 protein in its ability to mediate episome maintenance; however, there is very limited sequence similarity between these proteins.

KSHV Latent DNA Replication

Both EBV and KSHV hijack the cellular replication machinery and replicate during S phase in synchrony with the host cell (Yates and Guan 1991; Verma et al. 2007). The TR contains two *cis*-elements for DNA replication: (i) LBS1/2 (Garber et al. 2002) and (ii) a 29-32 bp replication element (RE) directly adjacent to LBS1/2 (Hu and Renne 2005) (Fig. 1-3A). LBS1 and LBS2 are spaced 22 bp apart, or two helical turns, allowing for a pair of LANA dimers to bind to the same helical face of the DNA (Garber et al. 2002). Two adjacent LANA binding sites are critical for efficient replication since deletion of one site reduces the replicative activity by about 50% (Garber et al. 2002).

The RE, directly upstream of LBS1/2, is absolutely required for KSHV latent DNA replication. Deletion of RE from TR abrogates the replicative competence of plasmids in LANA-expressing cells (Hu and Renne 2005). Plasmids containing the minimal replicator (RE and LBS1/2) replicate in a LANA-dependent fashion (Verma et al. 2007), indicating that the minimal replicator region alone functions as an origin. Additionally, treatment of cells with geminin, a compound that specifically inhibits assembly of cellular pre-replication complex (pre-RC), blocks replication of plasmids containing the minimal replicator, further demonstrating the dependence on cellular licensing factors for the initiation of latent DNA replication (Verma et al.

2007). Presumably, LANA directs the origin recognition complex (ORC) to assemble at RE for replication initiation, however, exact initiation sites within TR-plasmids or the viral genome are still undefined.

LANA has been shown to interact with and recruit ORC to assemble at the TR in late G1/early S phase, thus eliciting replication (Stedman et al. 2004). ORC is a conserved six-subunit protein complex that binds replication origin sites in an ATP-dependent manner and serves as a scaffold for other replication factors. ORC coordinates with the regulatory protein, Cdt1, and the pre-RC clamp loading factor, Cdc6, to recruit six mini-chromosome maintenance proteins (MCM2-7), forming the pre-RC (Dutta and Bell 1997; Takeda and Dutta 2005). Assembly of pre-RC occurs in a stepwise manner during late G1 (Nishitani and Lygerou 2002) and is temporally regulated by cyclin-dependent kinases (Cdks) (Sasaki and Gilbert 2007). The pre-RC progresses into a pre-initiation complex (pre-IC) during the transition to S phase. During this transition, the MCM2-7 complex is activated by Cdks to unwind DNA via its intrinsic helicase activity and recruits DNA polymerases to the origin. Following replication initiation, MCM2-7 leaves the origin, inactivating the pre-RC and preventing re-initiation. Re-loading of MCM2-7 is inhibited during S phase, ensuring that DNA is duplicated only once during each cell cycle (Sasaki and Gilbert 2007). The use of these cellular pathways for viral DNA replication is one way to ensure that KSHV episomes are maintained at a stable copy number in proliferating cells.

In addition to ORC, several other cellular proteins interact with TR. Heterochromatin components such as HP1α and methylated histone H3 are found associated with TR in a LANA-dependent manner (Sakakibara et al. 2004), suggesting that the chromatin architecture of the viral episome may be important for efficient long-term persistence. The TR is organized into

nucleosomes, and chromatin remodeling occurs in a temporally-regulated manner during G1 and S-phase (Stedman et al. 2004). Epigenetic modifications are thought to play an important role in permitting the DNA to be accessible to the replication machinery.

The transcription factor Sp1 contains three consensus binding sites within the TR (Hu and Renne 2005). Parp1, which modifies various nuclear proteins by poly-ADPribosylation, binds to the TR upstream of RE (Ohsaki et al. 2004). Recently, a number of additional cellular proteins have been reported to interact with the TR, including ATR, a protein involved in DNA damage, Brg1, an ATPase that associates with swi/snf to alter chromatin, and Npm1, a molecular chaperone for ribosome assembly (Si et al. 2006). However, these TR-interacting proteins are still uncharacterized as to their potential roles in episome replication and maintenance.

Partitioning Of KSHV Episomes During Mitosis

Like EBNA-1 and E2, LANA acts as a molecular linker between the viral genome and cellular chromosomes to ensure efficient partitioning of episomes to daughter cells. Consistent with the model of tethering viral genomes to chromosomes, LANA converges at sites along metaphase chromosomes in the presence of KSHV TR DNA (Ballestas et al. 1999; Cotter and Robertson 1999). Two chromosome binding sites (CBS) within LANA are important for this chromosome association, one in the proline-rich N-terminus comprised of amino acids 5-22 (Piolot et al. 2001; Wong et al. 2004) and a second in the C-terminus (Krithivas et al. 2000) (Fig. 1-3B). In the absence of TR DNA, LANA broadly paints chromosomes via its N-terminal region (Piolot et al. 2001), while the C-terminus localizes to discrete foci (Krithivas et al. 2002; Kelley-Clarke et al. 2007a; Kelley-Clarke et al. 2007b). LANA N-terminal residues 5-13 are sufficient to target heterologous proteins (GFP) to chromosomes (Barbera et al. 2004). Deletion of the first 22 N-terminal amino acids still allows LANA to localize to the nucleus, but prevents its

association with interphase chromatin, and abolishes episomal maintenance (Shinohara et al. 2002; Wong et al. 2004).

The N-terminal CBS has also been shown to contribute to LANA's role in DNA replication, and LANA mutants that can not interact with metaphase chromosomes have reduced activity in TR plasmid replication, providing evidence that chromosome association is not only important for tethering but also latent viral replication (Barbera et al. 2004; Lim et al. 2004). Recently, the N-terminus has been shown to interact directly with core histones H2A and H2B, enabling LANA to bind directly to chromosomes (Barbera et al. 2006).

Many cellular interacting partners have proposed roles in tethering and episome maintenance. LANA interacts with chromatin-associated proteins such as HP1α, histone methyltransferase SUV39H1, methyl CpG binding protein (MeCP2) which binds within the N-terminal CBS, and Dek, which binds to a region within the LANA C-terminus (Krithivas et al. 2002; Lim et al. 2003a; Sakakibara et al. 2004) (Fig. 1-3B), and associates with pericentromeric heterochromatin regions of cellular chromosomes (Szekely et al. 1999). LANA has been shown to recruit Brd2/RING3, a bromodomain protein, to heterochromatin (Platt et al. 1999; Mattsson et al. 2002). Another member of the double bromodomain family, Brd4, which has been implicated in E2-dependent tethering of papillomaviruses (You et al. 2004), has recently been shown to interact with LANA (You et al. 2006). Brd4, like Brd2, can bind acetylated histones H3 and H4, which are characteristic of a transcriptionally active chromatin state (Dey et al. 2003). Brd4 is unique in that it remains associated with mitotic chromosomes throughout mitosis (Dey et al. 2000).

Just as is the case for latent DNA replication, KSHV and EBV episomes are dependent on cellular pathways for partitioning of viral DNA. Viral episomes are faithfully segregated to

daughter cells by "piggy-backing" on sister chromatids. The foundation for high-fidelity chromatid separation during mitosis is actually set during late telophase, coinciding with pre-RC assembly, and maintained until anaphase of the next cell cycle (Nasmyth et al. 2000; Sasaki and Gilbert 2007). Protein complexes called cohesins are laid down between duplicated chromosomes and become responsible for the bipolar attachment of pairs of chromatids to the mitotic spindle. Cleavage of the cohesin subunit, Rad21 in humans, *Drosophila*, and *S. pombe*, occurs by a protease called separase, resulting in dissolution of the sister chromatids (Nasmyth et al. 2000; Nasmyth 2001). This enzyme is kept inactive in part by securin until all pairs of sister chromatids are attached to mitotic spindle. Recent work has shown that separase is also kept inactive by sequestration of Cdc20, an anaphase activator, via Mad2 to prevent premature anaphase entry (Ivanov and Nasmyth 2005; Nasmyth 2005). The correct assembly of the centromere, where two chromatids are tightly tied together, is also important in setting up the bilaterally symmetrical chromatids for spindle attachment so that chromatids can move to opposite poles in anaphase (Nasmyth et al. 2000).

The anaphase promoting complex (APC), an ubiquitin ligase, together with Cdc20, mediates the proteolysis of securin, marking the entry of anaphase (Alexandru et al. 1999; Nasmyth 2001). Upon chromosome separation, cells exit mitosis. Mitotic spindles dissolve, chromosomes decondense, and mitotic Cdks, which temporally regulate the onset of M phase, are degraded, creating a cellular environment permissive for re-assembly of the DNA replication machinery (Nasmyth 2001).

Much evidence indicates that episome partitioning is a non-random event. Initial observations with EBV *oriP* plasmids showed that when transfected into EBNA-1 expressing cells, plasmids are lost at slow rates. However, plasmid copy number had no influence on the

rate of loss and thus indicated that partitioning was a regulated event (Kirchmaier and Sugden 1995). More recently, elegant confocal microscopy studies on EBV infected cells have shown that EBNA-1 localizes symmetrically on pairs of mitotic sister chromatids in the presence of viral DNA, providing direct evidence of non-random partitioning (Kanda et al. 2007). For KSHV, studies looking at non-random episome tethering have yet to be done; however, the fact that viral episomes are maintained at stable copy numbers in latently infected PEL cells strongly suggests a non-stochastic model of episome partitioning.

Episome Establishment Is An Infrequent Event

PEL-derived cell lines, such as BCBL-1, can be readily established *ex vivo* and maintain between 20-150 stable viral copies per cell; however, KS-derived endothelial cells rapidly lose viral genomes upon *ex vivo* cultivation (Cesarman et al. 1995b; Aluigi et al. 1996). Studies on *de novo* infected cells in tissue culture indicates that the establishment and maintenance of KSHV genomes is an inefficient process (Lagunoff et al. 2002; An et al. 2006). Indeed, while many cell types are susceptible to infection with cell-free KSHV, cells fail to establish latency and lose viral genomes as they proliferate (Lagunoff et al. 2002; Bechtel et al. 2003). Similar observations have been made in the context of artificial replicons. TR-containing plasmids can be maintained in LANA-expressing cells under antibiotic conditions; however, in the absence of selective agents, rapid replicon loss has been reported (Ballestas et al. 1999; Grundhoff and Ganem 2004). This replicon instability and inefficient establishment cannot be explained merely by the absence of viral sequences outside of TR since both KSHV Bacmids and GFP-recombinant viruses behave similarly in the absence of selection following introduction into cells of either epithelial or lymphoid origin (Ye et al. 2004; Chen and Lagunoff 2005).

Based on these observations as well as studies on EBV episome maintenance (Leight and Sugden 2001), we and others have hypothesized that establishment of stable episome

maintenance is a rare event and may involve epigenetic modifications of incoming viral genomes. To address this central question of how KSHV episome establishment might be achieved, we employed an experimental system based on KSHV reporter replicons that can be monitored by GFP expression. This work is described in Chapter 2.

Virally-Encoded MiRNAs

A second major focus of my research has been the identification and functional characterization of KSHV-encoded microRNAs (miRNAs). This work is described in Chapters 3 and 4. In the following sections, I will briefly summarize our current knowledge of metazoan and viral miRNAs and miRNA-dependent post-transcriptional regulation of gene expression.

MiRNAs are small, non-coding, 19-24 nt RNAs that post-transcriptionally regulate gene expression by binding to 3'UTRs of target messenger RNAs (mRNAs), leading to translational repression and/or target mRNA degradation (Bartel 2004; Schafer et al. 2007). In 2004, Pfeffer et al. reported on the first virally encoded miRNAs expressed in human Burkitt's lymphoma B-cells latently infected with EBV B95-8, a laboratory adapted EBV isolate (Pfeffer et al. 2004). Five miRNAs were originally identified, and it is now known that EBV encodes at least 17 different miRNAs, 14 located within introns of the BART gene and three located next to BHRF1 (Cai et al. 2006; Grundhoff et al. 2006).

In 2005, our group and two other labs reported the identification of KSHV miRNAs (Cai et al. 2005; Pfeffer et al. 2005; Samols et al. 2005). Using size-fractionated RNA isolated from both lytically and latently infected BCBL-1 cells as well as latently infected endothelial cells (An et al. 2006), we cloned a total of ~650 sequences. Sequences were compared to the miRNA registry, as well as the human genome and KSHV genome using NCBI BLAST. Between 8.42% and 13.43% of the cloned sequences from BCBL-1 cells aligned to KSHV, representing 11 unique small RNAs between 19 to 23 nt in length. Computational analysis showed that these

small RNAs could arise from long precursor RNAs which can form hairpin structures, a hallmark of miRNA biogenesis. Additionally, the 19-23 nt miRNAs and ~60 nt precursors could be detected by Northern blot analysis in KSHV-infected cells (Cai et al. 2005; Pfeffer et al. 2005; Samols et al. 2005). Surprisingly, all KSHV miRNAs mapped to two regions within KLAR. To date, KSHV encodes a total of 12 miRNA genes (Grundhoff et al. 2006), 10 of which are located within a cluster (nt 119,839 to 122,426) within a previously non-annotated region of the KSHV genome between ORF71 and the kaposin locus, while two miRNAs are located within K12 (Fig. 1-4).

Additional miRNAs have been reported for several other herpesviruses, including γ-herpesviruses MHV68, RRV, and rhesus lymphocryptovirus (rLCV) (Cai et al. 2006; Pfeffer et al. 2005), as well as herpes simplex virus 1 (HSV-1) and human cytomegalovirus (HCMV) (Pfeffer et al. 2005; Cui et al. 2006; Gupta et al. 2006) (Fig. 1-5), and it is likely that all herpesviruses encode miRNAs (Samols 2006). The nine miRNAs encoded by MHV68 are unique in that they are located adjacent to tRNA genes, indicating they may be transcribed via RNA polymerase III, in contrast to the majority of cellular miRNAs which are processed from RNA pol II transcripts (Ambros 2004). RRV expresses eleven miRNAs located within a similar genomic region to that of the KSHV miRNAs- between ORF69, found directly upstream of the kaposin locus in KSHV, and ORF71 (Schafer et al. 2007). Both RRV and MHV68 are closely related to KSHV; however, the miRNAs expressed from these viruses lack any sequence homology. In fact, only rLCV, a non-human primate lymphocryptovirus, expresses nine out of 21 miRNAs with sequence identity to EBV miRNAs; the seven precursors from which these arise are also conserved (Cai et al. 2006b).

The majority of cloned herpesvirus miRNAs are located within intergenic regions, with the exception of several HCMV miRNAs found within ORFs dispersed throughout the viral genome (Fig. 1-5). EBV, KSHV, and MHV68 miRNAs are located within clusters, as has been observed for several cellular miRNAs. In fact, over 25% of metazoan miRNAs are found within clusters and processed from polycistronic mRNAs (Ambros 2004).

MiRNAs In Metazoans

The first identified miRNA, *lin-4,* was originally reported in 1993 in *Caenorhabditis elegans* (Lee et al. 1993; Wightman et al. 1993). The non-protein-coding *lin*-4 gene, known to control developmental timing, was found to produce two RNAs, one 22 nt in length, and the second ~60 nt in length with the potential to form a stem-loop structure with the 22 nt species present on one arm. Mutation of *lin*-4 resulted in developmental abnormalities and altered levels of the *lin-14* protein. Interestingly, *lin*-14 mutants with 3'UTR deletions exhibited a developmental phenotype similar to that of *lin-4* mutants. Further analysis showed that the *lin-4* 22 nt RNA was complementary to multiple regions within the 3'UTR of the *lin-14* transcript, and that *lin-4* could downregulate the *lin-14* protein levels without significantly altering the *lin-14* RNA levels via these complementary sites (Wightman et al. 1993). Thus, a new RNA regulatory function was proposed.

At the time, the regulatory RNA effect conferred by *lin-4* was thought to be specific to *C. elegans.* Since the discovery of *let-7*, a miRNA with homologs in *C. elegans, Drosophila,* and humans (Pasquinelli et al. 2000; Reinhart et al. 2000; Slack et al. 2000), studies have now shown that miRNAs are encoded by all metazoan organisms as well as plants and viruses (Ambros 2004; Bartel 2004; Cullen 2006; Samols and Renne 2006; Sullivan and Ganem 2005). *let-7* family members, like *lin-4,* are known to control developmental timing, regulating the L4-to-adult transition in *C. elegans* (Reinhart et al. 2000) by downregulating genes including hbl-1

(Lim et al. 2003b) and *lin-41* (Slack et al. 2000), thus permitting for expression of an adult-specific transcription factors. These short, non-coding RNAs are ~19-24 nt in length, have important functions in post-transcriptional control, and can greatly influence cellular transcriptomes/proteomes in a variety of organisms (Bartel 2004; Bartel and Chen 2004).

To date over 470 human miRNAs have been identified, several of which have known roles in development, hematopoiesis, apoptosis, cell proliferation, and cancer. One of the first vertebrate targets, HOX8, targeted by miR-196, was identified in 2004 and is a member of the HOX cluster with roles in mammalian development (Yekta et al. 2004). miR-181, first described in mouse development, is reported to control hematopoiesis (Chen et al. 2004). Members of the *let-7* miRNA family have roles in several of these processes. In lung cancer cells, the *let-7* miRNA has a growth-suppressive effect and can bind the 3'UTR of the oncogenic high mobility group A2 (HMGA2) mRNA (Lee and Dutta 2007). Work from the Bartel lab has recently shown that HMGA2 is often found at regions of chromosomal instability and because of this, exhibits disrupted pairing with *let-7* which enhances oncogenic transformation in many cancer types (Mayr et al. 2007).

MiRNA Biogenesis

MiRNA genes are transcribed within the nucleus via RNA polymerase II to form a long primary miRNA (pri-miRNA) (Fig. 1-6). While some miRNAs have their own promoter, the majority of miRNAs are located within intergenic regions (Ambros 2004). In fact, over 50% of mammalian miRNAs are located within introns (Rodriguez et al. 2004). Following transcription, the long pri-miRNA folds into a stem-loop structure which is cleaved by Drosha, releasing the precursor miRNA (pre-miRNA) which consists of an imperfect hairpin of approximately 60-80 nt. The remaining 5' and 3' pri-miRNA fragments are thought to be degraded rapidly in the nucleus and to date, have no reported function of their own (Cai et al. 2004).

Drosha is a conserved 160 kDa double-stranded RNA-binding protein with RNase III activity that is required for pri-miRNA processing (Lee et al. 2003). In humans, Drosha forms a complex with the DiGeorge syndrome critical region 8 protein (DGCR8), a regulatory co-factor called Pasha in *C. elegans* and *D. melanogaster*, which is thought to aid in recognition of the pri-miRNA (Denli et al. 2004; Han et al. 2006). Several studies indicate that substrate recognition is determined by the tertiary structure of the pri-miRNA itself, in particular, the length of the stem; cleavage occurs at a distance of approximately two helical turns from the terminal loop (Zeng et al. 2003; Zeng and Cullen 2005).

Cleavage by Drosha produces a duplex RNA with a 5'phosphate and ~2 nt 3'OH overhang (Lee et al. 2003). Following cleavage, the pre-miRNA is exported into the cytoplasm via the heterodimeric complex Exportin V/Ran-GTPase. Together, this complex recognizes and binds the 2 nt 3' overhang and pre-miRNA stem (Yi et al. 2003; Lund et al. 2004; Zeng and Cullen 2005). Within the cytoplasm, the pre-miRNA is bound by Dicer, an RNase III enzyme originally characterized for its participation in the RNA interference (RNAi) pathway. Dicer, with its co-factor TRBP, cleaves off the end loop of the pre-miRNA hairpin, leaving a ~21 nt miRNA duplex intermediate with a second 2 nt 3' overhang (Chendrimada et al. 2005; Hutvagner 2005).

One strand of the duplex is loaded into the RNA-induced silencing complex (RISC), while the passenger strand is degraded (Lee et al. 2004). Strand separation and loading of the mature miRNA into RISC was a mystery for some time. Studies on *Drosophila* RNAi proteins and their human orthologs have now shown that unwinding of the dsRNA and cleavage of the passenger strand is actually facilitated by Ago2, a RISC component, as well as TRBP (Gregory et al. 2005; Matranga et al. 2005; Rand et al. 2005). Strand selection is thought to result from the thermodynamic stability of the 5' end of the duplex, and the thermodynamically favored strand is

selectively incorporated into RISC (Hutvagner 2005). Interestingly, several mature miRNA originate from opposite strands of the same precursor. For example, KSHV miR-K12-4-5p and miR-K12-4-3p, arising from the 5' arm and 3' arm respectively, are both found expressed in latently infected cells (Cai et al. 2005; Pfeffer et al. 2005; Samols et al. 2005).

RISC has two major components: a small RNA entity such as a miRNA or siRNA that confers sequence specificity and Argonaute. Argonaute proteins contain two primary domains: an N-terminal PAZ (Piwi-Argonaute-Zwille) domain and a C-terminal PIWI domain (Parker and Barford 2006). The PIWI domain is responsible for the "slicer" function of Argonaute within RISC, and the dsRNA binding domain of Dicer has been shown to interact directly with the Ago2 PIWI domain, potentially for RNA loading (Brennecke et al. 2005; Parker and Barford 2006). Four Argonaute proteins are present in humans (Ago1, Ago2, Ago3, and Ago4); however, only Ago2 contains endonuclease activity. Tethering of Ago proteins to mRNA has been shown to recapitulate RISC activity (Brennecke et al. 2005; Pillai et al. 2005); however, the small RNA component of RISC acts as a guide for target mRNA specificity.

Regulation Of Gene Expression By MiRNAs

MiRNAs post-transcriptionally silence gene expression via imperfect base pairing to 3'UTRs of target mRNAs, leading to mRNA translational repression and/or cleavage (Ambros 2004; Bartel 2004). Only limited complementarity between a mature miRNA and mRNA target is required for target binding (Lewis et al. 2003; Lai 2004). As such, a single miRNA can modulate expression of several different mRNAs. Indeed, over one third of all human genes are predicted to be targeted by miRNAs (Bartel 2004; Burgler and Macdonald 2005).

Several models have been proposed as to the actual mechanism of miRNA post-transcriptional regulation. Studies with *let-7* have shown that RISC may interefere with cap recognition during translation initiation since it was observed that m(7)G-cap independent

translation is not downregulated by this miRNA (Brennecke et al. 2005; Pillai et al. 2005). Another study with *let-7* as well as *miR-125b* showed that these miRNAs contribute to accelerated removal of the mRNA poly(A) tail, the consequence of which is rapid mRNA decay (Wu et al. 2006). Experiments with *let-7a* and a *C. elegans lin-41* 3'UTR showed that polyribosomes sedimented together with the miRNA, the 3'UTR, and members of RISC in sucrose gradients, indicating that miRNAs might inhibit actively translating ribosomes (Nottrott et al. 2006). More recently, RISC has been shown to associate with the 60S ribosome subunit and eIF6, an anti-association factor that binds the 60S subunit and prevents 80S ribosome assembly, thus miRNAs could potentially inhibit productive polyribosome formation during translation (Chendrimada et al. 2007). Additionally, Ago2 itself contains a motif that allows the protein to bind directly to the m(7)-G cap, which could block recruitment of eIF4E to the cap and thus translation initiation (Brennecke et al. 2005; Kiriakidou et al. 2007). It is also possible that miRNAs utilize a combination of the proposed mechanisms for translational silencing.

Determinants Of MiRNA Targeting

Based on experimentally determined miRNA targets, a set of general rules has been developed for miRNA targeting. miRNA binding sites are located, with few exceptions, within the 3'UTRs of mRNAs. The presence of multiple miRNA binding sites within a 3'UTR makes it a more likely target (Lewis et al. 2003; Lewis et al. 2005). Mutational analysis has shown the importance of the 5' end of the miRNA for target recognition, a region known as the 'seed' (Lewis et al. 2003; Lewis et al. 2005). The 5' seed is 6 to 8 nt in length starting from nt 2 of the mature miRNA which perfectly base pairs to a 6 to 8 nt site within a 3'UTR (Lewis et al. 2003). The most 5' nt of the miRNA, often a uracil (Lau et al. 2001), is generally unpaired or binds with an adenosine. G:U pairing does not normally occur within the seed (Brennecke et al. 2005). Computational analysis of seed binding sites has shown that the seed is often flanked by

adenosines (Lewis et al. 2005). Seed sites are now referred to as 6mer, 7mer(A1), 7mer(m8), or 8mer depending on the length of perfect base pairing (Lewis et al. 2003; Lewis et al. 2005). In addition to the 5' seed, 3' compensatory sites have been reported (Brennecke et al. 2005) which may compensate for imperfect base pairing within the 5' end.

Like cellular miRNAs, cellular miRNA targets are also evolutionarily conserved. Additionally, extensive bioinformatics analysis on gene expression profiling data has revealed that miRNAs and miRNA targets have co-evolved, and thus in tissues where a specific miRNA is expressed, its targets are expressed at lower levels compared to tissues where that miRNA is not expressed (Farh et al. 2005; Sood et al. 2006).

Methods To Identify MiRNA Targets

Several target prediction programs have been built around the general guidelines of miRNA targeting. An RNA folding algorithm, RNAhybrid, has been used to predict *Drosophila* targets, and is based on a forced seed match within the 5' end of the miRNA as well as thermodynamic assessment of the minimal free energy for hybridization (Rehmsmeier et al. 2004). PicTar was designed to identify evolutionarily conserved miRNA targets in several species including human, chimpanzee, mouse, rat, dog, and chicken (Krek et al. 2005). The free energy for the miRNA:mRNA duplex as well as 5' seed binding is built into the algorithm as determinants for binding. TargetScanS, designed by the Bartel laboratory, uses RNAFold to calculate free energy of binding, and scores heavily for a 5' seed match which is flanked by an adenosine as well as multiple binding sites within a 3'UTR (Lewis et al. 2003; Lewis et al. 2005). All known miRNA targets are built into the algorithm, and it has an estimated ~25% false positive rate determined in part from the 11 confirmed targets out of the 15 predicted miRNA targets tested. TargetScanS has been used to predict a number of targets which have been validated experimentally (Reinhart et al. 2000; Yekta et al. 2004; Lewis et al. 2005).

miRanda, designed by Enright and John et al, was used to determine targets in *Drosophila* and humans (Enright et al. 2003; John et al. 2004). Pairing within the seed region as well as the cut-off free energy can be user-defined. miRanda relies on evolutionary conservation for target binding sites; however, the program can be manipulated to suit specific purposes using the open-source version (www.microrna.org).

While the algorithms built for miRNA target prediction are invaluable tools, the best approaches to examine miRNA targets are those achieved experimentally. Several experimental techniques have been implemented for this purpose. Reporter assays to validate miRNA targeting of a single 3'UTR are widely used (Lewis et al. 2003; Stark et al. 2003; Brennecke et al. 2005; Krek et al. 2005). Cloning of specific transcripts bound by RISC has recently been used by Vatolin et al (Vatolin et al. 2006). Finally, to globally investigate targets, expression profiling studies to identify genes downregulated in response to specific miRNAs is a very practical approach since miRNA targeting often leads to mRNA decay (Ambros 2004; Bagga et al. 2005; Calin and Croce 2006; Volinia et al. 2006).

Targets Of Viral MiRNAs

Since the identification of viral miRNAs, a major research focus has been to elucidate the biological roles of these novel viral regulators; in particular, determining whether they target host and/or viral mRNAs and the biological consequences of this regulation. EBV miR-BART2 has been proposed to facilitate cleavage of the EBV BALF5 mRNA which encodes the viral DNA polymerase for lytic replication (Pfeffer et al. 2004). A miRNA encoded by HSV-1, miR-LAT, has been shown to confer resistance to apoptosis by downregulating transforming-growth factor (TGF-β) and SMAD3 (Gupta et al. 2006). The functions of the majority of herpesvirus

miRNAs, including those expressed by KSHV, are still unknown; however, we have recently identified several genes targeted by the KSHV miRNA cluster (Samols 2007).

Sequence analysis of KSHV miRNAs has shown they are not evolutionarily conserved with other viral miRNAs (Samols et al. 2005; Samols 2006); however, based on the miRNA targeting requirements and the importance of the seed sequence outlined above, we identified one miRNA, miR-K12-11, with seed sequence homology to miR-155. Overexpression of miR-155 has been linked to several malignancies, including various B cell lymphomas, as well as breast, lung, and colon cancers, thus miR-155 has been proposed to be an oncogenic miRNA (Eis et al. 2005; Iorio et al. 2005; Tam and Dahlberg 2006; Volinia et al. 2006). Very recently, miR-155 has been implicated in B and T cell development (Rodriguez et al. 2007; Thai et al. 2007). Based on the seed sequence homology of miR-K12-11 and miR-155, I hypothesized that these miRNAs might regulate similar cellular targets. A major portion of my research has been investigating the targets of miR-K12-11 and miR-155 and their potential contributions to tumorigenesis. This work is presented in Chapter 3.

Chapters 3 to 5 focus on two different aspects of KSHV biology, the major players of which originate from KLAR. In Chapter 2, the roles of LANA and the TR in the establishment and maintenance of viral episomes are discussed. In particular, I focused on early events contributing to the establishment of episomes as well as contributory viral *cis*-elements within the TR. In Chapters 3 and 4, targets of KSHV-encoded miRNAs are described. I first focused on identifying and characterizing targets of a single miRNA, miR-K12-11, which has homology to the oncogenic miR-155 family. Later, I expanded my work to include all miRNAs encoded within the KSHV miRNA cluster and aided in identifying several KSHV miRNA targets.

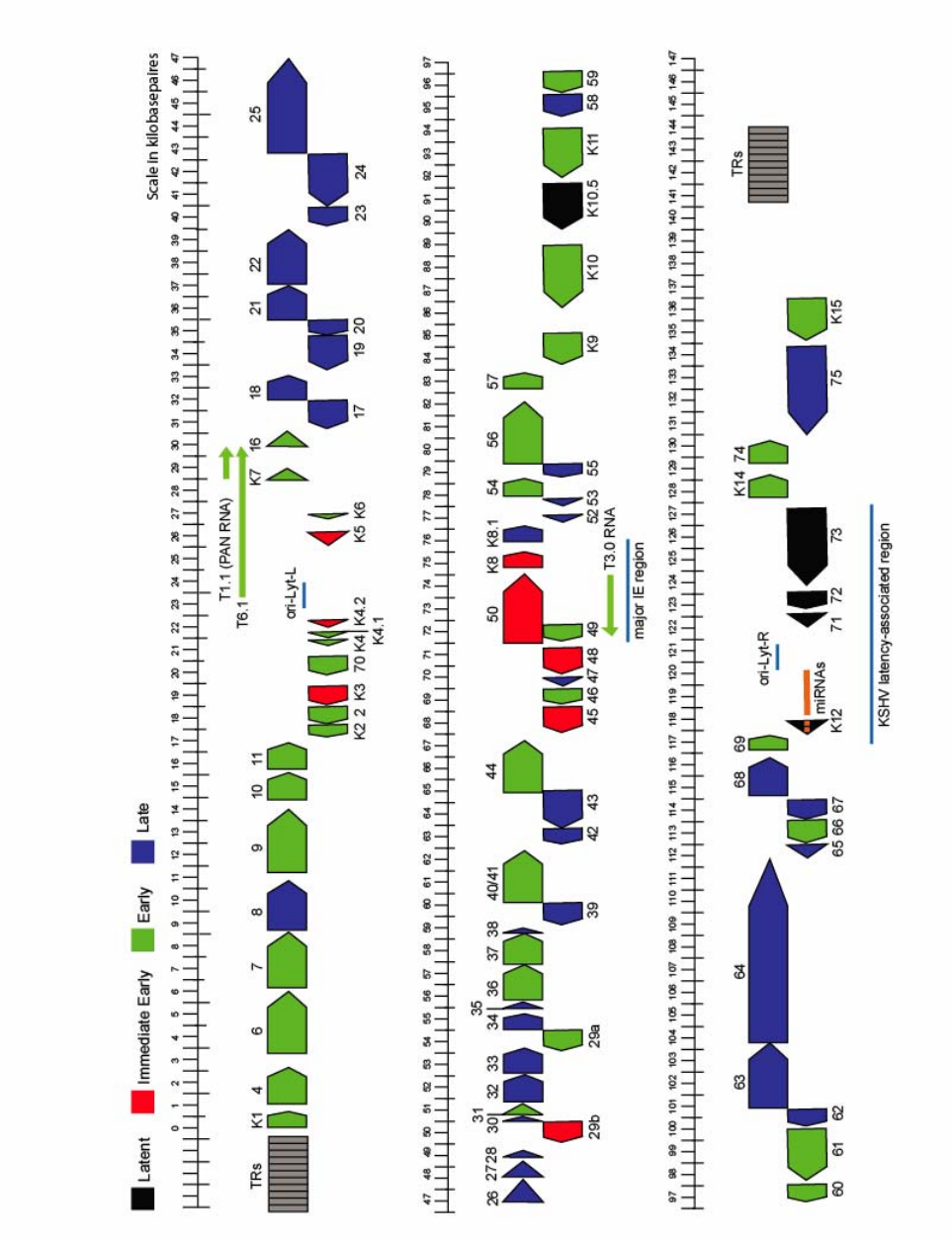

Figure 1-1. The KSHV Genome. Terminal repeats (TRs) are depicted in gray boxes at either end of the unique long coding region. Open reading frames (ORFs) are color coded according to immediate early, early, late, and latent genes. The KSHV latency associated region is underlined in blue.

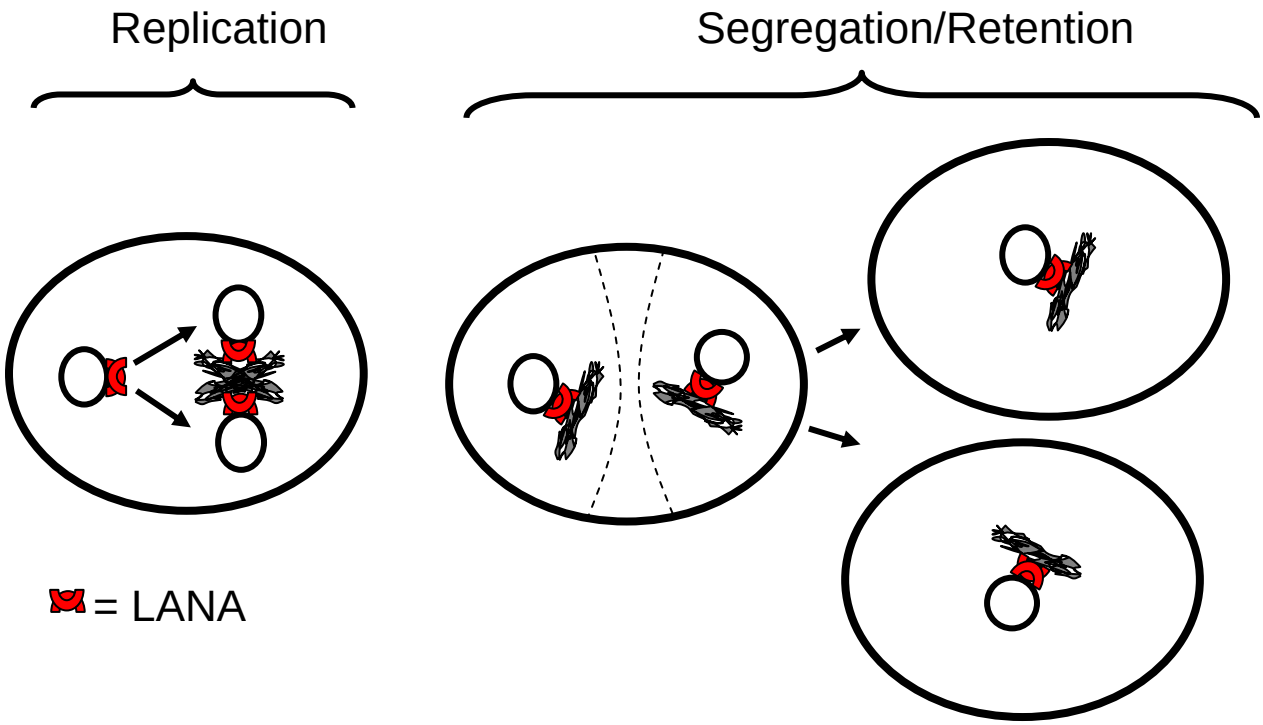

Figure 1-2. Episome maintenance model. The two distinct steps of episome maintenance, replication and segregation, are outlined. Viral episomes are depicted as black circles while latent viral proteins, such as LANA, are shown in dark orange, linking the episomes to cellular chromosomes.

A

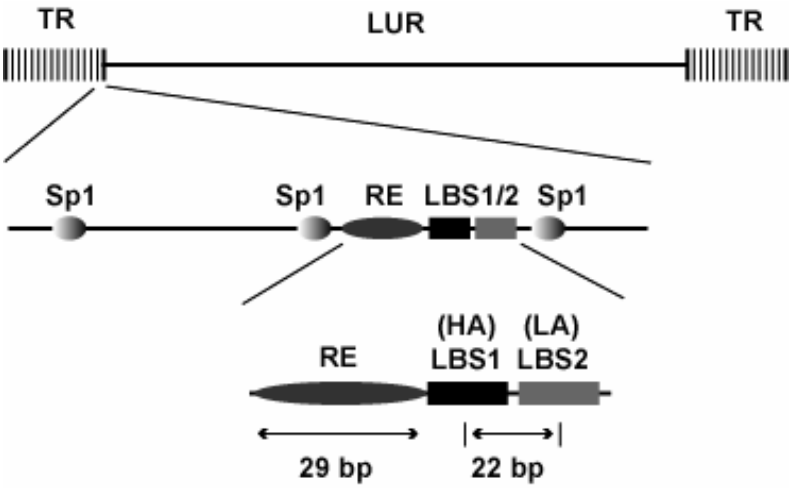

B

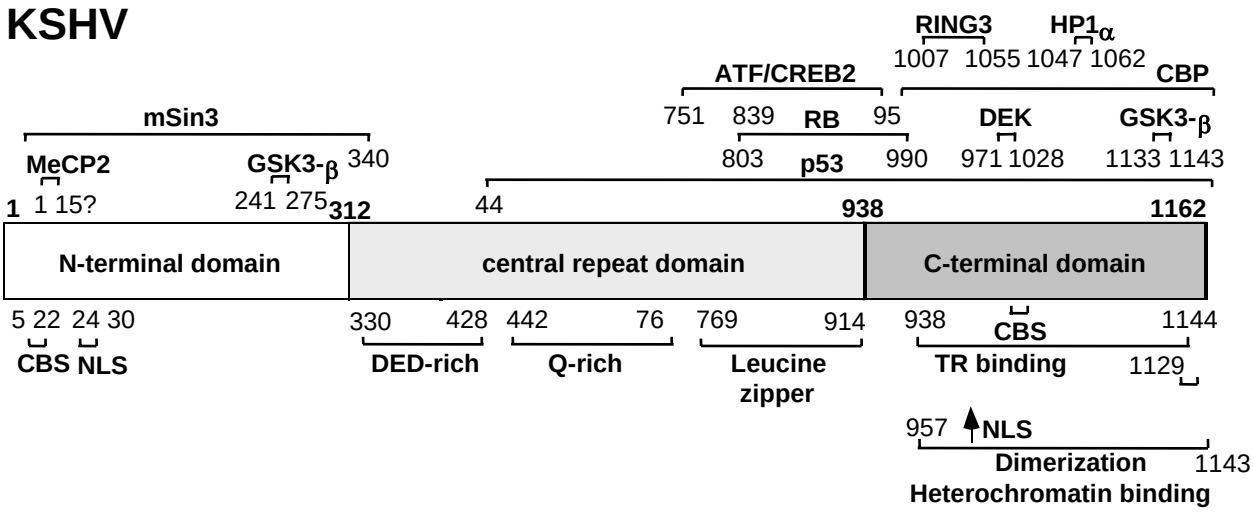

Figure 1-3. Schematic of cis-elements within TR and domains of LANA. A. A single TR unit (801 bp) is shown containing three Sp1 binding sites, the 29 bp RE, and LBS1/2 which are distanced by 22 bp center to center (From Hu and Renne, 2005). B. Schematic of the LANA protein with three distinct domains. Listed above are all cellular proteins known to interact with LANA; below are the assigned functions to each region of the protein. CBS = chromosome binding site; NLS = nuclear localization signal.

A

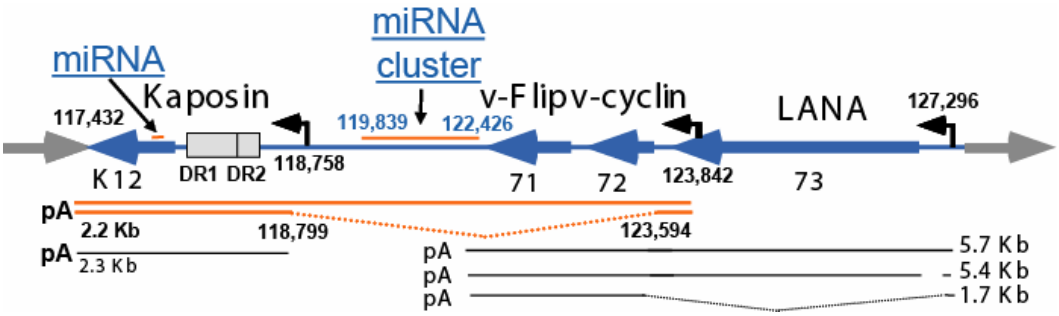

B

Name	Sequence	position
KSHV-miR-K12-1	AUUACAGGAAACUGGGUGUAAG	121911
KSHV-miR-K12-3-5p	UCACAUUCUGAGGACGGCAGCGA	121608
KSHV-miR-K12-4-5p	AGCUAAACCGCAGUACUCUAGG	121476
KSHV-miR-K12-4-3p	UAGAAUACUGAGGCCUAGCUGA	121438
KSHV-miR-K12-5	UAGGAUGCCUGGAACUUGCCGGU	121287
KSHV-miR-K12-6-3p	UGAUGGUUUUCGGGCUGUUGAG	120786
KSHV-miR-K12-11	UUAAUGCUUAGCCUGUGUCCGAU	120601
KSHV-miR-K12-7	UGAUCCCAUGUUGCUGGCGCUC	120380
KSHV-miR-K12-8-3p	CUAGGCGCGACUGAGAGAGCAC	119967
KSHV-miR-K12-9-3p	GCUGGGUAUACGCAGCUGCGU	119326
KSHV-miR-K12-10	UUAGUGUUGUCCCCCCGAGUGGC	117992

Figure 1-4. KSHV miRNAs and their position within KLAR. A. Schematic of the KSHV latency-associated region (KLAR). All nucleotide annotations are based on the BC-1 KSHV sequence. ORFs, transcripts, direct repeats 1 and 2 (DR1 and DR2), and promoters are drawn as described in (Dittmer et al. 1998, Li et al. 2002, Sadler et al. 1999, Talbot et al. 1999). The miRNA cluster, as well as the proposed Kaposin transcripts by Li et al, are shown in orange. B. Sequences of cloned miRNA species and nucleotide positions within KLAR (Samols et al. 2005).

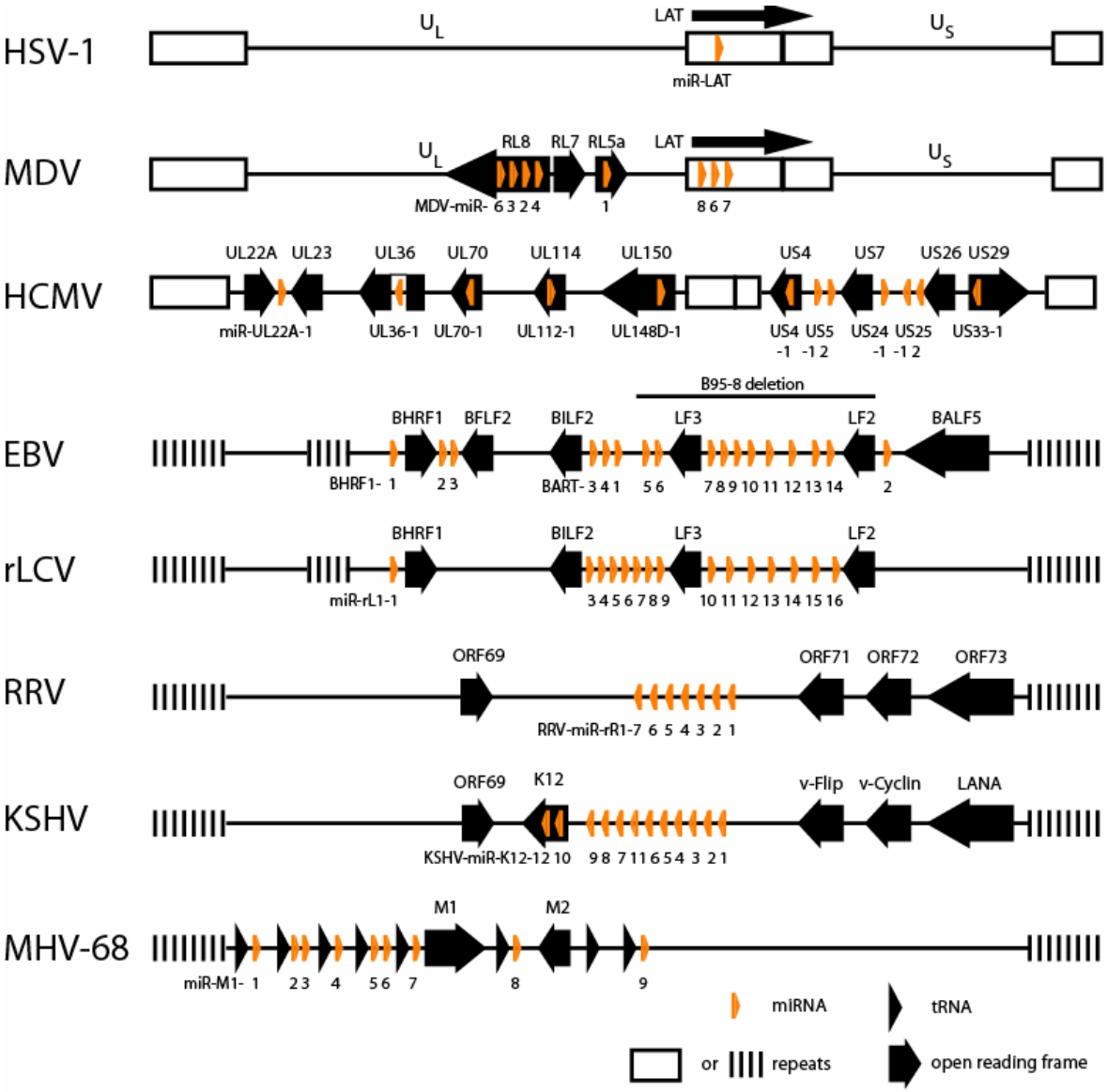

Figure 1-5. Virally-encoded miRNAs. Genomes are represented for α-herpesviruses, HSV-1 and MDV, β-herpesvirus HCMV, and γ-herpesviruses EBV, rLCV, RRV, KSHV and MHV-68 with black arrows for ORFs and black bars for repeat sequences. The locations of miRNAs are indicated with orange arrows. Genomes are not drawn to scale.

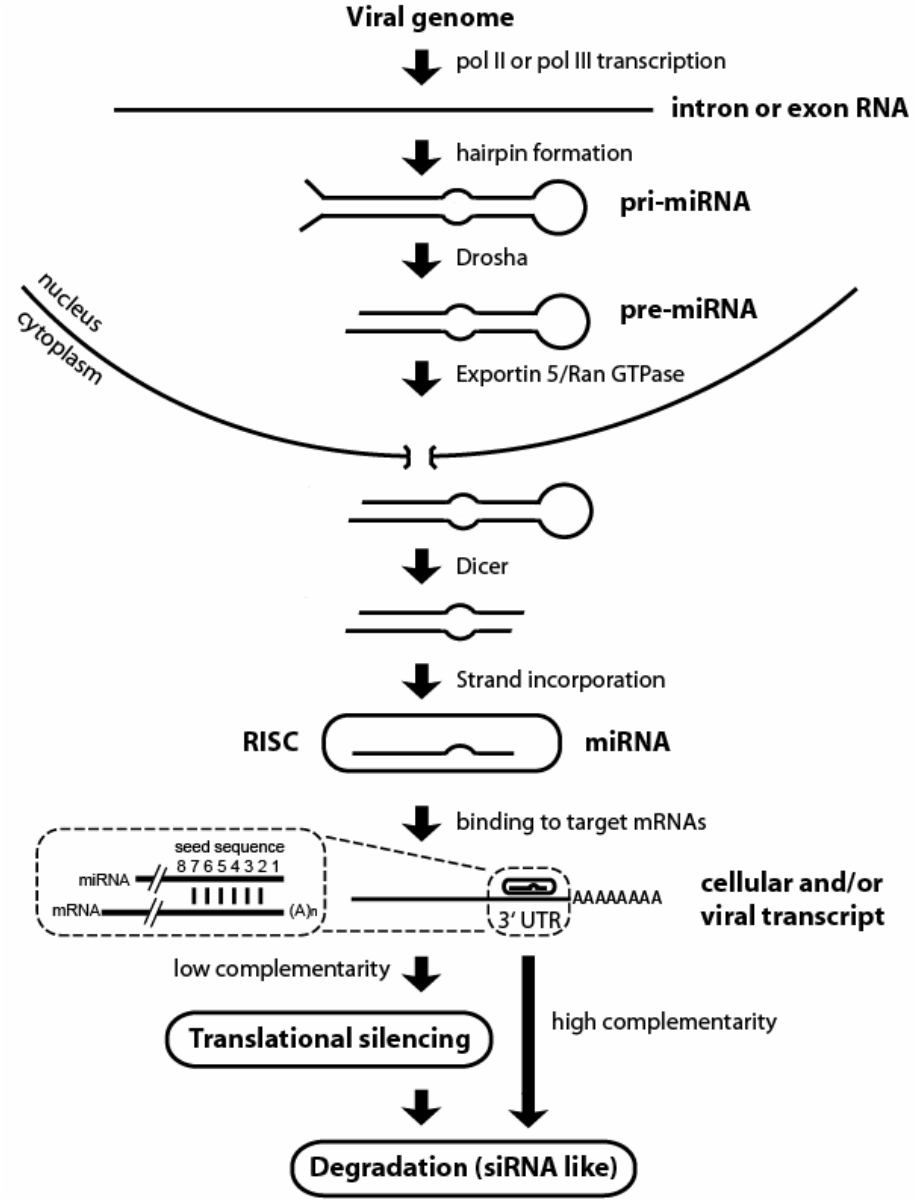

Figure 1-6. miRNA biogenesis. MiRNA precursors originate from introns or exons of RNA pol II or pol III transcripts, forming ~110 nt hairpin structures. Drosha cleaves the long primary miRNA (pri-miRNA) to leave a ~80-60 nt stem loop pre-miRNA which is exported into the cytoplasm via Exportin 5/Ran GTPase. In the cytoplasm, Dicer cleaves off the terminal loop, leaving a 21-24 nt duplex RNA molecule. The mature miRNA is incorporated into the RISC, where it binds to 3'UTRs of target transcripts, and induces either translational silencing or transcriptional degradation depending on the level of complementarity. Important for targeting is nt 2-7 of the mature miRNA, termed the "seed."

CHAPTER 2
ANALYSIS OF VIRAL CIS-ELEMENTS CONFERRING KSHV EPISOME PARTITIONING AND MAINTENANCE

Abstract

Maintenance of Kaposi's sarcoma-associated herpesvirus (KSHV) episomes in latently infected cells is dependent on the latency-associated nuclear antigen (LANA). LANA binds to the viral terminal repeats (TR), leading to recruitment of cellular origin recognition complex proteins. Additionally, LANA tethers episomes to chromosomes via interactions with histones H2A and H2B (Barbera et al. 2006). Despite these molecular details, less is known about how episomes are established after de novo infection. To address this, we measured short-term retention rates of GFP-expressing repliconsin proliferating lymphoid cells. In the absence of antibiotic selection, LANA significantly reduced the loss rate of TR-containing replicons. Additionally, we found that LANA can support long-term stability to KSHV replicons for over two months under non-selective conditions. Analysis of cis-elements within TR that confer episome replication and partitioning revealed that these activities can occur independently, and furthermore, both events contribute to episome stability. We found that replication-deficient plasmids containing LANA binding sites (LBS1/2) exhibited measurable retention rates in the presence of LANA. To confirm these observations, we uncoupled KSHV replication and partitioning by constructing hybrid origins containing the EBV dyad symmetry for plasmid replication and KSHV LBS1/2. We demonstrate that multiple LBS1/2 function in a manner analogous to the EBV family of repeats by forming an array of LANA binding sites for partitioning of KSHV genomes. Our data suggests that the efficiency by which KSHV establishes latency is dependent on multiple LANA activities, which stabilize viral genomes early after *de novo* infection.

Introduction

Kaposi's sarcoma-associated herpesvirus (KSHV/HHV8) is a DNA tumor virus present in Kaposi's sarcoma (KS) and lymphoproliferative diseases such as primary effusion lymphoma (PEL) and multicentric Castleman's disease. Like other DNA tumor viruses, including Epstein-Barr virus (EBV) and papillomaviruses, KSHV genomes are maintained as multi-copy episomes in the nuclei of latently infected cells (Raab-Traub 1989; Cesarman et al. 1995a).

Conceptually, maintenance of viral episomes in dividing cells can be described as the sum of two distinct processes: (i) DNA replication and (ii) partitioning/segregation. Critical for episome maintenance are virally encoded origin binding proteins (OBPs), which support DNA replication by binding to *cis*-regulatory elements within their respective origins of replication. The latency-associated nuclear antigen (LANA) of KSHV is a functional homologue of the EBV nuclear antigen 1 (EBNA-1) in that it is the only viral protein required for episome maintenance (Ballestas et al. 1999; Cotter and Robertson 1999; Yates et al. 1985). LANA binds cooperatively to two LANA binding sites (LBS1/2) (Garber et al. 2002) within the 801 bp highly G+C rich terminal repeats (TR), 35-45 copies of which flank the unique long coding region of KSHV (Lagunoff and Ganem 1997). LANA interacts with the cellular origin recognition complex (ORC), which assembles at the TR in late G1/early S phase, thus eliciting replication (Stedman et al. 2004; Verma et al. 2006). Our laboratory identified a 32 bp replication element (RE) directly adjacent to LBS1/2 within the TR that is absolutely required for LANA-dependent replication (Hu and Renne 2005) and plasmids containing the minimal replicator (RE and LBS1/2) replicate in synchrony with host chromosomes once per cell cycle (Verma et al. 2007). While the minimal *cis*-regulatory elements for replication have been defined (Hu and Renne 2005), whether additional *cis*-elements within TR and/or the number of LANA binding sites within TR have a direct role in episome partitioning and maintenance has not been determined.

First evidence demonstrating that LANA plays a key role in partitioning of viral episomes came from experiments involving G418 selection of Z6-cosmids harboring multiple TR copies (Ballestas et al. 1999). Subsequently it was shown that, under selection, two copies of TR are required to efficiently maintain plasmids in a LANA-dependent fashion, while one copy of TR conveys maintenance with less efficiency (Ballestas and Kaye 2001). Hence, all necessary *cis*-regulatory elements for both initiation of latent DNA replication and episome partitioning are located within TR sequences.

Extensive studies have been done on EBV oriP, a 1.8 kbp long region containing two distinct *cis*-elements: the dyad symmetry (DS) and the family of repeats (FR) (Yates et al. 1984; Lupton and Levine 1985). EBNA-1 recruits ORC to oriP (Chaudhuri et al. 2001) and facilitates long-term maintenance of oriP plasmids (Yates et al. 1985). The DS contains four EBNA-1 binding sites and functions as a replication origin, while the FR contains multiple EBNA-1 binding sites to facilitate episome partitioning (Rawlins et al. 1985; Reisman et al. 1985; Harrison et al. 1994). The organization of *cis*-elements within the latent replication origins of EBV and KSHV exhibits some similarities in that the spacing between OBP binding sites is 21 bp for EBNA-1 compared to 22 bp for LANA (Hu and Renne 2005). Unlike EBV however, KSHV genomes do not contain an obvious FR element. Given that KSHV genomes have 35-45 TR copies, each containing high affinity LANA binding sites, we hypothesized that multiple LBS1/2 function as a *cis*-partitioning element in a manner analogous to FR.

LANA, encoded by ORF73, is 222-234 kDa in size and can be divided into distinct functional domains. Piolot et al first demonstrated that amino acids 5 to 22 within the proline-rich N-terminus of LANA are required for the tethering of viral episomes to mitotic chromosomes (Piolot et al. 2001). Furthermore, this N-terminal domain conveys chromosomal

attachment when fused to heterologous proteins such as GFP (Piolot et al. 2001; Krithivas et al. 2002). Consistent with the tethering model, LANA converges at sites along metaphase chromosomes in the presence of TR DNA (Cotter and Robertson 1999). Several LANA-interacting chromatin-associated proteins including Brd4, Brd2/RING3, HP1α, histone methyltransferase SUV39H1, methyl CpG binding protein MeCP2, and Dek have been proposed as potential targets for LANA-dependent episome tethering (Krithivas et al. 2002; Lim et al. 2003a; Sakakibara et al. 2004; Viejo-Borbolla et al. 2005; Ottinger et al. 2006). Recently, Barbera et al provided biochemical and genetic evidence that the LANA N-terminus interacts directly with core histones H2A and H2B for episome tethering (Barbera et al. 2006). The LANA C-terminus contains a sequence-specific DNA binding domain (DBD) and a dimerization domain, both of which are required for DNA replication (Schwam et al. 2000; Garber et al. 2002; Lim et al. 2002; Komatsu et al. 2004). As such, the N-terminus of LANA is responsible for tethering viral episomes that are bound by the C-terminus to host chromosomes.

Both the N- and C-termini of LANA can facilitate multiple protein/protein interactions with cellular proteins including members of the wnt family of transcriptional regulators and the tumor suppressor proteins RB and p53, although recently is has been shown that p53 pathways in PEL cells are intact (Friborg et al. 1999; Radkov et al. 2000; Fujimuro et al. 2003; Petre et al. 2007). As a result, LANA modulates both cellular and viral gene expression (Renne et al. 2001; Naranatt et al. 2004).

In contrast to the growing knowledge on the molecular details by which LANA contributes to the initiation of DNA replication and tethering of episomes, a lot less is known about how episome maintenance is established. Indeed, studies of either *ex vivo* cultivated KS tumor cells or *de novo* infected cells suggest that these processes are rather inefficient (Cesarman et al. 1995b;

Aluigi et al. 1996; Lagunoff et al. 2002; Bechtel et al. 2003; An et al. 2006). While PEL-derived cell lines can be readily established and contain 20-150 stable copies, KS-derived endothelial cells rapidly lose viral genomes upon *ex vivo* cultivation. Additionally, *in vitro* infection studies have revealed that although many cell types are susceptible to infection with KSHV, cells fail to establish stable latency and lose viral genomes (Lagunoff et al. 2002; Bechtel et al. 2003). Similar observations have been made with artificial KSHV replicons; in the absence of antibiotic selection, rapid loss of TR-plasmids from transfected cells has been reported, and provision of LANA had no measurable effect (Grundhoff and Ganem 2004).

Based on these observations, we and others have hypothesized that the establishment of latency, defined here as stable episomal maintenance, occurs with very low frequency and may involve epigenetic modifications of the incoming viral genomes. Indeed, rare cases in which cells of endothelial origin (TIVE and SLK) support stable latency after *de novo* infection have been reported (Bechtel et al. 2003; Grundhoff and Ganem 2004; An et al. 2006).

To quantitatively access these rare events, we examined the kinetics of TR-containing replicons within proliferating cell populations in the absence and presence of LANA under non-selective conditions. Contrary to previous reports, we observed a significant effect of LANA on the short-term retention of KSHV replicons. In our model system, LANA improves plasmid retention two fold when provided *in cis* and four fold when provided *in trans*. Additionally, long-term maintenance of KSHV replicons can be observed at low frequencies. Using this system in conjunction with colony formation assays, we show that the *cis*-regulatory elements conferring episome partitioning consist of multiple LANA binding sites within multiple TRs which function in a manner analogous to the FR element of EBV. Our data indicates that the

early replication and partitioning events mediated by LANA are fundamental to initiating episome establishment and maintenance within dividing cells.

Results

LANA significantly increases the retention of KSHV replicons in the absence of antibiotic selection. Previous reports indicate that TR-plasmids are maintained in the presence of LANA only under selective conditions (Ballestas et al. 1999; Grundhoff and Ganem 2004). The fact that latent viral genomes are readily detectable within 36 hrs post-infection (Bechtel et al. 2003) suggests that LANA has a significant effect on episome establishment early after infection. To examine these early events in a quantitative manner, we measured the short-term retention rates of GFP-expressing replicons in the absence of selective agents.

First, we constructed a series of KSHV replicons containing a GFP reporter gene, allowing us to track cells that maintain replicons by microscopy and flow cytometry (Fig. 2-1A). The complete replicon, pLANA-2TR-GFP (11.3 kb), contains all required viral elements for episome replication and maintenance. Derivatives used for controls include p2TR-GFP (7.0 kb), lacking the LANA expression cassette, and pGFP (5.4 kb), lacking both *cis* (TR) and *trans* (LANA) elements. LANA expression from pLANA-2TR-GFP was confirmed by Western blot analysis (Fig. 2-1B).

To investigate replicon kinetics at early time points after transfection, we implemented a novel transfection method which enables us to transfect cells at high efficiencies while preserving cell viability (amaxa, inc.). To further recapitulate events after *de novo* infection, we introduced the lowest amount of DNA possible, which calculates to an optimized 5,000 copies per cell (~150 to 200 ng per 5 million cells). Equimolar amounts of plasmid DNA were introduced into BJAB cells, a B cell lymphoma line previously shown to replicate TR-plasmids in the presence of LANA (Grundhoff and Ganem 2003). 18 hrs post-transfection, cells were

FAC-sorted, and equal numbers of GFP-positive cells seeded and maintained in non-selective media. Cells were analyzed every 24 hrs for GFP expression and the percent of GFP positive cells was plotted over time.

GFP expression in pGFP and p2TR-GFP transfected populations followed similar kinetics, decreasing rapidly to about 1% within five days post-FACS (Fig. 2-2A). While GFP expression in cells transfected with pLANA-2TR-GFP also declined, the presence of LANA significantly slowed plasmid loss. At four days post-FACS, 13.9% of cells were GFP positive compared to less than 3% in the controls. By seven days post-FACS, the level of GFP expression stabilized at 3% ± 0.5% for pLANA-2TR-GFP (compared to 1.2% ± 0.3% for pGFP and 1.2% ± 0.1% for p2TR-GFP) and remained at this level indefinitely (Fig. 2-2A and data not shown). To compare the retention ability for each plasmid, we calculated the rate of plasmid loss per cell generation (Table 2-1). With LANA expression, TR-plasmids were lost at a rate of 13.6% ± 0.2% per cell generation. In contrast, control plasmids were lost at rates of 27.8% ± 0.3% (pGFP) and 25.6% ± 0.3% (p2TR-GFP) per generation. These data demonstrate that TR-containing replicons are retained two times more efficiently when LANA is provided *in cis* (Fig. 2-2A and Table 2-1).

Previously, it has been shown that LANA targets the wnt/β-catenin pathway (Fujimuro et al. 2003) thus promoting S-phase. To rule out that LANA-expressing BJAB cells have a growth advantage, thereby affecting our measurements of replicon maintenance, we monitored growth of FAC-sorted BJAB cells but observed no differences (Fig. 2-2B).

To confirm that the observed differences in GFP expression are due to LANA activity, we tested plasmid replication. Episomal Hirt-extracted DNA prepared four days post-transfection was subjected to *DpnI* digestion for over 72 hrs and subsequently amplified by PCR. *DpnI*

resistant species were readily detectable in cells transfected with pLANA-2TR-GFP (Fig. 2-2C, lanes 5-8), but not with p2TR-GFP (lanes 1-4) demonstrating LANA-dependent replication.

To determine whether provision of LANA *in trans* would enhance replicon retention in our model system, we monitored plasmid kinetics in LANA-inducible BJAB/TetOn/ORF73 cells (described in (An et al. 2005)). Cells were transfected with plasmids containing either one or two copies of TR. Following FAC-sorting, we again observed rapid loss of GFP expression from LANA negative cells (Fig. 2-2D, dashed lines). Provision of LANA *in trans* significantly reduced the loss of TR-plasmids, and plasmids containing only a single copy of TR behaved similarly to p2TR-GFP (Fig. 2-2D, solid lines). The loss rate of p2TR-GFP was 5.9% in LANA-expressing cells compared to 26.9% in BJAB controls (Table 2-1), resulting in a four-fold increase in retention. This retention is two times higher than when LANA was provided *in cis* (Fig. 2-2A). These data show that provision of LANA *in cis* or *in trans* significantly enhances the retention of TR-plasmids in proliferating cells under non-selective conditions.

To rule out the potential effect of plasmid size on retention and stability, we introduced p2TR-GFP into BJAB/TetOn/ORF73 cells grown in dox-plus media for 72 hrs. Following FAC-sorting, cells were re-seeded in either dox-plus or dox-minus media. Cells released from dox-induction retained GFP expression less efficiently than cells maintained in dox-plus media (Fig. 2-2E). This decrease in plasmid retention was tightly linked to the loss of LANA expression as monitored by Western blot (Fig. 2-2F). We have also tested a replicon containing an EBV replication origin (pDS-GFP) (Fig. 2-3A), and observed no differences in plasmid kinetics in the presence or absence of LANA (Fig. 2-3B), demonstrating that LANA has no effect on plasmids that lack TR. Thus, GFP expression correlates directly with retention of TR-containing

plasmids. Together, these data suggest that LANA increases viral episome retention early after infection.

KSHV replicons can be episomally maintained long-term in rare subpopulations in the absence of drug selection. Several reports have shown that KSHV and EBV replicons are unstable and can not be maintained long-term in the absence of antibiotic selection (Grundhoff and Ganem 2004; Leight and Sugden 2001); however, we have observed GFP expressing colonies in 293/LANA cells transfected with p2TR-GFP after 14 days post-transfection (Fig. 2-4A) and replicating TR-plasmids in GFP-positive LANA-expressing BJAB cells as long as 4 weeks post-transfection (Fig. 2-4B and C). Additionally, we have observed that the percent of GFP-positive cells stabilizes at ~3% within seven days post-FACS for either cells transfected with pLANA-2TR-GFP or dox-induced cells transfected with p2TR-GFP (Fig. 2-2). Thus, we hypothesized that rare cells within a population are competent in establishing episome maintenance and such events occur at a low frequency.

To demonstrate long-term LANA-dependent replication of TR-containing plasmids, BJAB or dox-induced BJAB/TetOn/ORF73 cells were transfected with p2TR-GFP. At days indicated, plasmid DNA was Hirt-extracted, digested with *DpnI,* and resistant species amplified by PCR. At 10 days post-transfection, BJAB cells were ~0.2% GFP positive and tested negative for *DpnI* resistant DNA while LANA-expressing cells were ~13% GFP positive and exhibited *DpnI* resistant replicated plasmid forms (Fig. 2-2G, lanes 2 and 4). To enrich for cells maintaining replicons, GFP-expressing LANA-positive cells were FAC-sorted at day 10, and Hirt extracts prepared 10 and 16 days later for PCR analysis. At 20 and 26 days post-transfection (10 and 16 days post-FACS), *DpnI* resistant plasmids continued to be present in LANA-expressing cells. Interestingly, at these later time points, the intensity of *DpnI* digested bands is similar to that of

input DNA, suggesting that LANA-positive cells are replicating and maintaining p2TR-GFP as stable episomes (Fig. 2-2G, lanes 5 and 6).

We next examined plasmid maintenance on an individual cell basis. BJAB cells were transfected with p2TR-GFP or pLANA-2TR-GFP and single cells were FAC-sorted into 96-well plates. At day four post-FACS, 21 of 49 wells contained GFP positive, viable cells for p2TR-GFP and 19 of 52 wells for pLANA-2TR-GFP were GFP positive. After 10 days, three wells for p2TR-GFP and seven wells for pLANA-2TR-GFP remained GFP positive (Fig. 2-5A).

At 14 days, three subpopulations from pLANA-2TR-GFP and all three p2TR-GFP subpopulations were triturated, expanded, and remained under continuous microscopic observation for over 2 months (Fig. 2-5B). LANA-expressing populations sustained a much higher percentage of GFP expressing cells, ranging from 16.3% to 55.3% GFP positive while control populations were significantly lower, ranging from 0.3% to 6.2% (Fig. 2-5C), suggesting that cells were maintaining KSHV replicons.

To verify that pLANA-2TR-GFP plasmids were maintained as episomes, Hirt-extracted DNA was analyzed ten weeks post-transfection by PCR. Cells transfected with p2TR-GFP (Fig. 2-5D, lanes 1-3) were negative, indicating that the small number of GFP expressing cells in these populations harbor integrated plasmids. However, cells transfected with pLANA-2TR-GFP (lanes 4-6) were positive, indicating the presence of episomal DNA. To confirm these results in a PCR-independent fashion, we performed Southern blot analysis. Hirt extracted DNA at eight or ten weeks post-FACS tested positive (Fig. 2-5E), demonstrating that these subpopulations (L-A3 and L-C3) stably maintained replicons. Semi-quantitative Southern blot analysis revealed low plasmid copy numbers, averaging three to 10 molecules per cell.

These results demonstrate that, in the presence of LANA, TR-containing plasmids can be maintained as episomes at a low frequency over a long period of time in dividing cells. Additionally, this data suggests that a small fraction of cells is competent to support the establishment of episomes in a LANA-dependent fashion under non-selective conditions.

Replication-deficient TR-plasmids are initially retained in the presence of LANA, but with less efficiency. Episome maintenance can be described as the sum of two processes: replication and partitioning. The EBV oriP contains two distinct sequence elements for these processes. DS conveys EBNA-1 dependent replication while FR facilitates partitioning (Yates et al. 1984; Lupton and Levine 1985; Rawlins et al. 1985; Reisman et al. 1985). For KSHV, all required sequences are located within the TRs (Ballestas et al. 1999). The minimal replicator has been mapped to a 71 bp region (nt 539-610) containing LBS1/2 and an adjacent 32 bp G+C rich replication element (RE), and confers replicative activity at about 25% that of wt TR (Hu and Renne 2005; Verma et al. 2007). Sequence requirements for LANA-dependent partitioning, on the other hand, have not been investigated. Several reports suggest that multiple TRs are needed for efficient long-term maintenance (Ballestas and Kaye 2001; Grundhoff and Ganem 2004); however, whether LBS1/2 alone or additional TR sequences contribute to partitioning is not known.

To address this question, we first asked whether plasmids containing LBS1/2 but not RE, therefore unable to replicate, could be retained in LANA-expressing cells. We compared retention of wt TR (p1TR-GFP), the minimal replicator (pRE-LBS1/2-GFP), or a plasmid containing 3 sets of LBS1/2 in tandem (p3XLBS1/2-GFP) in BJAB and LANA-inducible BJAB/TetOn/ORF73 cells.

In LANA-negative cells, GFP expression was lost rapidly irrespective of the transfected plasmids (Fig. 2-6A, dashed lines). In congruence with data shown above, LANA expression greatly reduced the loss of wt TR (Fig. 2-6A, solid squares). While pRE-LBS1/2, and p3XLBS1/2, which does not replicate, were lost faster than wt TR, the presence of LANA significantly reduced the loss of these plasmids (Fig. 2-6A, solid lines). Loss rates, calculated for each plasmid, showed that LBS1/2-containing plasmids were retained approximately 2.5 to 3 times more efficiently with LANA (Fig. 2-6C). By performing Southern blot analysis of Hirt-extracted DNA 96 hrs post-transfection, we detected pRE-LBS1/2 and p3XLBS1/2 only in LANA expressing cells (Fig. 2-6B, lanes 1 and 2). Importantly, by 72 hrs post-transfection, over 95% of the transfected DNA is degraded in the absence of LANA (data not shown). Thus, early on, LANA seems to stabilize LBS1/2-containing plasmids in the absence of DNA replication.

Multiple LBS1/2 function as a cis-partitioning element analogous to FR of EBV oriP. Based on our data in Fig. 2-6, we hypothesized that although replication and partitioning are LANA-dependent, both steps occur independently. To directly test this, we uncoupled replication and partitioning elements by constructing hybrid origins which contain the DS element of EBV oriP and various TR mutants in the background of pPur (Fig. 2-7A) and performed colony formation assays. Hybrid origins should replicate in an EBNA-1-dependent fashion, but require LANA for efficient partitioning. Similar hybrid origins have successfully been utilized to separate *cis*-elements of other DNA tumor viruses (Silla et al. 2005).

Starting with pDS-FR (wt EBV oriP), we replaced the FR element with either one or two TRs (pDS-1TR, pDS-2TR), or two TRs both lacking RE (p2TRΔRE). 293 cells stably expressing EBNA-1 (a kind gift from Dr. Ashok Aiyar) were co-transfected with each hybrid origin and either pPur-LANA or pPur as control. After transfection, equal numbers of cells were seeded,

selected with puromycin, and after two weeks outgrowing colonies were stained and enumerated. The number of outgrowing colonies is a direct measure of the efficiency of long-term maintenance. As a negative control, we tested a replication-defective plasmid, p2TRΔRE, in 293/LANA cells and observed no colonies (Fig. 2-9A). In congruence with previous reports, pDS-FR produced 1516 ± 83 colonies per 50,000 plated cells while pDS did not form colonies (Fig. 2-7C; (Hebner et al. 2003)). In the absence of LANA, pDS-2TR and pDS-1TR gave a low number of colonies, but produced 1483 ± 461 and 645 ± 51 colonies, respectively, when co-transfected with pLANA (Fig. 2-7C), demonstrating that these assays allow us to monitor LANA-dependent maintenance. Importantly, co-transfection of pDS-2TRΔRE with pLANA produced 506 ± 109 colonies, proving that LANA can partition episomal DNA that is replicated in an EBNA1-dependent fashion.

To address whether LANA binding sites alone can confer partitioning, we tested hybrid origins containing either two or three copies of LBS1/2 (pDS-2XLBS1/2 and pDS-3XLBS1/2) (Fig. 2-7A). Both plasmids formed colonies in a LANA-dependent fashion, and increasing the number of LBS1/2 significantly increased the number of colonies produced (Fig. 2-7B and D). These observations indicate that LBS1/2 within the TR functions as a *cis*-partitioning element comparable to the EBV FR element.

We observed that the number of colonies formed from plasmids containing minimal LBS1/2 was greatly reduced compared to full length TR. For instance, while pDS-2TRΔRE generated over 500 colonies, pDS-2XLBS1/2 produced 26 ± 6 colonies, which were strictly dependent on the presence of LANA (Fig. 2-7C and D). One possible explanation for this difference is due to the spacing between the sets of LANA binding sites within the viral genome. Spacing between adjacent EBNA-1 binding sites within EBV FR has been shown to be critically

important for stable oriP plasmid maintenance (Hebner et al. 2003). In both wt p2TR and pDS-2TRΔRE, consecutive sets of LBS1/2 are spaced about 800 bp apart. In contrast, for pDS-2XLBS1/2 the sets of LANA binding sites are directly adjacent to each other, spaced by only 6 bp. Accordingly, we generated pDS-2XLBS1/2+800 by inserting an 808 bp spacer of unrelated DNA in between the two sets of LBS1/2 (Fig. 2-7A); however, no significant differences in the number of colonies were observed (Fig. 2-7E). In summary, these results suggest that while multiple copies of LBS1/2 convey LANA-dependent partitioning, sequences outside of the minimal replicator region may contribute to the efficiency of this process.

Hybrid origins containing LBS1/2 are episomally maintained. To confirm that all hybrid origins which formed colonies were indeed maintained as episomes, we prepared Hirt extracts from puromycin-resistant cell pools and analyzed episomal DNA by Southern blot. Consistently, we detected strong signals for hybrid orgins co-transfected with pLANA, while those transfected with pPur showed no signal (Fig. 2-8 A, B, and C, left panels).

To verify hybrid origins had not undergone genetic rearrangements, Hirt extracts were subjected to *DpnI* digestion and re-transformed into *E. coli.* Restriction enzyme analysis showed that rescued plasmids were the correct size (Fig. 2-8 A, B, and C, right panels). Thus, hybrid origins containing minimal LBS1/2 are maintained as episomes in dividing cells. These data formally prove that LBS1/2 sites within the TR function in a manner analogous to the FR element of EBV.

The number of LANA binding sites within TR affects the outcome of stable plasmid maintenance. KSHV viral genomes contain between 35 and 45 copies of TR (Lagunoff and Ganem 1997). Our results shown in Fig. 2-2D and previous reports indicate that plasmids bearing multiple TRs are more efficient in episome maintenance (Ballestas and Kaye 2001;

Grundhoff and Ganem 2004). To test this in a quantitative manner, we examined long-term maintenance of plasmids containing either two or four copies of TR in 293 cells that stably express LANA (Fig. 2-9B). We observed a two-fold increase in the number of outgrowing colonies with plasmids containing four TRs compared to plasmids containing only two TRs (Fig. 2-9A). Similarly, an increase in TR copies from one to two yielded more colonies (Fig. 2-7B and C). These data show that multiple TRs enhance the efficiency of long-term episome maintenance.

Discussion

In this study, we used a GFP-reporter replicon system to follow the establishment and maintenance of TR-containing plasmids in a LANA-dependent fashion. Additionally, we generated EBV/KSHV hybrid origins to define *cis*-regulatory elements required for LANA-mediated episome partitioning.

LANA significantly increases the retention rate of TR containing plasmids early after transfection. To monitor kinetics of KSHV replicons in the absence of selection, we used nucleofection in combination with FAC-sorting. Both efficient plasmid delivery and rapid GFP expression allowed us to examine retention events during the first few cell divisions in a highly repeatable and quantifiable fashion. TR-containing replicons were retained two to four times more efficiently in the presence of LANA (Fig. 2-2), and such retention was conferred both by active DNA replication and LANA-mediated partitioning (Fig. 2-2 and 2-6). Surprisingly, we found that TR mutants incapable of replication exhibited measurable retention rates in the presence of LANA, suggesting that binding of LANA to TR also stabilizes and/or protects incoming DNA from degradation (Figure 2-6B). Importantly, GFP expression correlated well with the presence of episomal DNA which was monitored by both PCR and Southern blot analysis (Fig. 2-2 and 2-5). The fact that we observed a loss of GFP expression from LANA-

expressing cells can be explained in at least two ways. Either cells maintaining replicons are outgrown by those that do not, or the stabilization and establishment of replicons occurs over several cell divisions. More likely, this is the latter since re-sorting of LANA-expressing cells at two or four days post-FACS results in similar loss kinetics up until approximately day seven when the percentage of GFP expressing cells becomes constant (Fig. 2-2 and Fig. 2-10). Thus, these initial experiments reveal that replication and partitioning of KSHV episomes, although LANA-dependent, occur independently and that events early after *de novo* infection, here recapitulated by transfection, are critical for episome establishment.

Episome maintenance of TR-plasmids can occur in the absence of antibiotic selection. Analysis of clonal populations revealed that a small percentage of cells retain KSHV replicons for several months post-transfection in the absence of antibiotic selection. These cells maintain episomal DNA in the presence of LANA as shown by both Southern blot and PCR analysis (Fig. 2-5). Although the frequency of clones was low (<7%), these experiments suggested that LANA and TR can indeed confer episome maintenance in dividing cells under non-selective conditions. Furthermore, this low establishment frequency mimics that observed following *de novo* infection *in vitro* (Bechtel et al. 2003; An et al. 2006).

Episome maintenance is a long standing paradigm for γ-herpesvirus latency (Liebowitz and Kieff 1993), but lately has been brought into question. Most cells infected *in vitro* with KSHV fail to establish stable latency and lose viral genomes as they proliferate (Lagunoff et al. 2002; Bechtel et al. 2003). Additionally, long-term maintenance of KSHV replicons was reported to require antibiotic selection (Grundhoff and Ganem 2004). In response to these observations, Grundhoff et al. proposed a new model potentially explaining the fact that the majority of cells within KS tumors are infected albeit the lack of an efficient mechanism to

segregate latent genomes. Rather than stable episome maintenance, a minority of cells could spontaneously reactivate to produce progeny virions, thereby continuously replenishing the pool of infected cells (Grundhoff and Ganem 2004). Indeed, early *in situ* hybridization studies showed that a small number of cells within KS tumors express lytic markers (Staskus et al. 1997).

This reasoning, however, leaves out an important genetic argument which stems from the fact that all γ-herpesviruses encode origin-binding proteins and have *cis*-regulatory elements that convey OBP-dependent origin activity. Additionally, stable episomal maintenance is observed in LCLs, BL- and PEL-derived cell lines (Renne et al. 1996; Cesarman 2002b, 2002a; Hammerschmidt and Sugden 2004). LANA knock-down experiments in PEL cells result in decreased KSHV copy numbers (Godfrey et al. 2005), demonstrating that the maintenance of episomal DNA, even in PELs, requires LANA. Likewise, KSHV bacmids, in which LANA expression is genetically disrupted, are no longer maintained in proliferating cells even under selective conditions (Ye et al. 2004).

Based on these observations and our data, we propose that the fate of the incoming viral DNA early after *de novo* infection is dependent upon robust expression of LANA. Interestingly, recent reports on viral gene expression profiling of *de novo* infected endothelial cells show that there is a competition between ORF50 and LANA expression (Krishnan et al., 2004). Moreover, both proteins can regulate their counterpart promoters (Jeong et al. 2004; Lan et al. 2004; Lan et al. 2005).

The presented data here, together with the out-growth of a small number of stably infected KSHV-positive endothelial-derived SLK and HUVEC cells reported by the Ganem lab and us (Bechtel et al. 2003; Grundhoff and Ganem 2004; An et al. 2006), suggest that a crucial event in

the establishment of episome maintenance is the initial retention and stabilization of episomes by LANA. Elegant experiments by the Sudgen and Ganem labs demonstrated that stable episomes are genetically intact, and cells in which episomes are established are also not genetically altered since newly introduced episomes are lost as rapidly from stable cells as naïve cells. Hence, it was proposed that epigenetic modifications *in cis* occur for episome establishment (Leight and Sugden 2001; Grundhoff and Ganem 2004).

In this context, LANA interacts with a variety of chromatin components (Krithivas et al. 2002; Lim et al. 2003a; Sakakibara et al. 2004; Barbera et al. 2006; Ottinger et al. 2006). Additionally, EBV latent genomes are packaged into nucleosomes (Shaw et al. 1979), and it is known that KSHV TR is organized into nucleosomes, at which cell-cycle dependent histone modifications occur for initiation of DNA replication (Stedman et al. 2004). Thus, the chromatin status of an episome is likely an important determinant in viral latency. Interestingly, recent work has shown that LANA can recruit Dnmt3a, a *de novo* methyltransferase, to cellular and viral promoters, resulting in hypermethylation and subsequently, transcriptional silencing (Shamay et al. 2006). We propose that the LANA interaction with DNA methyltransferases also contributes to episome retention early after infection. In this model, LANA would interact with the viral genome and recruit DNA methyltransferases, facilitating epigenetic modifications as an initial step in sequestering and/or associating viral genomes with chromatin. In congruence with this model, we have tested *in vitro* methylated TR-plasmids in maintenance assays and found that they did not yield colonies (Fig. 2-11), suggesting that LANA-mediated recruitment of chromatin associated factors, including DNA methyltransferases, are important initial steps in stabilizing episomes. In summary, we propose that γ-herpesvirus OBPs support episome

establishment within a cell population by reducing the loss of viral genomes from individual dividing cells early after infection, permitting epigenetic stabilization events to occur.

Partitioning elements of KSHV episomes. While sequence requirements for LANA-dependent DNA replication have been characterized (Hu and Renne 2005), *cis*-regulatory elements conferring partitioning are less defined. Both bovine papillomavirus minichromosome maintenance element and EBV FR facilitate chromosome attachment and maintenance as part of hybrid origins containing a polyomavirus replication origin, showing that viral *cis*-elements are interchangeable (Silla et al. 2005). Using EBV-DS/KSHV-TR hybrid origins, we demonstrate that (i) multiple copies of LBS1/2 form an array of OBP binding sites to confer LANA-mediated partitioning and (ii) replication and partitioning occur independently.

We observed that minimal LBS1/2 conferred partitioning, but less efficiently than 2TRΔRE (Fig. 2-7). Similarly, we observed a reduction in the short-term retention of plasmids containing RELBS1/2 compared to wt TR (Fig. 2-6). These data indicate that sequences outside of LBS1/2 enhance episome maintenance. TR contains binding sites for several cellular proteins including PARP1 (Ohsaki et al. 2004) and transcription factors such as Oct-1 and Sp1 (Hu and Renne 2005; Verma et al. 2006) as well as a variety of chromatin-associated proteins (Si et al. 2006). Additionally, a low affinity LANA binding site within TR has been demonstrated *in vitro* (Cotter et al. 2001). Alternatively, the observed differences may be due to a disruption in chromatin architecture surrounding LBS1/2. Indeed, nucleosome positioning and chromatin remodeling are important factors in viral DNA replication (Stedman et al. 2004; Zhou et al. 2005), and likely have a role in episome partitioning/tethering. In summary, our results suggest that while other TR-binding proteins may not be essential for partitioning, they may enhance episome stability.

Uncoupling replication and partitioning. Our data indicates that replication and partitioning play compensatory roles in retention of viral episomes early after infection. Two lines of evidence support this observation. First, plasmids containing either RELBS1/2 (replicating) or 3XLBS1/2 (non-replicating) exhibit similar retention kinetics (Fig. 2-6). Thus, increasing the number of LBS1/2 from one to three somewhat compensates for the defect in replication, resulting in a comparable retention rate to a replication-competent plasmid. Second, DS-plasmids with a single TR show the same maintenance efficiency as pDS-2TRΔRE, despite the twice as many LANA binding sites present within pDS-2TRΔRE (Fig. 2-7). These data suggest that transfected plasmids can be stabilized/retained either by replication or by LANA-dependent chromatin association prior to the cell entering S-phase.

Interestingly, within the EBV oriP, 3 copies of DS can replace FR in maintenance (Wysokenski and Yates 1989), suggesting that the mere presence of multiple OBP binding sites in an appropriate conformation conveys EBNA1-dependent tethering. While the number of EBNA-1 binding sites within FR does not affect DNA synthesis, at least four EBNA-1 sites spaced 14 bp apart are required for efficient oriP maintenance (Hebner et al. 2003). For KSHV, plasmids bearing a single TR replicate with the same efficiency as those containing two TR as shown by short-term replication assays (Hu et al. 2002). In contrast, for long-term maintenance, the number of TRs, or more specifically the number of LBS1/2, directly affects the outcome of plasmid maintenance: two TRs are twice as efficient as one TR, and four TRs are twice as efficient as two TRs (Fig. 2-7 and 2-9). Since LANA oligomerizes when bound to LBS1/2 via its C-terminal DBD (Schwam et al. 2000; Garber et al. 2002; Komatsu et al. 2004) and EBNA-1 dimerization is required for binding to its cognate sequences (Bochkarev et al. 1996), the requirement of multiple OBP binding sites for efficient maintenance may be due in part to the

higher order structure which γ-herpesvirus OBPs form as they interact simultaneously with the viral episome via protein/DNA interactions and host chromatin via protein/protein interactions.

Chromosome association plays important roles in both the replication and tethering functions of EBNA-1 (Hung et al. 2001; Sears et al. 2003) and LANA. A region within amino acid residues 5-22 of the LANA N-terminus (CBS) is required for episome maintenance, interacts directly with core histones H2A and H2B, and can be substituted with histone H1 for maintenance of artificial replicons (Piolot et al. 2001; Shinohara et al. 2002; Barbera et al. 2006). The LANA C-terminal DBD supports DNA replication at about 20% of wt levels (Hu et al. 2002), and residues within the N-terminal CBS contribute to replication activity (Barbera et al. 2004). In congruence, we have observed that replicons expressing only the LANA C-terminus exhibit low retention rates, while addition of the N-terminus partly rescues retention (Fig. 2-12), indicating that LANA-mediated tethering of KSHV replicons early after transfection brings DNA into a nuclear context where it is stabilized and can be efficiently replicated once the cell enters S-phase. Importantly, LANA has been shown to overcome G1 cell cycle arrest (An et al. 2005) and cause nuclear accumulation of β-catenin (Fujimuro et al. 2003), subsequently promoting S phase entry. A fine mapping of TR sequences and examination of potential cellular proteins which may further support these early events is currently ongoing.

In summary, the dogma of γ-herpesvirus episome maintenance has shifted away from a simple picture in which episomes are segregated with absolute efficiency as is observed in LCLs or PELs. However, the data presented here clearly demonstrate that a mechanism exists which confers maintenance of KSHV episomes and that this multi-step process is LANA-dependent. Early on, various LANA activities may contribute to episome establishment by soliciting chromatin remodeling factors and/or facilitating epigenetic modifications of viral DNA. We like

to suggest that the inefficiencies of episome maintenance observed in tissue culture are due in part to experimental parameters utilized. For example, the dramatic reduction of transfected DNA in our model system allowed us for the first time to measure LANA-dependent retention rates of TR-plasmids. Finally, we speculate that episome establishment may be more efficient *in vivo,* compared to fast growing, transformed cells in tissue culture, due to the impact of LANA on cell signaling processes directly related to cell cycle control and S-phase induction, which can influence the establishment of latency. Therefore, combining our experimental system with the use of primary cells should increase our understanding of these important γ-herpesvirus specific processes.

Materials And Methods

Plasmids. pGFP was constructed by inserting a green-fluorescent protein (GFP) cassette from pHPT-GFP (kindly provided by Dr. Stanton Gerson, Case Western Reserve University) into pCRII (Invitrogen). GFP expression is driven by the EF1α promotor which augments strong expression over long periods of time without being translationally silenced (Salmon et al., 2000). p2TR-GFP contains two copies of TR in tandem (described in (Hu et al. 2002)) while p1TR-GFP contains one 801 bp TR at *NotI*. p2TRΔ512-556 was derived from pTRΔ512-556 (described in (Hu and Renne 2005)). Expression of LANA, a 1003 aa full-length variant (Garber et al. 2002), is driven by a CMV promoter. Plasmids containing RELBS1/2 or two or three sets of LBS1/2 were constructed from oligonucleotides (Integrated DNA Technologies, inc.). Puromycin-containing plasmids are based on pPur (Invitrogen). pPur-DS-FR and pPur-DS were gifts from Dr. Ashok Aiyar. TRs or derivatives were inserted at the *PvuII* site of pPur or pPur-DS. All constructs were confirmed by restriction enzyme digestion and/or sequencing and are illustrated in Figures 2-1 and 2-6.

Cell lines and transfections. BJAB, an EBV/KSHV-negative Burkitt's lymphoma B-cell line, and BJAB/TetOn/ORF73 previously described (An et al., 2005) were maintained in RPMI 1640 supplemented with 10% FBS and 5% penicillin/streptomycin. For plasmid retention assays, cells were kept in the log phase of growth (10^5 to 8 x 10^5 cells/ml) at all times. Cell counts were determined by trypan blue exclusion. 72 hrs prior to transfection, BJAB-TetOn-ORF73 were induced to express LANA by the addition of 1 μg/ml doxycycline. BJAB cells were transfected either by traditional electroporation methods in Opti-MEM reduced serum media (Invitrogen) using 15 μg of plasmid DNA, 950 μF and 250V (BioRad Genepulser) or by nucleofection using 0.04 fmoles of plasmid DNA per 5 x 10^6 cells, solution T, program O-17 as per manufacturer's instructions (amaxa, inc.). For colony formation assays, 293, 293/LANA, and 293/EBNA-1 cells were grown in supplemented DMEM and transfected using Effectene (QIAGEN, inc.) as per manufacturer's protocol. 48 hrs post-transfection, cells were plated and 1 μg/mL puromycin (Calbiochem) was added.

Immunoblotting. Whole cell lysates were separated on 8% SDS-PAGE and transferred to Immobilon-P membranes (Millipore). Polyclonal rabbit anti-LANA (An et al. 2005), anti-tubulin (Oncogene Research, CA), or mouse anti-actin (Santa Cruz Biotechnology, inc.) antibodies were used to detect proteins. Blots were developed with peroxidase-conjugated antibodies and enhanced chemiluminescent substrate (Pierce).

FAC-sorting and flow cytometry analysis. To obtain clonal populations, cells were sorted into 96-well plates at 3 cells per well 48 hrs post-transfection (Elite ESP, Beckman Coulter). Photomicrographs of GFP positive cells were taken with an inverted fluorescent microscope (Nikon). For short-term maintenance assays, cells were batch-sorted at 18-22 hrs post-transfection, achieving >95-99% GFP positive cell populations (FACS-Diva, Becton

Dickinson), and resuspended in complete media at equal cell densities. To measure GFP expression, cell aliquots were fixed in 2% paraformaldehyde in phosphate-buffered saline (PBS) at selected time points and stored at 4ºC until time of analysis. GFP percentages are based on gated viable cells using CellQuest software and always compared to a BJAB negative control (FACS-Calibur, Becton Dickinson). Episome loss follows first-order exponential decay, defined by the equation $N(t)=N_0e^{-kt}$, where t is the number of cell generations and k is the rate of plasmid loss defined as the percent of cells losing plasmids per cell generation as measured by GFP expression. Since cells were FAC-sorted at the beginning of each experiment, $N_0 = 100\%$. This equation model is used to calculate k values at 5 days post-transfection shown in Table 1-1.

PCR and Southern hybridization. Episomal plasmid DNA was prepared from cells using either the method of Hirt (Hirt 1967) as described previously (Garber et al. 2002) or a modified Hirt extraction method as described (Arad 1998). Hirt extracts were resuspended in 50 µl of distilled H2O containing RNase A or 50 µl of 10mM Tris-EDTA, pH 8.0 for the modified protocol. PCR amplification was performed using primers specific for the GFP gene, fwd 5'-AGATCCGCCACAACATCGAG-3'; rev 5'-CCATGCCGAGAGTGATCC-3' and products visualized on 1.5% agarose gels. For Southern blot analysis, extracted DNA was loaded directly into wells of 0.8% agarose gels and transferred to Immobilon-Ny+ membranes (Millipore) following electrophoresis. Radioactive probe was prepared by random-prime labeling plasmid DNA (Amersham Biosciences) with [^{32}P]dCTP and purifying with quick-spin columns (Roche). Hybridization and washing was performed as described (Hu et al. 2002). Following hybridization, southern blots were exposed to a phosphor screen and signals captured on phosphoimager using ImageQuant software (Molecular Dynamics).

DpnI PCR-based replication assays. 10% of Hirt extracted DNA was digested with 70 units *DpnI* (New England Biolabs, MA) at 37ºC for >72 hrs to eliminate bacterially methylated input DNA. Plasmid DNA which has undergone at least 2 rounds of DNA synthesis in eukaryotic cells is resistant to *DpnI* cleavage. As control for input, equivalent amounts of extract were subjected to the same buffer conditions in the absence of enzyme. To detect *DpnI* resistant species, digests were heat-inactivated and an aliquot of each sample was subjected to 27 to 30 PCR amplification cycles using GFP-specific primers.

Colony formation assays. Cells were co-transfected with 0.7 μg replicon DNA and 0.3 μg pLANA or pPur. 24 hrs post-transfection, cells were washed twice in PBS, trypsinized, and plated at equal densities (2 x 10^4, 5x10^4, 1x10^5, or 2x10^5 cells) in 10cm plates. Cells were grown in the presence of puromycin for over two weeks. To visualize colonies, cells were fixed in 80% methanol and stained in 30% methanol in PBS containing 0.1% crystal violet.

Plasmid rescue assay. *DpnI* digested Hirt-extracted DNA at >15 days post-transfection was transformed into chemically competent DH5α and plated onto ampicillin LB plates. Bacterial colonies were analyzed by *NcoI* restriction enzyme digestion following plasmid purification.

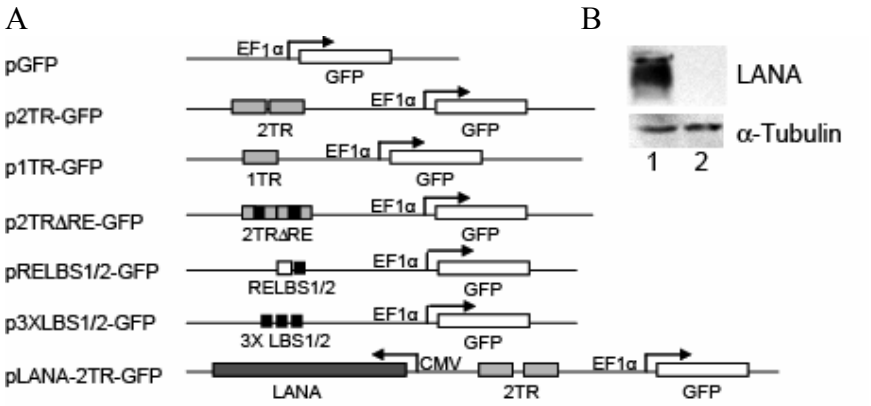

Figure 2-1. KSHV replicons. A. Schematic of plasmid constructs used in retention assays. GFP is inserted into pCRII (Invitrogen) at XhoI to XbaI; TRs or derivatives are at NotI; LANA is at EcoRV. Plasmid p2TRΔRE-GFP was derived from pTRΔ512-556 (described in (Hu and Renne 2005)) and contains two copies of TR in tandem, each lacking the G+C rich region encompassing RE directly adjacent to LBS1/2. pRELBS1/2-GFP contains 71 bp of the minimal replicator inserted HindIII to NotI, while p3XLBS1/2-GFP contains three sets of minimal LBS1/2 at NotI in tandem. B. LANA expression at 24 hrs in 293 cells transfected with 1 μg pLANA-2TR-GFP (lane 1) or p2TR-GFP control (lane 2). □-tubulin was used as loading control.

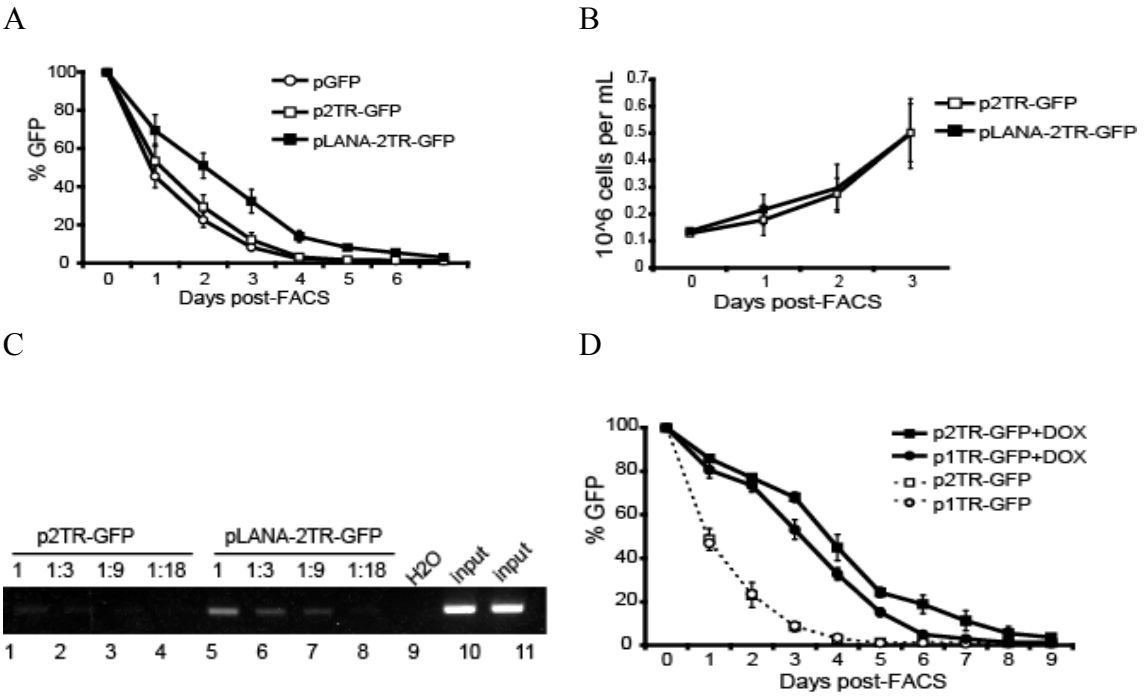

Figure 2-2. LANA significantly increases the retention of TR-plasmids. A. Short-term retention of KSHV replicons. BJAB cells were transfected with 5,000 copies per cell plasmid DNA using nucleofection (amaxa, inc.). 20 hrs post-transfection, cells were FAC-sorted and GFP expression monitored by flow cytometry. Curves represent the average of 4 transfections. By Student's t-test, $p<0.01$ for pLANA-2TR-GFP compared to p2TR-GFP or pGFP. B. Growth of FAC-sorted cells was monitored by trypan-blue exclusion. C. LANA expression in cis facilitates replication of KSHV replicons. Hirt-extracts (day 4) were prepared from cells transfected with p2TR-GFP (lanes 1-4 and 10) or pLANA-2TR-GFP (lanes 5-8 and 11). DpnI resistant or undigested DNA (input lanes) was PCR amplified using GFP-specific primers (product of 203 bp). Digests were diluted 1:3, 1:9, or 1:18 prior to PCR. D. LANA in trans enhances replicon retention. BJAB or doxycyline-induced BJAB/TetOn/ ORF73 (+Dox) were transfected as in (A) and monitored post-FACS. Shown is the average of 2 transfections. By Student's t-test, $p<0.01$ for BJAB versus BJAB/TetOn/ORF73. E. LANA is required for retention of GFP expressing replicons. GFP-positive BJAB/TetOn/ORF73 cells transfected in duplicate with p2TR-GFP were grown in the presence (+Dox) or absence (No Dox) of doxycycline following FACS. By Student's t-test, $p<0.01$ for +Dox compared to No Dox (days 5 to 8). F. Western blot analysis of LANA expression in BJAB/TetOn/ORF73 cells following release from dox-induction. Negative control = BJAB lysate; actin is shown as loading control. G. Long-term replication of KSHV replicons. BJAB or induced BJAB/TetOn/ORF73 (Dox) were transfected with 50,000 copies per cell p2TR-GFP. At day 10 post-transfection, GFP positive LANA-expressing cells were FAC-sorted. Hirt-extracted DNA was prepared at days 4, 10, 20, and 26 days post-transfection. Equal amounts of DpnI resistant DNA and input DNA corresponding to 2000 cell equivalents were PCR-amplified using GFP-specific primers.

E

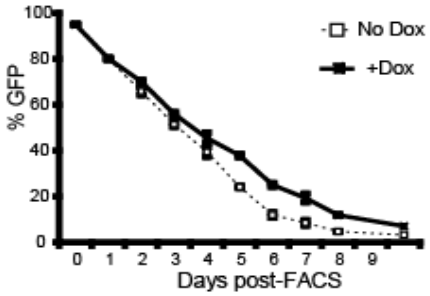

F

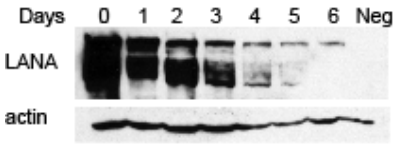

G

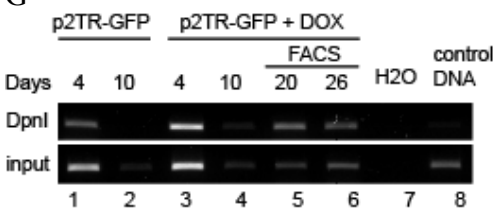

Figure 2-2 continued

A

B

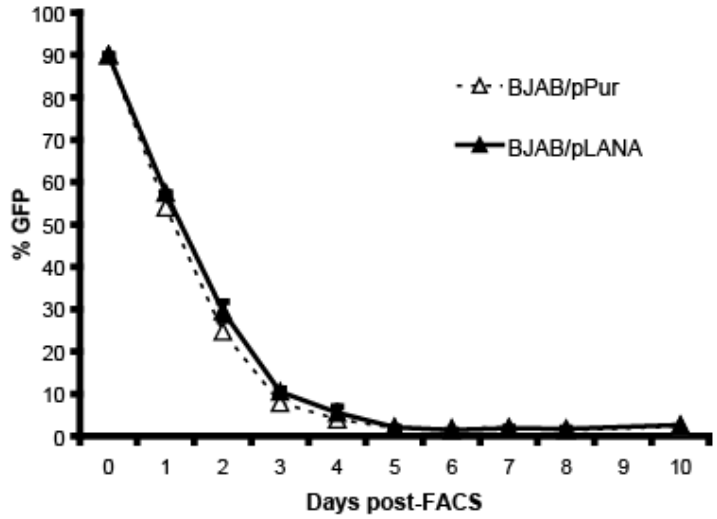

Figure 2-3. LANA does not affect the retention of plasmids containing EBV replication origins. A. Schematic of pDS-GFP. B. BJAB or BJAB/pLANA cells were transfected with 5,000 copies per cell plasmid DNA and GFP expression was monitored post-FACS. Shown is the average of two independent transfections.

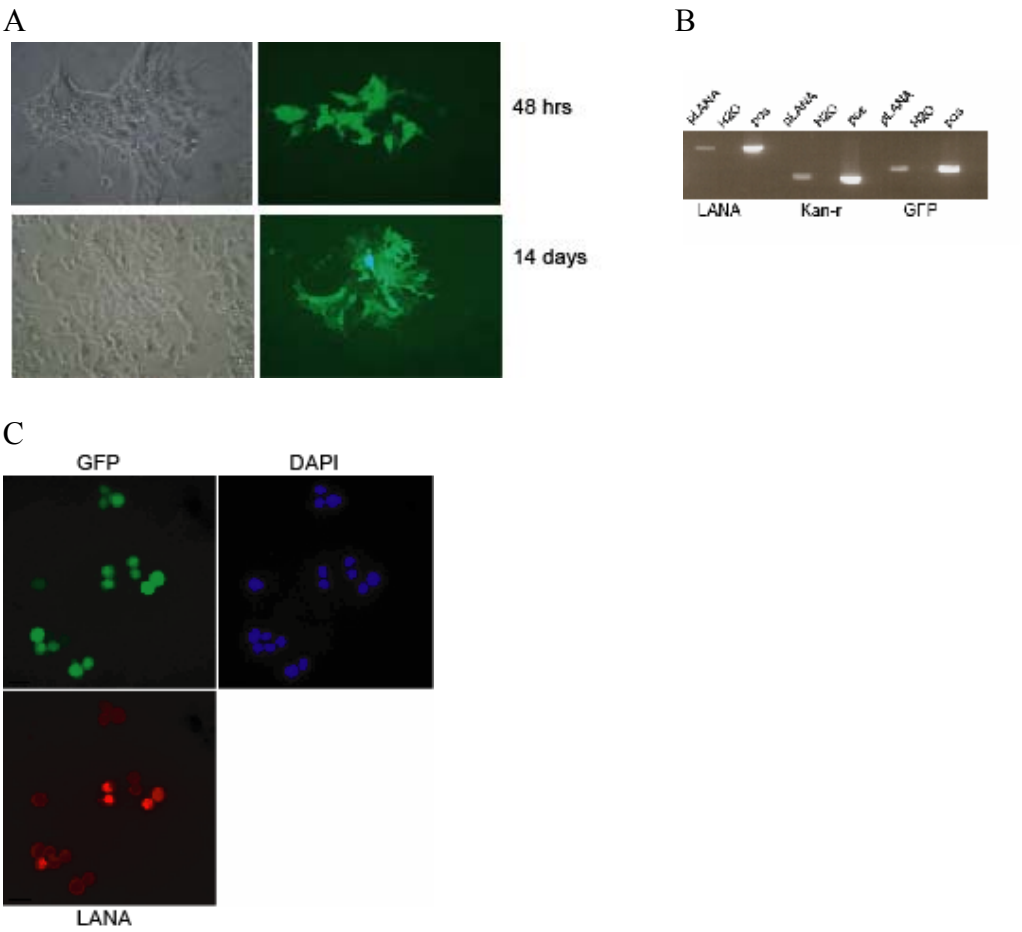

Figure 2-4. KSHV replicons are maintained without antibiotic selection. A. 293/LANA cells were transfected with p2TR-GFP using Effectene (QIAGEN) and maintained in non-selective for 14 days. Shown are bright phase and GFP fluorescent photomicrographs at 48 hrs and 14 days post-transfection. B. BJAB cells were transfected with 5,000 copies per cell pLANA-2TR-GFP, FAC-sorted at 20 hrs, and cultured for seven days. At day seven, cells were re-sorted and maintained in non-selective media for over four weeks. Hirt extracted episomal DNA was digested with DpnI and analyzed by PCR using primers to three different regions of the plasmid. 25 pg pLANA-2TR-GFP is shown as positive control. C. LANA expression was evaluated by immunofluorescent staining. GFP positive BJAB cells (green) were fixed and stained with a polyclonal antibody to LANA; a secondary Texas-red conjugated antibody was used to visualize the protein (red). Nuclear DAPI staining is shown in blue.

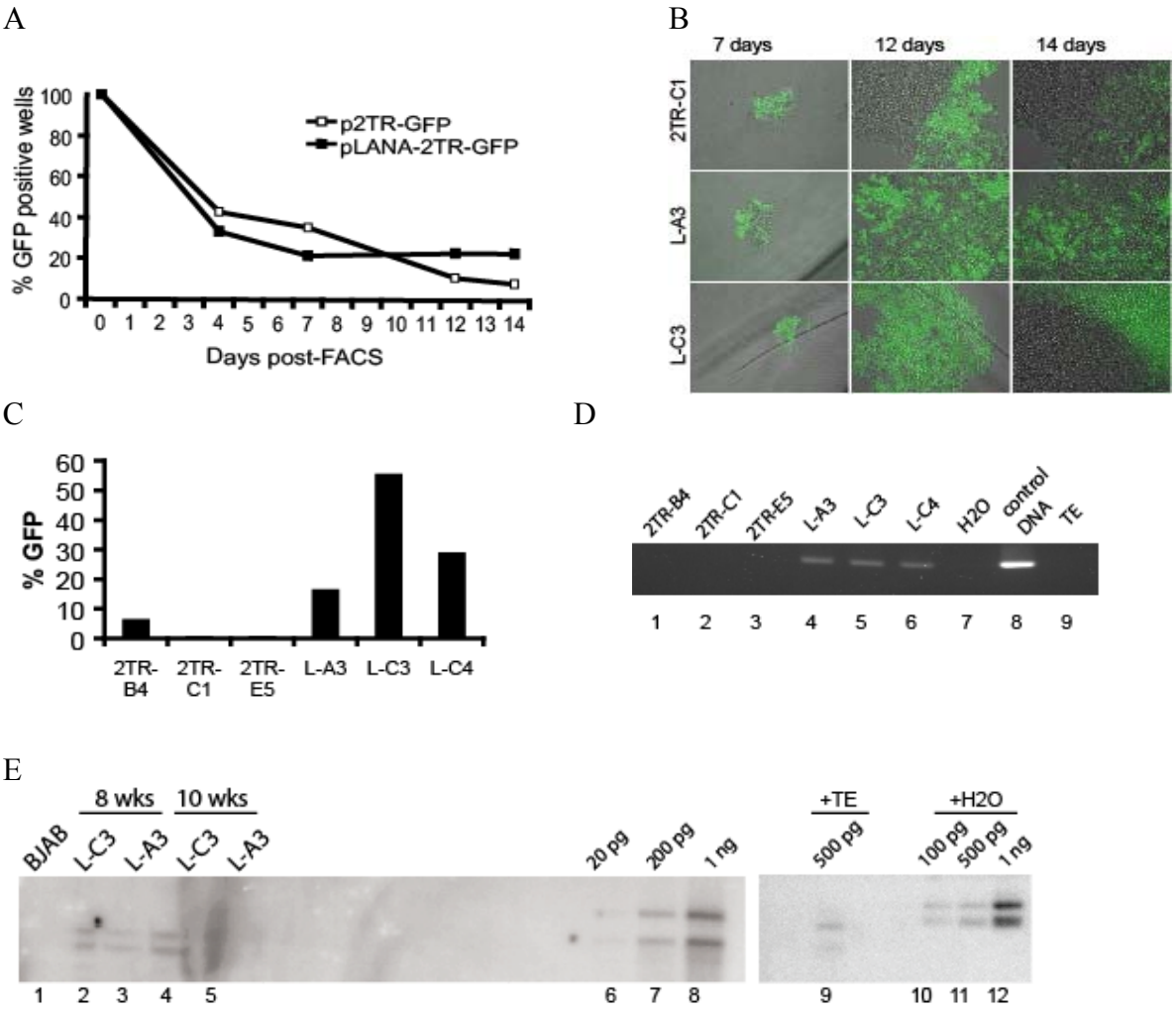

Figure 2-5. Subpopulations maintain replicons as episomes long-term in the absence of selection. A. BJAB cells were FAC-sorted into 96-well plates 48 hrs post-transfection and scored for GFP expression by fluorescent microscopy. The percent of GFP positive wells was determined from the ratio of GFP positive wells to wells containing viable cells. B. Photomicrographs of 3 clones from 96-well plates post-FACS. C. GFP expression by flow cytometry for p2TR-GFP (2TR) and pLANA-2TR-GFP (L) subpopulations at >2.5 months. D. PCR analysis of Hirt extracted DNA at 2.5 months post-FACS. 50 pg of p2TR-GFP plasmid DNA was used as positive control (lane 8); TE = Tris-EDTA (lane 9). E. Southern blot analysis of 2 pLANA-2TR-GFP populations at 8 wks (lanes 2-3) and 10 wks (lanes 4-5) post-transfection. Episomal DNA prepared using a modified Hirt-extraction protocol from 2 x 106 cells was detected using p2TR-GFP as a probe. Episomal DNA is observed in two forms: a top band corresponding to open circular and a lower band corresponding to covalently closed circular. Indicated amounts of pLANA-2TR-GFP control DNA are on right as standards for quantification (lanes 6-8). At far right, control DNA was loaded in TE Hirt resuspension buffer or water to show differences in migration due to buffer conditions (lanes 9-12).

A

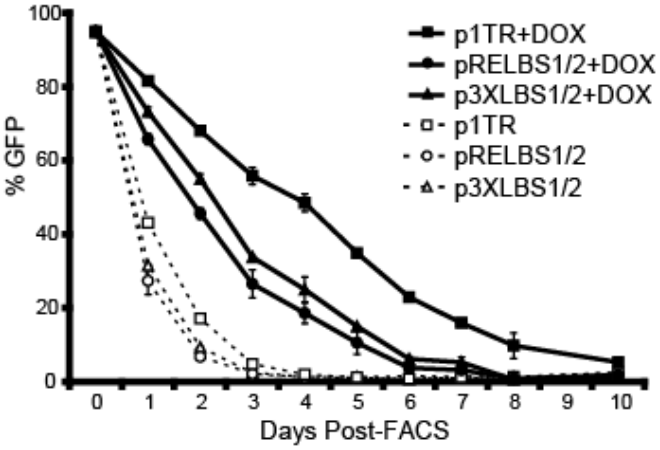

B

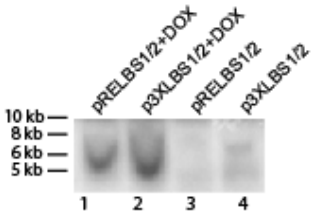

C

Loss Rate	
9.7%	p1TR+DOX
23.7%	pRELBS1/2+DOX
20.2%	p3XLBS1/2+DOX
57.9%	p1TR
58.4%	pRELBS1/2
59.6%	p3XLBS1/2

Figure 2-6. Replication-deficient plasmids exhibit moderate retention in the presence of LANA. A. BJAB (dashed lines) or LANA-positive BJAB/TetOn/ORF73 (+Dox) cells (solid lines) were transfected with equimolar amounts of plasmid DNA corresponding to 5,000 copies per cell, FAC-sorted at 20 hrs post-transfection, and monitored by flow cytometry. Transfections were done in duplicate. B. Replication-deficient plasmids are retained as episomes in LANA-expressing cells. Hirt-extracted DNA at four days post-transfection was analyzed by Southern blot. Undigested episomal DNA was detected using pGFP as probe. C. Loss rates for each plasmid were calculated between one and four days post-FACS. According to Student's t-test, $p<0.01$ for LANA-positive versus BJAB cells and $p<0.01$ for p1TR compared to pRELBS1/2 and p3XLBS1/2.

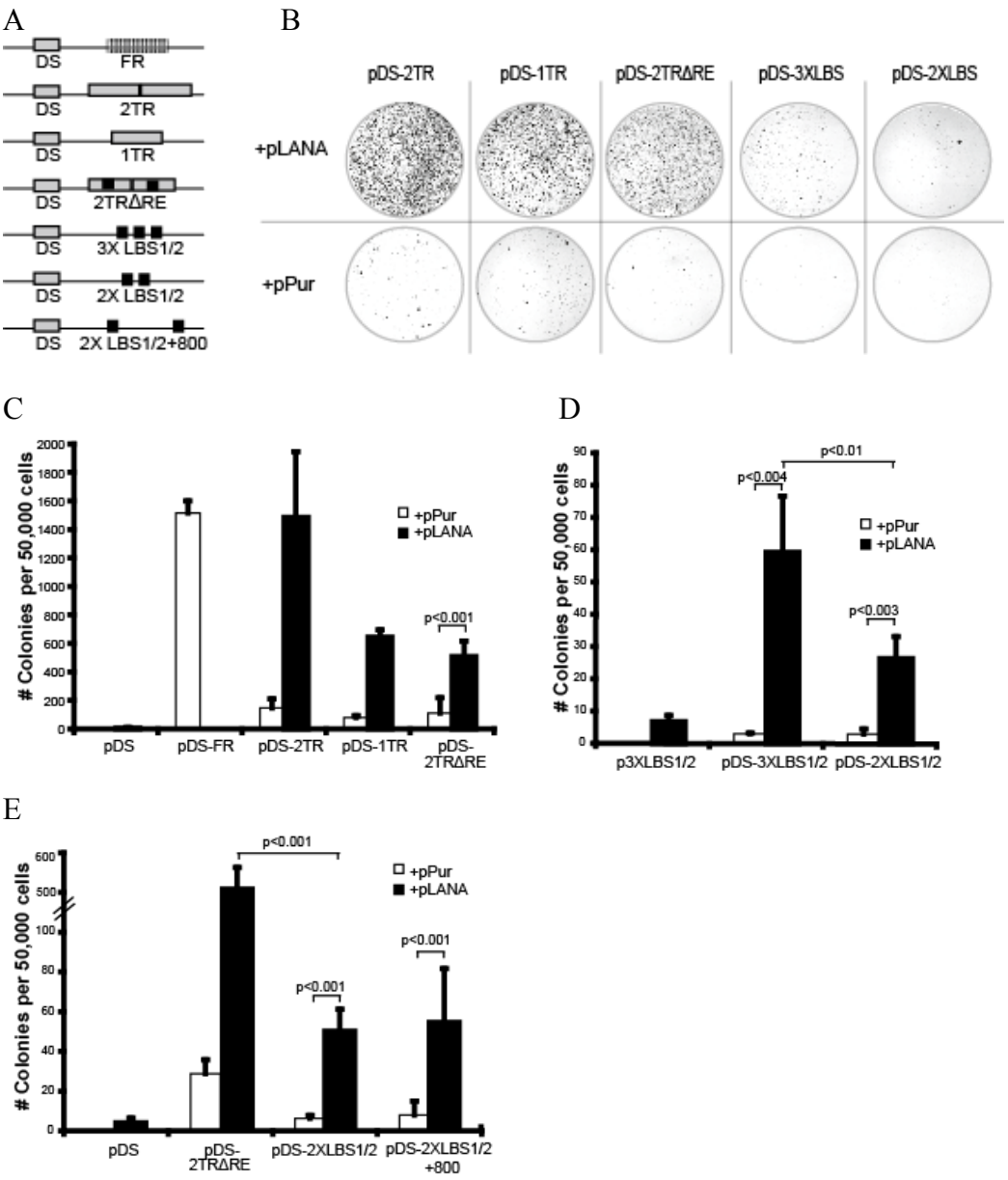

Figure 2-7. LBS1/2 functions as a cis-partitioning element. A. Schematic representation of hybrid origin constructs used in colony formation assays. Plasmids contain pPur as the vector backbone and EBV DS as a replication origin. EBV FR is replaced with various TRs or TR mutants, all oriented in tandem. B. Hybrid origins were co-transfected with a puromycin plasmid expressing full-length LANA (pLANA) or empty vector (pPur) into 293/EBNA1 cells. At 24 hrs post-transfection, cells were washed in PBS, trypsinized, and plated at equal densities. Puromycin selection was applied 48 hrs post-transfection. Crystal violet staining was performed two weeks following selection and colonies are shown for indicated plasmids. C-E. Enumeration of puromycin-resistant colonies. Graphs represent the average of at least four plates from two independent transfections. Solid bars indicate co-transfection with pLANA; open bars indicate co-transfection with pPur. Statistical p values are reported according to Student's t test.

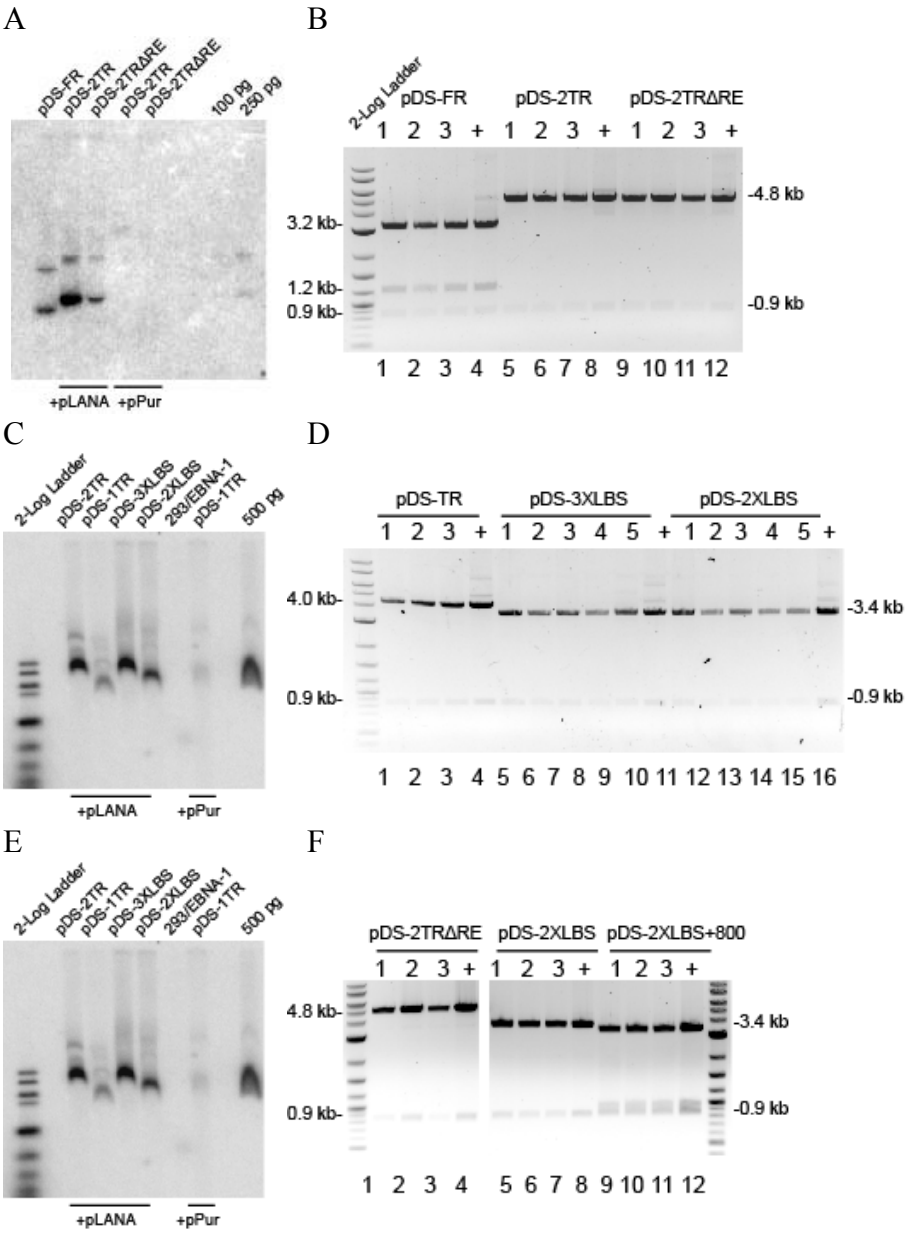

Figure 2-8. Hybrid origins are maintained as episomes. A, C, E. Southern blot analysis of Hirt-extracted DNA from 293/EBNA1 cell pools transfected with hybrid orgins 15 to 17 days following puromycin selection. Prior to Hirt-extraction, cells were washed twice in PBS. Undigested episomal DNA is detected using pPurTR-TRΔRE as probe. B, D, F. Plasmid rescue assay. 10% of each Hirt-extract was digested >48 hrs with DpnI and retransformed into E. coli. Hybrid origins co-transfected with pLANA yielded a significant number of bacterial colonies (~300 to 600) while plasmids co-transfected with pPur yielded less than five or none. Three to five individual colonies for each hybrid origin co-transfected with pLANA were selected for restriction enzyme analysis. DNA is digested with NcoI and expected fragment sizes are indicated; (+) indicates 250 ng control plasmid DNA.

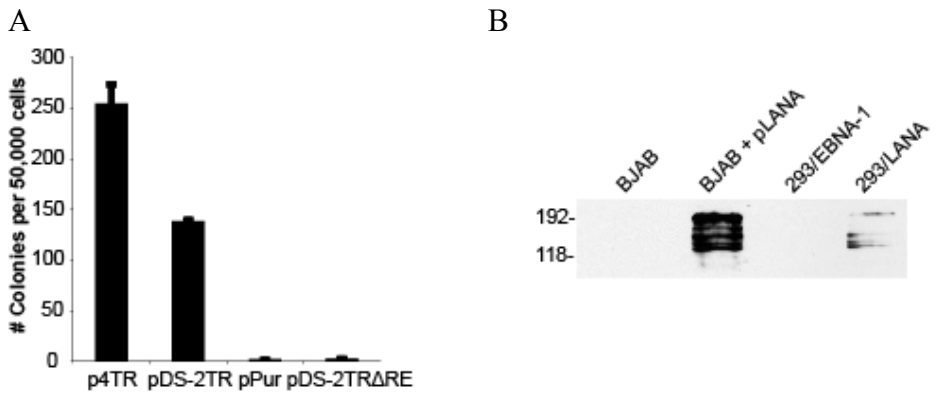

Figure 2-9. Long-term maintenance is more efficient with multiple TRs. A. 293/LANA cells were transfected with plasmids indicated, and colony formation assays were performed as described in Methods and Fig. 5. Puromycin-resistant colonies were quantified following crystal violet staining. Graph represents the average of four plates from two transfections. B. LANA expression by Western blot analysis in BJAB cells transfected with pLANA and 293/LANA cells. BJAB and 293/EBNA1 are shown as negative control. Lysates are from 1 x 105 cells.

A

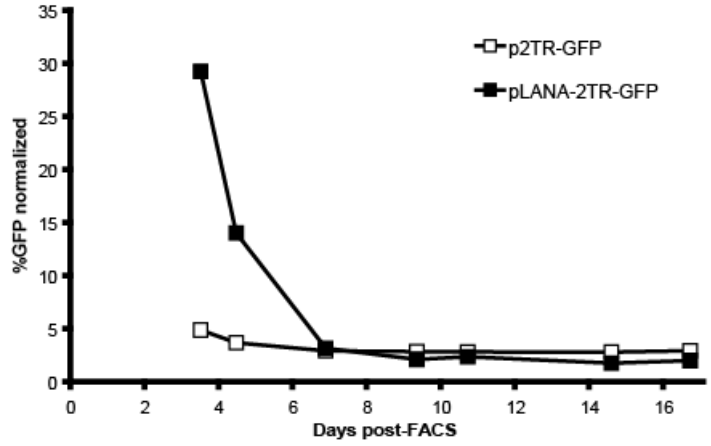

B

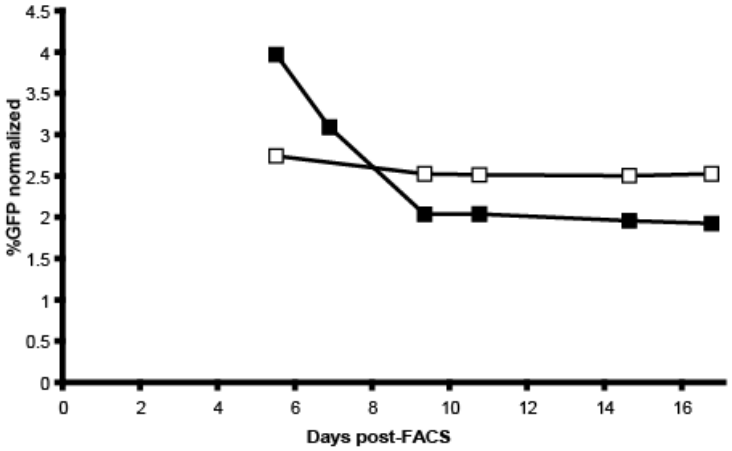

Figure 2-10. Replicons exhibit similar kinetics following re-sorting at two or four days. GFP positive BJAB cells from figure 2A were re-sorted at A. two or B. four days following initial FACS. GFP expression was monitored by flow cytometry. GFP expression is normalized to the percent of GFP positive cells within each population at time of re-sort.

A

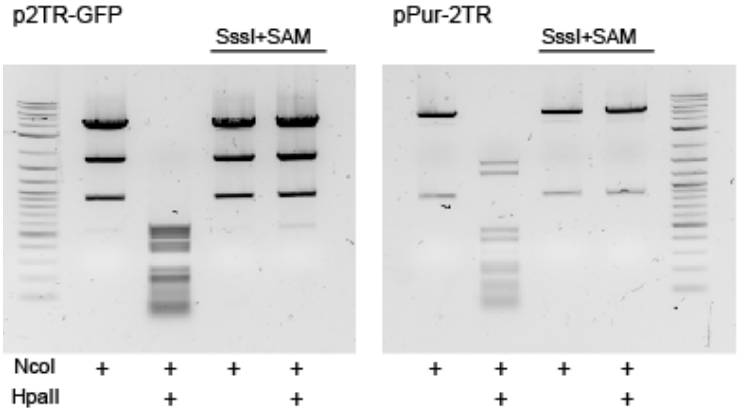

B

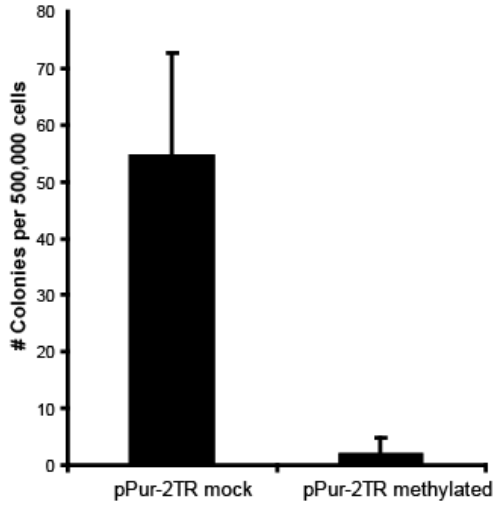

Figure 2-11. In vitro methylated TR-plasmids are not maintained. A. 2.5 □g of p2TR-GFP or pPur-2TR was methylated by SssI methyltransferase in the presence of s-adenosylmethionine (SAM). To check for methylation, 500 ng plasmid DNA was digested overnight with NcoI, which cuts at three sites in p2TR-GFP and two sites in pPur-2TR, and HpaII, which cuts at >60 sites per plasmid and is blocked by CpG methylation. B. 293 cells were transfected with mock-treated or methylated pPur-2TR and used for colony formation assays to measure plasmid maintenance. A parallel set of transfections with mock-treated or methylated p2TR-GFP resulted in a transfection efficiency ~30% for mock and methylated plasmids as determined from GFP expression (not shown). Outgrowing colonies were stained with crystal violet and enumerated. Shown is the number of colonies per 500,000 cells from four independent transfections.

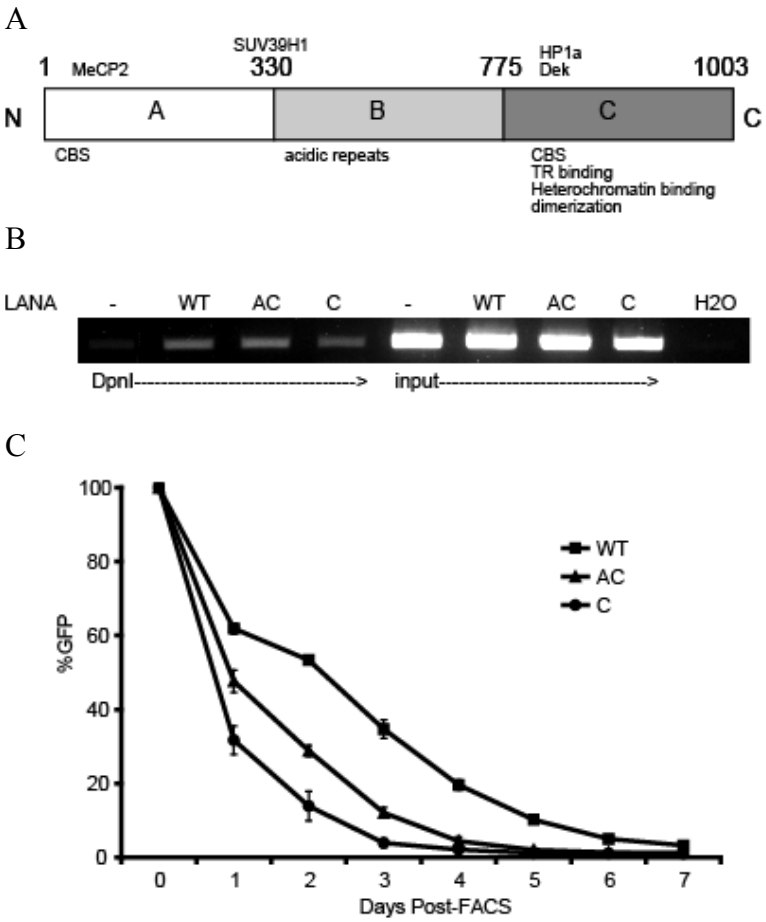

Figure 2-12. LANA mutants exhibit low TR-plasmid retention rates. A. Schematic of the LANA protein (1003 aa) with domains A, B, and C. Listed above are cellular proteins that have been reported to interact with LANA; below are the regions of LANA that bind to viral DNA and mitotic chromosomes. B. Modified short-term replication assay. Hirt extracted DNA from day 4 post-transfection was digested with excess DpnI and subjected PCR amplification. p2TR-GFP was used as negative control (neg). Equivalent amounts of template were used for DpnI and input PCR. C. GFP expression in FAC-sorted BJAB cells expressing LANA (WT), LANA-AC (AC), or LANA-C (C) in cis. Curves represent the average of two independent experiments with error bars. Transfections were performed with separate plasmid preparations. According to Student's t-test, $p<0.01$ for WT vs AC or C.

Table 2-1. Average loss rates of KSHV replicons

Plasmid	k (% rate loss/generation) ± SDa	n
pGFP	27.8 ± 0.3	4
p1TR-GFP	26.6 ± 0.2	2
p2TR-GFP	25.6 ± 0.3	6
pLANA-2TR-GFP	13.6 ± 0.2	6
p1TR-GFP+Dox	8.2 ± 0.2	4
p2TR-GFP+Dox	5.9 ± 0.2	4

[a] Average loss rates per cell generation (k) with standard deviations (SD) are calculated from days zero to four post-FACS.

CHAPTER 3
KAPOSI'S SARCOMA-ASSOCIATED HERPESVIRUS ENCODES AN ORTHOLOG OF THE MIR-155 MicroRNA FAMILY

Abstract

KSHV infection is linked to several malignancies, including primary effusion lymphoma (PEL). To date, 60 γ-herpesvirus-encoded microRNAs have been identified. KSHV encodes 12 miRNAs, but only a few regulatory targets are known. We found that KSHV-miR-K12-11 shares 100% seed-sequence homology with hsa-miR-155, a miRNA frequently found up-regulated in lymphomas and solid tumors. Based on this seed-sequence homology, we hypothesized that both miRNAs might regulate a common set of target genes. Examination of five PEL lines showed that PELs do not express miR-155, but do express high levels of miR-K12-11. Bioinformatics tools predicted >1158 potential target genes for both miRNAs, including the transcriptional repressor BACH-1. Ectopic expression of either miR-155 or miR-K12-11 inhibited a BACH-1 3'UTR containing reporter, further implicating BACH-1 as a target. To experimentally investigate additional targets, we generated miRNA-expressing cell lines and performed genome-wide gene expression profiling. In response to miR-K12-11, 264 genes were down-regulated and for miR-155, 109 genes were decreased. 64 genes were commonly down-regulated and of these, 18 3'UTRs contained seed binding sites. MiRNA targeting was confirmed for select genes by luciferase reporter assays. Thus, based on *in silico* predictions, expression profiling data, and reporter assays, miR-K12-11 and miR-155 can regulate overlapping cellular targets. Together, these findings indicate that KSHV miR-K12-11 is an ortholog of miR-155.

Introduction

MicroRNAs (miRNAs) are 19 to 23 nucleotide (nt) non-coding RNAs that post-transcriptionally regulate gene expression through translational inhibition and/or mRNA

degradation. In the nucleus, precursor miRNAs are processed by Drosha and DGCR8, exported into the cytoplasm via Exportin 5, and subsequently processed by Dicer (Ambros 2004; Bartel 2004). One strand of the cytoplasmic miRNA duplex is incorporated into the RNA-induced silencing complex (RISC), which guides binding of mature miRNAs to 3'UTRs of target messenger RNAs (mRNAs) (Ambros 2004; Bartel 2004). Originally identified in *C. elegans* as important regulators of development, it is now known that all metazoan organisms encode miRNAs (Lagos-Quintana et al. 2001; Ambros 2004; Bartel 2004). Recently, miRNAs have been identified in several DNA viruses including polyomaviruses and herpesviruses (Sullivan and Ganem 2005; Cullen 2006; Samols 2006). Epstein-Barr virus (EBV) encodes at least 17 miRNAs (Pfeffer et al. 2004; Cai et al. 2006b; Grundhoff et al. 2006) while 12 miRNA genes have been reported for Kaposi's sarcoma-associated herpesvirus (KSHV) (Cai et al. 2005; Pfeffer et al. 2005; Samols et al. 2005), a virus linked to Kaposi's sarcoma and lymphoproliferative disorders (Chang et al. 1994; Cesarman 2002b). Unlike metazoan miRNAs which are often highly conserved between species (Bartel 2004), viral miRNAs are much less conserved and lack sequence homology amongst themselves as well as their host counterparts. Thus the question remains whether herpesvirus-encoded miRNAs regulate host cellular and/or viral gene expression.

Investigating miRNA targets is complicated by the fact that miRNAs require limited complementarity for 3'UTR binding (Lewis et al. 2003; Bartel 2004; Brennecke et al. 2005). Consequently, a single miRNA can modulate expression of multiple genes. Analysis of the entire human transcriptome *in silico* in combination with experimental verification has revealed that binding of a miRNA to a specific 3'UTR is critically dependent on 5' nucleotides 2 to 7 of the

mature miRNA. This sequence, termed the "seed", classifies miRNAs into families (Lewis et al. 2005).

We aligned seed sequences of human herpesvirus miRNAs with the human microRNA database. Here, we report on a KSHV-encoded miRNA which has an identical seed sequence to that of hsa-miR-155, and provide evidence that both miRNAs can regulate a common set of cellular genes.

Results

DNA tumor virus-encoded miRNAs share seed sequence homology with human oncogenic miRNAs. Herpesvirus-encoded miRNAs lack strong sequence homology to metazoan miRNAs which are highly conserved between species. We therefore asked whether seed sequences, demonstrated to be critically important in mRNA target recognition, exhibit conservation. We aligned all known KSHV, EBV, herpes simplex virus (HSV-1), and human cytomegalovirus (HCMV) miRNAs against the miRNA registry containing 474 human miRNA sequences (microrna.sanger.ac.uk). 5' nts 2 to 7 of both cloned (Pfeffer et al. 2004; Cai et al. 2005; Pfeffer et al. 2005; Samols et al. 2005; Cai et al. 2006b; Gupta et al. 2006) and predicted (Grundhoff et al. 2006) miRNAs were analyzed.

Sequence alignments revealed that at least six viral miRNAs harbored seed sequences homologous to human miRNAs. 5' nt 1-8 of KSHV-miR-K12-11 are 100% identical to hsa-miR-155, while 5' nt 3-10 of miR-K12-6-5p are identical to hsa-miR-15a and miR-16. 5' 2-7 of EBV-BART5 are homologous to hsa-miR-18a/b (Fig. 3-1). Interestingly, both miR-15a and miR-16 are thought to have tumor suppressor activity and induce apoptosis by targeting BCL2 (Cimmino et al. 2005). In contrast, miR-155 and miR-18 are highly expressed in several human malignancies. Human miR-18 is expressed from the miR-17-92 cluster on chromosome 13q31, a region often amplified in B-cell lymphomas, and has been proposed as oncogenic since over-

expression of this cluster accelerates c-myc induced lymphomagenesis in transgenic mice (He et al. 2005; Hwang and Mendell 2006).

MiR-155 is an evolutionarily conserved miRNA, processed in humans from exon 3 of the non-protein-coding *BIC* (B cell integration cluster) RNA (Lagos-Quintana et al. 2002; Tam et al. 2002) (Fig 3-2A). *BIC* was originally identified in chicken B cell lymphomas which developed following infection with avian leukosis virus (ALV) (Tam et al. 1997). Tam et al. was the first to show that a region of the *BIC* RNA, now known to encode the miR-155 hairpin precursor, accelerated c-myc associated lymphomagenesis in chickens (Tam et al. 2002). More recently, both *BIC* and miR-155 has been found highly expressed in several B-cell lymphomas as well as breast, lung, and colon cancers (van den Berg et al. 2003; Iorio et al. 2005; Kluiver et al. 2005; Volinia et al. 2006; Yanaihara et al. 2006). Additionally, transgenic mice over-expressing mmu-miR-155 from a B-cell specific promoter exhibit splenomegaly and lymphopenia at early ages and by 6 months of age, develop high grade B-cell neoplasms (Costinean et al. 2006). Together, these observations strongly suggest that miR-155 is an oncogenic miRNA. In humans, miR-155 expression can be detected in activated B and T cells (Haasch et al. 2002; van den Berg et al. 2003). Most recent reports link miR-155 to B and T lymphocyte development (Rodriguez et al. 2007; Thai et al. 2007). Thus, dysregulation of miR-155 can have important implications in B cell differentiation processes.

Based on the identical seed sequences of miR-155 and miR-K12-11, and the association of KSHV with lymphoproliferative disorders including primary effusion lymphoma (PEL) and multicentric Castleman's disease (Cesarman 2002b), we hypothesized that both miRNAs might regulate a common set of cellular genes thereby contributing to pathogenesis. First, we analyzed *BIC* and miR-155 expression in KSHV latently infected PEL-derived cell lines. Total RNA was

isolated using RNA-Bee (Tel-Test), RNA was reverse-transcribed using random hexamers, and PCR analysis performed using primers indicated (Fig 3-2A and Table 3-1). EBV positive Burkitt's lymphoma cells (Raji) expressed readily detectable levels of *BIC* (Fig. 3-2B). In contrast, all KSHV-positive PEL lines tested did not express *BIC* (Fig. 3-2B), and did not express miR-155 as determined by Northern blot analysis (Fig. 3-2C). However, PEL cells highly express miR-K12-11 as shown by Northern blot analysis (Fig. 3-2C) and previously reported (Cai et al. 2005; Pfeffer et al. 2005; Samols et al. 2005). Hence, miR-K12-11 could hypothetically mimic miR-155 dependent regulation in these B cell lymphomas.

Generation of miR-155 and miR-K11 expression and sensor vectors. Given that miR-155 and miR-K12-11 have identical seed sequences, we hypothesized these miRNAs could target a common set of genes via seed matching. To test this idea, we generated pmiR-155 and pmiR-K12-11 by introducing the region encompassing each primary miRNA into pcDNA3.1/V5/HisA under control of a CMV promoter (Fig. 3-3A). To monitor miRNA expression from these constructs, we generated miRNA-sensor vectors containing two anti-sense complementary binding sites within the 3'UTR of a luciferase reporter (Fig. 3-3B). Co-transfection of each miRNA expression vector with the respective sensor showed a 70%-80% knockdown of luciferase expression (Fig. 3-3C, middle bars). Note that this inhibition reflects a siRNA-like mediated effect since the miRNA and target 3' UTR are 100% complementary, and thus rapidly induce mRNA degradation.

We next tested whether miR-155 could target the miR-K12-11 sensor and vice versa. As shown in Figure 3-3C (right bars), both miRNAs inhibited luciferase expression from both reporters, and as expected, the observed inhibition levels were less, approximately 50%. Importantly, neither miR-155 nor miR-K12-11 had any effect on an unrelated sensor, and an

unrelated miRNA, miR-K12-3-5p, did not affect either the miR-K12-11 or miR-155 sensors (Fig. 3-3D). Hence, the importance of the miRNA seed for 3'UTR targeting is confirmed by the fact that both miR-155 and miR-K12-11 can inhibit luciferase expression from their opposite sensor vectors.

miR-155 and miR-K12-11 can target the BACH-1 3'UTR. To date, miR-155 is reported to target genes associated with hematopoietic stem cell differentiation (Georgantas et al. 2007) and can regulate lymphocyte function (Rodriguez et al. 2007; Thai et al. 2007). Additionally, miR-155 targets the angiotensin II type I receptor in fibroblasts (Martin et al. 2006). KSHV miR-K12-11 has no published targets. Using three available target-prediction algorithms (miRanda, PicTar, and TargetScan) (Enright et al. 2003; John et al. 2004; Krek et al. 2005; Lewis et al. 2005), we identified BACH-1 (Btb and CNC homolog 1) as a candidate target for both miR-155 and miR-K12-11 as it contains four perfect seed match sites within its 3,315 nt long 3'UTR (Fig. 3-4A). BACH-1 is a transcriptional regulator which binds NF-E2 sites and coordinates transcription with small Maf (musculoaponeurotic fibrosarcoma oncogene homolog) proteins (Igarashi and Sun 2006).

To examine whether BACH-1 can be regulated by miR-155 and/or miR-K12-11, we co-transfected 293 cells with pGL3-BACH1, containing nt 658-2495 of the BACH-1 3' UTR downstream of luciferase, and increasing amounts of miRNA expression vectors. This cloned region of BACH-1 3'UTR encompasses all four predicted miRNA binding sites (Fig. 3-4A). We observed a dose-dependent knockdown of luciferase expression in response to both miR-155 and miR-K12-11, demonstrating that the BACH-1 3'UTR can be targeted by both miRNAs (Fig. 3-4B).

Co-transfection of pGL3-BACH1 with miR-K12-3-5p, which has no predicted BACH1 binding sites, had no effect on reporter, ruling out non-specific effects of ectopic miRNA expression (Fig. 3-4B). We have also performed de-repression assays utilizing miRNA antagomirs. 2'OMe oligoribonucleotides antisense to miRNAs are potent inhibitors of RISC-associated miRNA acitivity (Hutvagner et al. 2004; Meister et al. 2004). Co-transfection of miR-155 or miR-K12-11 expression vectors with the BACH-1 reporter resulted in inhibition as previously shown, while addition of a miRNA-specific antagomir released this inhibition (Fig. 3-4C and 3-4D). These assays further indicate the observed expression differences from the BACH-1 reporter are due to sequence–specific interactions of the miRNA and its target.

miR-155 and miR-K12-11 target BACH-1 predominantly via seed match site two. To confirm that the observed BACH-1 inhibition depends on the presence of miR-155 and miR-K12-11 seed match sites, we performed a detailed mutational analysis of the BACH-1 3'UTR. First, 3'UTR truncation mutants were generated by restriction enzyme digestion containing one or more of the predicted seed match sites (Fig. 3-5A). Co-transfection of these mutant reporters with miRNA-expressing vectors identified specific regions within the 3'UTR that were important for targeting. Deletion of all four sites (Fig. 3-5B, "A") or sites two, three, and four (Fig. 3-5B, "C") abrogated the miRNA-dependent inhibition. Deletion of site one alone had no significant effect on the inhibition level of luciferase expression (Fig. 3-5B, "B"). Thus, these data show that the region encompassing sites two, three, and four within the BACH-1 3'UTR is likely targeted by these miRNAs.

To further confirm this, we used quick-change site-directed mutagenesis to delete individual or multiple seed match sites. Seed match sites (6mers) one to four alone or in combination within pGL3-BACH1 were replaced with *XhoI* restriction enzyme sites and

luciferase assays were performed. Deletion of binding sites one, three or four alone had no effect on miRNA-inhibition of the reporter; however, we observed a 15% increase in luciferase expression with deletion of binding site two alone (Fig. 3-5C). Analysis of double mutants showed that deletion of site two with any other site completely abrogated the effect of both miR-155 and miR-K12-11 on the BACH-1 reporter (Fig. 3-5C). In contrast, deletion of sites three and four together showed the same downregulation as the wildtype BACH-1 reporter (Fig. 3-5C). Together, these data demonstrate that the BACH-1 3'UTR is targeted by miR-155 and miR-K12-11 predominantly via site two in combination with any other site. Interestingly, for BACH-1, there appears to be no difference in target site selection for either miRNA.

***In silico* predictions suggest that miR-155 and miR-K12-11 can regulate a common set of cellular targets.** To investigate additional targets, we first scanned a library of over 21,000 human 3'UTRs (www.ensembl.org) for putative miRNA binding sites using miRanda (Enright et al. 2003)(www.microRNA.org). For miR-K12-11, 5686 genes were predicted as targets while 2079 genes were predicted for miR-155. Of those predicted, 1158 3'UTRs were overlapping (Fig. 3-6A). We then restricted the analysis to those 3'UTRs containing seed match sites. 63 overlapping targets were predicted for both miR-K12-11 and miR-155, representing 9.3% to 13.5% of the total miRanda-predicted 3'UTRs with seed match sites for each miRNA (Fig. 3-6B). Thus, *in silico*, these two miRNAs can regulate a common set of genes.

Gene expression profiling reveals a common set of down-regulated genes in response to miRNA expression. To experimentally investigate the influence of these miRNAs on the cellular transcriptome, we generated 293 cells which stably express miR-155, miR-K12-11, or vector control (pcDNA3.1) and performed Affymetrix-based gene expression profiling. MiRNA expression in 293/miR-155 and 293/miR-K12-11 cells was confirmed both by luciferase

derepression assays using specific miRNA-sensor vectors and antagomirs (Fig. 3-7A) and Northern blot analysis (Fig. 3-7B). To avoid the risk of analyzing integration events, we examined cell pools rather than individual cell clones.

RNA was harvested at two time points from two independent cultures of each cell line. A total of twelve samples were used to synthesize cRNA and hybridized to Affymetrix U133 2.0 plus human GeneChips containing over 47,000 human probe sets. RNA extraction, quantification, cRNA synthesis, hybridization, and washing steps were performed as recommended by the manufacturer and previously described (Samols 2007). Figure 3-8 shows a heat map representing the expression profiles of genes significantly altered in the presence of miR-K12-11 or miR-155.

In both 293/miR-155 and 293/miR-K12-11 cells, a total of 195 annotated genes, represented by 208 probe sets, were found altered when compared together to vector control. Of those genes altered, we found 137 genes (70%) downregulated. A cross-validation analysis (CV) showed that of these 137 genes, 78 exhibited a CV of 75% or greater (Table 3-3). This analysis, base on *t*-values of signal intensities, gives statistically robust data while including probe sets with relatively small fold changes. In the final data set, a common set of 64 genes was significantly downregulated between –1.11 to –11.05 fold in response to both miR-155 and miR-K12-11.

Downregulated genes contain potential seed-match binding sites. Using an *ad hoc* miRNA seed match scanning algorithm (Samols 2007), we examined those genes exhibiting altered expression patterns in response to miR-155 or miR-K12-11 for potential 3'UTR miRNA binding sites. Of the 137 genes found downregulated in both 293/miR-155 and 293/miR-K12-11 cells, 33 3'UTRs (24%) contained 6mer (nt 2-7) sites for both miRNAs while 13 3'UTRs

contained 7mer (nt 2-8) sites. Within the set of 64 genes commonly downregulated by both miRNAs, 18 3'UTRs (28%) contained 6mer sites (Fig. 3-9).

Luciferase reporter assays confirm miRNA targeting of TM6SF1. Based on the bioinformatics data, we chose three genes for further examination. Selected 3'UTRs were inserted into pGL3-promoter downstream of the luciferase gene. Reporter constructs were co-transfected into 293 cells with pmiR-155, pmiR-K12-11, or pcDNA3.1 as control. Neither miRNA had any effect on the *FLJ37562* or *PHF17* 3'UTRs (Fig. 3-10). In contrast, we observed a significant inhibition of luciferase from a reporter containing the 3'UTR of *TM6SF1* when miR-155 or miR-K12-11 was present. *TM6SF1,* transmembrane 6 superfamily member 1, is an uncharacterized 370 aa protein with predicted transmembrane domains (Carim-Todd et al. 2000). A control miRNA, miR-K12-3-5p, which lacks predicted binding sites within the *TM6SF1* 3'UTR, had no effect on luciferase expression. Thus, *TM6SF1* is a target of both miR-155 and miR-K12-11.

Discussion

The goal of this study was to determine whether the known oncogenic hsa-miR155 and the tumorvirus-encoded miR-K12-11, which both contain identical seed match sequences, can regulate a common set of target genes, and therefore might target similar regulatory pathways. Using a combination of bioinformatics tools and gene expression profiling, we identified 64 genes which are potentially targeted by both miRNAs. 28% of these common targets contained seed match sites within their 3'UTRs, and reporter assays verified that one of these genes, *TM6SF1,* was regulated by both miRNAs (Fig. 3-10). We are currently in the process of evaluating additional 3'UTRs. To the best of our knowledge mir-K12-11 is the first example of a virally-encoded miRNA with seed sequence homology to a human miRNA and the proven ability to regulate similar targets as its host counterpart.

Sequence alignments revealed that additional herpesvirus-encoded miRNAs shared seed sequence homology with human miRNAs (Fig. 3-1). KSHV miR-K12-6-5p has homology to miR-15a and miR-16, both associated with tumor suppressor activity (Cimmino et al. 2005) while EBV BART5 has homology to miR-18, a member of the oncogenic miR-17-92 cluster (He et al. 2005). This indicates that herpesviruses, through co-evolution with their human hosts, have pirated miRNA genes in addition to the nine known KSHV genes including v-Interleukin 6, v-Cyclin, v-IRF, which are all homologues of cellular proteins that modulate the host environment (Russo et al. 1996; Neipel et al. 1997). Interestingly, the precursor miRNAs from which miR-155 and miR-K12-11 arise are vastly different (not shown). However, precursors for members of the *let-7* miRNA family are also not conserved despite the fact they share a common seed sequence and can target similar 3'UTRs (Abbott et al. 2005; Johnson et al. 2005) (microrna.sanger.ac.uk).

By utilizing reporter assays and detailed mutational analysis, we found that both miR-155 and miR-K12-11 specifically target seed match sites within the BACH-1 3'UTR (Fig. 3-3 and 3-4). In contrast to the reporter assays, the RNA levels of BACH-1 were not altered in miRNA expressing 293 cells as shown by expression profiling. Possible explanations could be that miR155/mirK12-11-dependent BACH-1 regulation occurs at the level of translational inhibition as has been previously shown for some miRNA targets (Bartel 2004) or the fact that observed BACH-1 transcript levels in 293 cells were very low. However, BACH-1 mRNA levels are downregulated in KSHV latently infected endothelial cells (An et al. 2006). BACH-1 is a broadly expressed transcriptional repressor, which regulates genes involved in hypoxia response such as heme-oxygenase-1 (*HMOX1)* (Igarashi and Sun 2006). Increased levels of *HMOX1*, which enhances cell survival and proliferation, have been reported following *de novo* KSHV

infection of endothelial cells (McAllister et al. 2004). While the increase of *HMOX1* has been attributed in part to the KSHV G-protein coupled receptor (v-GPCR) (Marinissen et al. 2006), the observed downregulation of BACH-1 may also be due to miR-K12-11 expression during latency.

The seed sequence homology of these two naturally occurring miRNA orthologs also provides an opportunity to analyze the contribution of sequences outside the seed match to mRNA targeting and target site selection. A detailed analysis of the BACH-1 3'UTR demonstrated that both mir155 and miR-K12-11 preferentially utilized seed match site two for targeting; however sites three and four also contributed (Fig. 3-4). Further analysis of the 64 downregulated genes using miRanda showed that >30% of 3'UTRs are predicted to contain miR-155 or miR-K12-11 binding sites; notably, greater than 50% of these 3'UTRs contained exact seed match sites. Hence, this bioinformatics analysis revealed a significant enrichment for seed match containing 3'UTRs within the 64 altered genes and furthermore, supports the chosen experimental approach to identify potential miRNA targets.

The biological consequences of these newly identified miRNA targets are currently under investigation. Using Biocarta (Biocarta, Inc.), we found that the majority of pathways affected by genes changed in response to miRNA-expression included cell signaling, cell division, apoptosis, and T cell activation. Additionally, we identified several miR-155 and miR-K12-11 responsive genes known to be aberrantly expressed in human malignancies. These include *LDOC1,* a regulator of apoptosis (Inoue et al. 2005; Mizutani et al. 2005), as well as several Bcl-2 and Bcl-6 family members (*BCLAF1, BCL2L11, BCL6B*).

BCLAF1, Bcl-2 associated transcription factor 1 (Btf), has been shown to interact with the anti-apoptotic Bcl-2 and Bcl-xL family members, and when overexpressed, to induce apoptosis

(Kasof et al. 1999). *BCL2L11*, known as Bim, inactivates the Bcl-2-like proteins thereby inducing apoptosis (Cory et al. 2003; Adams and Cory 2007). *BCL6B,* a transcriptional repressor also known as BAZF, is an NF-κB regulator and homolog of the Bcl-6 oncogene; however, unlike Bcl-6 which is ubiquitously expressed, BAZF is expressed predominantly in the heart, lung, and stimulated lymphocytes (Okabe et al. 1998). Both Bim and BAZF also have roles in cellular immunity. Bim is required apoptosis of activated T-cells following viral infection, critical for limiting anti-viral immune responses (Pellegrini et al. 2004). BAZF is required for secondary responses of memory CD8+ T-cells (Manders et al. 2005), and recently, was also linked to the homeostasis of hematopoietic progenetors (Broxmeyer et al. 2007). Thus, the observed downregulation of these genes by miR-155 or miR-K12-11 suggests important roles in regulation of immune responses to infection as well as targeting apoptosis to regulate cell survival during lymphocyte differentiation. It is interesting to note that to date of the only ~50 experimentally determined human miRNA targets, a significant proportion are regulators of apoptosis, such as miR-15a and miR-16 (Cimmino et al. 2005). Furthermore, both KSHV- and HSV-encoded miRNAs have recently been reported to target apoptosis regulators (Gupta et al. 2006; Samols 2007).

While there are only few experimentally confirmed targets for miR-155, it was the first human miRNA suggested to be oncogenic (Tam and Dahlberg 2006) and was recently shown to be important for lymphocyte differentiation and immunity. MiR-155 is expressed in activated macrophages following treatment with TLR ligands, suggesting that miR-155 has a role in innate immunity (O'Connell et al. 2007). Recently, it was shown that *BIC*/miR -155 plays a significant role in B and T lymphocyte maturation (Rodriguez et al. 2007; Thai et al. 2007). *BIC* is absent in resting and progenitor B cells but induced upon activation; miR-155 is expressed shortly

thereafter, and regulates the germinal center (GC) reaction during B cell maturation (Thai et al. 2007). The late stages of B cell development, particularly the affinity maturation in conjunction with helper T cell signaling, are critically dependent upon a timely miR-155 expression (Thai et al. 2007).

Intriguingly, KSHV-associated PELs are of B cell lineage and have a distinct developmental phenotype. We showed that PEL cells do not express miR-155, but do express high levels of miR-K12-11 (Fig. 3-2). PEL cells have rearranged immunoglobulin (Ig) genes as well as somatic point mutations within rearranged Ig variable genes (Matolcsy et al. 1998; Fais et al. 1999), indicating that B-cell activation during the GC reaction has occurred. Accordingly, the PEL developmental phenotype was classified as plasmablastic (Klein et al. 2003), and expression profiling studies suggest that PEL represent B cells blocked late in their differentiation pathway towards a antibody secreting plasma cell (Jenner et al. 2003). Exactly some of these late steps seem to be dependent upon a short miR155 expression burst during normal B cell development (Thai et al. 2007).

Based on our data demonstrating common targets for both miRNAs, it is tempting to speculate that miR-K12-11 continues to regulate a set of miR-155 targets at a stage when miR-155 is not expressed, and thereby, directly contributes to dysregulated non-mature B cell proliferation and potentially, lymphomagenesis. Clearly, this hypothesis will have to be tested in appropriate *in vivo* models, such as NOD/SCID mice that allow the study of human B cell maturation.

In conclusion, these data show that the oncogenic human miR-155 and the virally-encoded KSHV miR-K12-11 can regulate a common set of target genes, and that miR-K12-11 is an

ortholog of miR-155. The recent link of miR-155 to B cell maturation suggests a similar role for miR-K12-11 which therefore, may contribute directly to KSHV pathogenesis.

Finally, we found a total of four additional viral miRNAs with perfect seed match sequence identity to cellular miRNAs. Most importantly, three of these are potential orthologs of human miRNAs known to have either oncogenic or tumor suppressor activity. Hence, these observations strongly suggest that DNA tumor viruses have utilized molecular mimicry of microRNA genes to regulate host cellular environment in the same fashion as the long list of pirated cytokines, growth factors, and immune modulatory genes, commonly found in DNA tumor virus genomes (Russo et al. 1996; Neipel et al. 1997).

Materials And Methods

Plasmids and Oligonucleotides. MicroRNA sensor plasmids were constructed using pGL3-Promoter (Promega). Oligonucleotides were annealed and inserted at *FseI* and *XbaI*. Constructs were verified by restriction enzyme digestion.

- *miR-155* fwd:5'CTAGACCCCTATCACGATTAGCATTAACTCGAGCCCCTATCACGATTAGCATTACGGCCGG-3'
- *miR-155* rev: 5'CCTTAATGCTAATCGTGATAGGGCTCGAGTTAATGCTAATCGTGATAGGGGT-3'
- *miR-K12-11* fwd: 5'CTAGAATCGGACACAGGCTAAGCATTAATTATTATCGGACACAGGCTAAGCATTAAGGCCGG-3'
- *miR-K12-11* rev 5'CCTTAATGCTTAGCCTGTGTCCGATAATAATTAATGCTTAGCCTGTGTCCGATT-3'.

3' UTR sequences were obtained from the Ensembl database (www.ensembl.org) or NCBI and PCR amplified (TripleMaster, Eppendorf) from either BCBL-1 or 293 genomic DNA (DNAzol, Molecular Research Center, Inc., OH). Primers were designed using Vector NTI (Invitrogen) and are indicated in Table 3-3. PCR products were cloned into pCRII-TOPO (Invitrogen), excised, and inserted into the 3'UTR of pGL3-promoter.

For construction of pmiR-K12-11 and pmiR-155, ~180 nt encompassing the stem-loop pre-miRNA were PCR-amplified from BCBL-1 genomic DNA using primers indicated in Table 3-3. PCR products were TOPO-cloned, excised with *HindIII* and *XhoI*, and inserted into pcDNA3.1V5/HisA (Invitrogen) at corresponding sites.

2' O-methylated RNA oligonucleotides were synthesized by Dharmacon, Inc and are antisense to the mature miRNA sequence. All bases are modified at the 2' position.

Quick-change site-directed mutagenesis was performed using primers indicated in Table 3-2 according to manufacturer's protocols (Stratagene). Primer design was done using PrimerX (www.bioinformatics.com). Each 6mer seed match site was mutated to an *XhoI* restriction enzyme site and mutants were analyzed by restriction enzyme digestion.

Cell lines and transfections. BCP-1 (a gift from Dr. Denise Whitbey at NCI), BC-1, VG-1, JSC-1 (gifts from Dr. Dirk Dittmer at UNC), RAJI (a gift from Dr. Sankar Swaminathan at UF), BCBL-1, and BJAB cell lines were grown in RPMI 1640 supplemented with 10% fetal bovine serum and 5% penicillin/streptomycin (Gibco). 293 cells were maintained in DMEM supplemented with 10% FBS and 5% penicillin/ streptomycin. For stable cell lines, cells were transfected with 10 μg plasmid DNA using Lipofectamine 2000 (Invitrogen) and selected with 500 μg/mL G418 (Mediatech, Inc.) for 4 wks. Transfections for luciferase assays were performed in 6-well or 24-well plates with Lipofectamine 2000 according to manufacturer's protocols. Cells were cultured 48-72 hrs prior to harvest.

Affymetrix array-based gene expression profiling. RNA isolation was performed using the RNeasy kit as per manufacturer's instructions (QIAGEN). RNA labeling was done using the GeneChip Eukaryotic One-Cycle Target Labeling Assay as directed by Affymetrix (www.affymetrix.com) and used to probe Affymetrix U133 2.0 plus human GeneChips.

Hybridization was performed at 45ºC for 16 hrs, then chips were washed and stained using Affymetrix protocol EukGE-WS2v5_450. Array scanning and analysis was performed as described in (Samols 2007).

Luciferase Assays. Luciferase activity was quantified using the Luciferase assay system (Promega) according to manufacturer's protocols. Briefly, transfected 293 cells were lysed in cell culture lysis reagent (Promega) and 20% of each cell lysate assayed for firefly luciferase activity. Light units are normalized to total protein, determined using the BCA protein assay kit (Pierce) according to manufacturer's instructions or *Renilla* luciferase using the dual luciferase reporter kit (Promega).

RNA Extraction for RT-PCR. Total RNA was prepared using RNA-Bee (Tel-Test, Inc., TX), according to manufacturer's protocols. For detection of *BIC* expression, 1 μg of DNAse-treated RNA was reversed-transcribed using SuperScript III Reverse Transcriptase (Invitrogen) and random hexamers in the presence of RNase-OUT Recombinant RNase Inhibitor (Invitrogen) to create a cDNA pool. 10% of each RT reaction was used for PCR-amplification. *BIC* and β-actin primers are noted in Table 3-3.

Northern Blot analysis. 30 μg of total RNA was loaded onto 15% 8M urea polyacrylamide gel and transferred onto Genescreen Plus (Perkin Elmer) following electrophoresis. Probe labeling was performed using T4 polynucleotide kinase (New England Biolabs) in the presence of αP^{32} γ-ATP.

Figure 3-1. Herpesvirus miRNAs share seed sequence homology with human miRNAs. MiRNA sequences from KSHV, EBV, HCMV, and HSV-1 were aligned to the human miRNA database. MiRNAs with seed sequence homology are in bold.

A

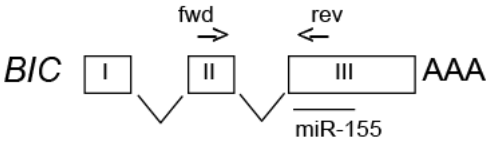

B

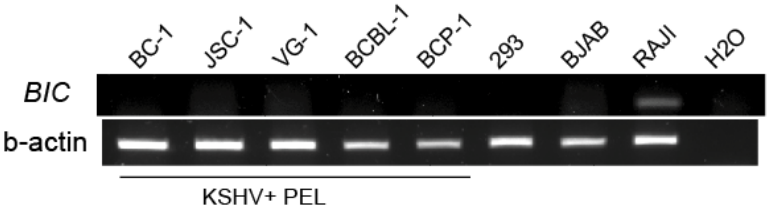

C

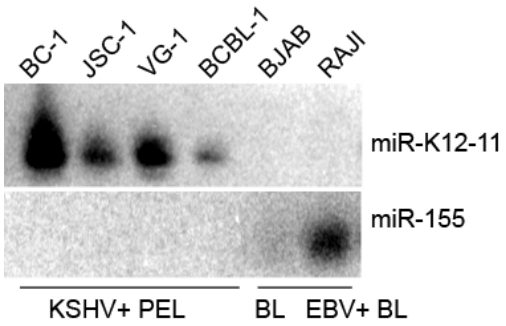

Figure 3-2. PEL cells do not express miR-155. A. miR-155 is expressed from exon 3 of the non-protein-coding BIC. Primers (fwd and rev) for RT-PCR analysis of BIC expression are indicated. B. RT-PCR analysis shows that BIC is not expressed in KSHV-infected primary effusion lymphoma (PEL) cell lines. RAJI, an Epstein-Barr virus (EBV) infected Burkitt's lymphoma (BL) cell line was used as a positive control. H2O indicates no template control. C. Northern blot analysis of KSHV-miR-K12-11 and hsa-miR-155 expression. 25 μg of total RNA was loaded per lane and hybrized to probes for either miR-K12-11 or miR-155.

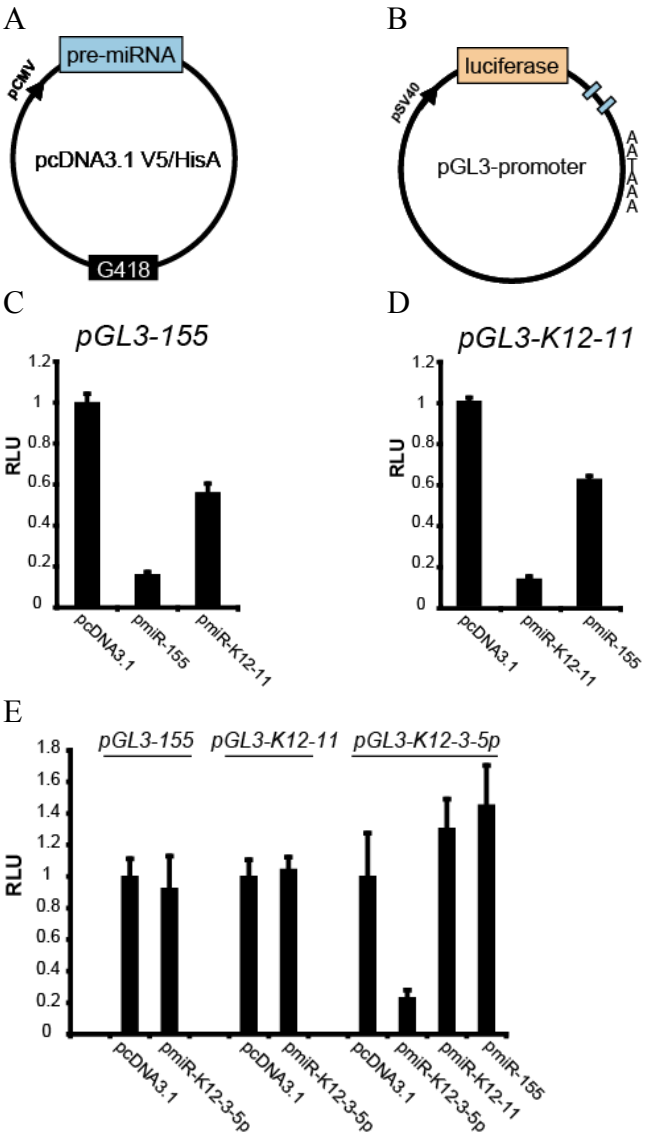

Figure 3-3. Importance of the seed sequence for miRNA targeting. A. Schematic of miRNA expression vector. A region encompassing the pre-miRNA for miR-155 or miR-K12-11 was PCR-amplified and cloned downstream of the CMV promoter in pcDNA3.1. B. Schematic of miRNA sensor vector. Two antisense complementary binding sites for each miRNA were inserted into the 3'UTR of pGL3-promoter (Promega). C and D. Luciferase expression from miRNA sensors (pGL3-155 or pGL3-K12-11) is downregulated in reponse to ectopic miRNA expression. Additionally, miR-K12-11 can target the miR-155 sensor vector and vice versa (right bars); by Student's t test, $p<0.01$. 293 cells were transfected with 40 ng sensor and 800 ng miRNA expression vector using Lipofectamine 2000 (Invitrogen). Lysates were analyzed at 72 hrs post-transfection (Promega). Light units are normalized to total protein determined by BCA (Pierce). E. Luciferase assays to control for ectopic miRNA effects. MiRNA expression and sensor vectors for KSHV-miR-K12-3-5p, a miRNA with no sequence homology to either miR-K12-11 or miR-155, were used as controls.

A

BACH-1 3'UTR nt 658-2495

TCTAGAAAGTCTGGCTACATGAATAGATTTAAGTGTCACTTTCCCTCCCTGCCCCCCGCTTCAGTCTCTACCATATCTG
GTCCCATCATGGACTTCCTATTTCCTGGCATTTTTGTCCCTTTGGAAGAAGAAATAGGACTCAGAATACAGTGGCATG
AGTGATTACACTGGCAGCATTATCTCAGGCTCCCTAGAATCTGGAGAGCTTACCAACATGTAAAGCTGTTCATTTTTC
CACCGTGGGTCACCAATGCCAGAAAACCAGACATCACGGGGAAAGAATGTTGCTTACTTTTTACCAGGAGTGCAGTT
CATTTTTTTCACCCTGTTTTTGAAGTCGTATTATTCACTTGTAAAAATGATTGTAACAGATAAAAAATGTATCTGCAGCA
ACTCTGCAGGTTTGTGAAATAGGATGAAACTCAATCTTTTTCTATTGTGGGTTTGCATTTGAAAAGCAGGTTGAATCCT
TGCTCTCTTCTCCAAATTTGGTGTGGTATAAAGACACACAAATCATTTTAACTTGGACATTTAAAGATCAGTCTTAGTGT
TTGTTCAGTCCTGTTACAAAATAGATAACTGAGCACCTATCGCATAACATTTTGCGGTGGCTTTTAGCCATGCTGGGG
TTAGATGTGTTTGAGAGTCAAATGAAAGCTATGGATCTTCTCAGCAATTAAAAAAAATGCATATATTCACATTCACAGA
AACATTGGCAGAACCCAGTTTTAATGGTACAGAGGAGTAGTTTATAGTGTTGATTTCACCAAAATCAGAGGGCTGAAA
GAGACACTTCTATAGACTGCATCCTGAGCCTAGTGCAGGGCTTGTCTAGCTAATGTGGGCAGCCACCACCCACTGTG
TATGAACAAGTCTGAAGCAAGTTGGCCTTGCCCTTGAGAGTATATGGGGACCAGTCTTCATGTCTTGGAGTAATTTGT
CAAATGTTACCCTTTTTGATCAGGGTGTAGGGGGAGGATATTGCTAGTATATTTTCAGTGGTTTGTATGTTCTCTCTGT
CACTGACTTATTTGTAAGAGAAAATTAGTTGGACTTGTTTATTTTCTAGTAGCTTTTATAAGTACACTCAAGAATTTGTC
AGGGAGAATAATTCTGATAGTGCATCCCATACTGCAAAAGAATTTGTGTGTGTGTGTGTGTGTGTGTGTGTGTGTG
TATGTGTATGTATACATATATATCTCTCCATATAGGTATTTCTTTGATACTTGTAATTTTAAATTTCAGCTTCACGATATA
AAATAATATAAGAACTTCTGGTTTACAAAATGTAAAATCTTAAGCCAATGGAACCCTTGATTTCCTACCTCAGTGTACA
CCCAACTATTGGTTGTATCAGTTTGTGTATGTGCAAATGTCAAATAATCTTTTGCTTTAATTGCTACTGTACTTGCTTTG
AAAGATTACCTACTATTTTATGATAAAATGTAGTTGTCTCCAGAGCTTAAATATAATTTGTAAAGCACTTGGTTTAAATTT
CTCTCTACCTATAAACAGTTTAGCATTAAGGGTTTCTATTAATGACACAGAATTATTGGCCAAGTGTAATTTCTTAAAAT
TTAGCATTACTTTAAATAGCCAGCATGTAATACAAGTAACTACACTACCTCATATCTACATGATTTTCAAGTTGTAATGC
AGATGGACAGATAAAAAAGATTTTACGTTTGTCTTTTGGCCATAAGTGGGAAAGTTTTCTGTATATTGCATAGCATTAC
ACATTTATGCCTATTTTAACATTAACTTCTAAAGAAGTTTTTTCTAAGAAAATGTTTCAAGGCAATATTTTTTTTGAGGCT
GCCGAAGACAAATGACAGG

B

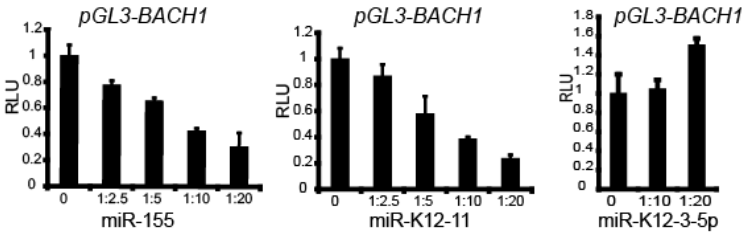

C

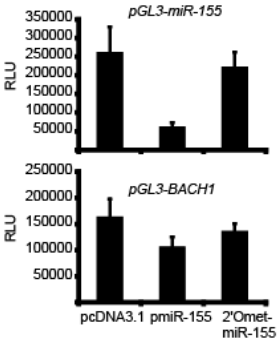

D

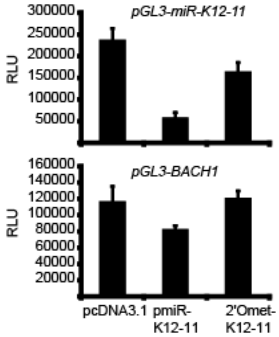

Figure 3-4. BACH-1 is targeted by miR-K12-11 and miR-155. A. The BACH-1 3'UTR contains four seed match sites (highlighted) based on three target prediction programs (miRanda, PicTar, TargetScan). B. A region of the BACH-1 3'UTR (nt 658-2495) encompassing the predicted miRNA binding sites was cloned downstream of luciferase (pGL3-BACH1). Co-transfection of pGL3-BACH1 with pmiR-155 or pmiR-K12-11 into 293 cells shows a dose-dependent inhibition of luciferase. Ratios on the X-axis indicate the amount of miRNA vector to reporter. pcDNA3.1 was used as filler. Co-transfection of pGL3-BACH1 with miR-K12-3-5p, which lacks potential binding sites within BACH-1, does not inhibit luciferase. C. and D. De-repression assays with antagomirs. 293 cells were transfected with indicated sensor vectors (top graphs) or pGL3-BACH1 (bottom graphs), miRNA expression vectors or pcDNA3.1 control, and antagomirs specific to each miRNA. For control transfections (two right bars for each graph), the antagomir to miR-K12-10 was used for filler. Light units are normalized to total protein determined by BCA (Pierce).

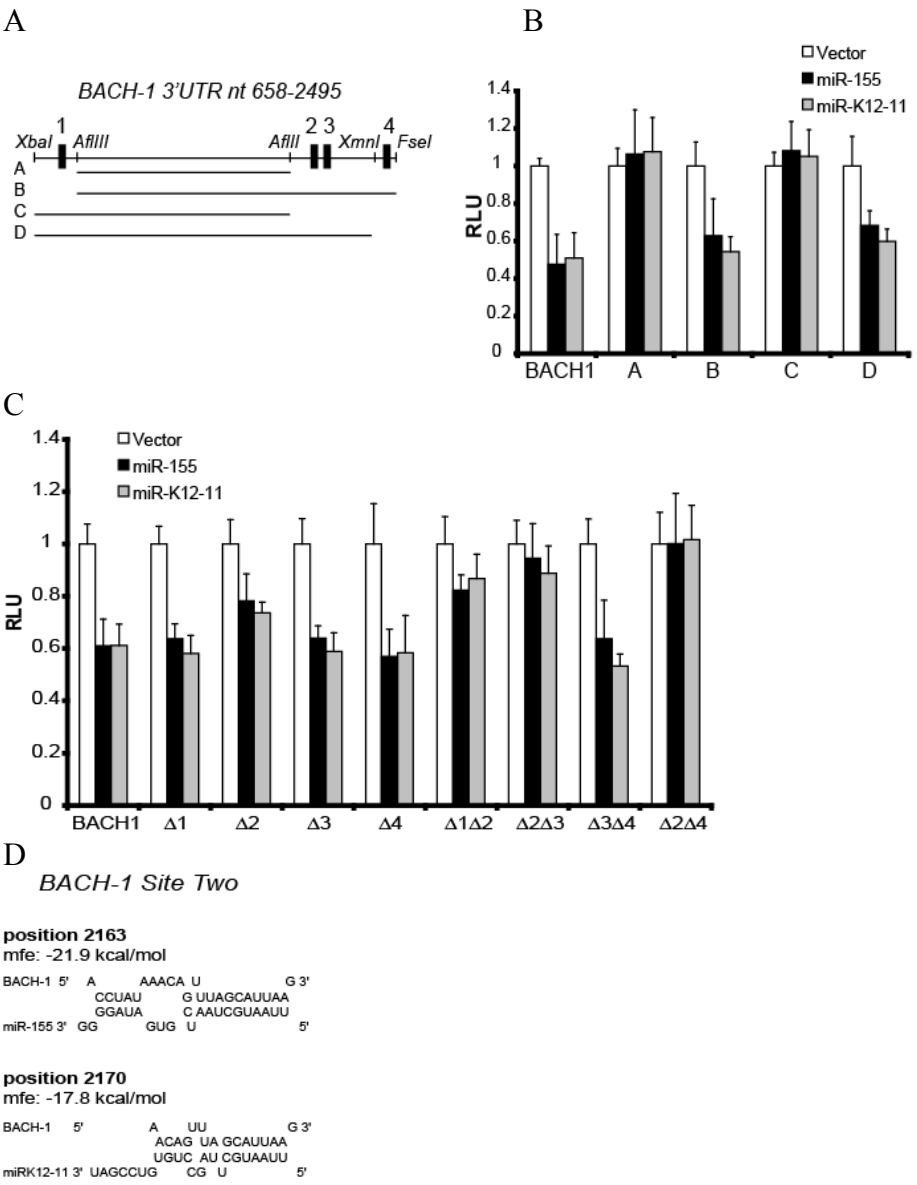

Figure 3-5. miR-155 and miR-K12-11 target BACH-1 via site two. A. Schematic of the BACH-1 3'UTR with miRNA seed-match sites (1-4). A-D are truncation mutants generated by restriction enzyme digestion. B. Mapping of miRNA binding sites. BACH-1 fragments A-D were inserted into pGL3 and 40 ng of each reporter was co-transfected with 10 ng pEF-RL (renilla) and either 800 ng pcDNA3.1 (vector), pmiR-155, or pmiR-K12-11 into 293 cells. C. Site-directed mutagensis to validate mapping data. Individual or double seed match sites were mutated to an XhoI site. Mutation of site 2 alone (□2) or in combination with site 1, 3, or 4 released the miRNA effect on the BACH-1 3'UTR, indicating that both miRNAs use site 2 for targeting. D. Potential miR-155 and miR-K12-11 binding to site 2 within the BACH-1 3'UTR (RNA-hybrid). Binding position within the 3'UTR and the minimum free hybridization energy (mfe) for each miRNA are shown. For B. and C., lysates were harvested at 72 hrs and light units are normalized to renilla luciferase.

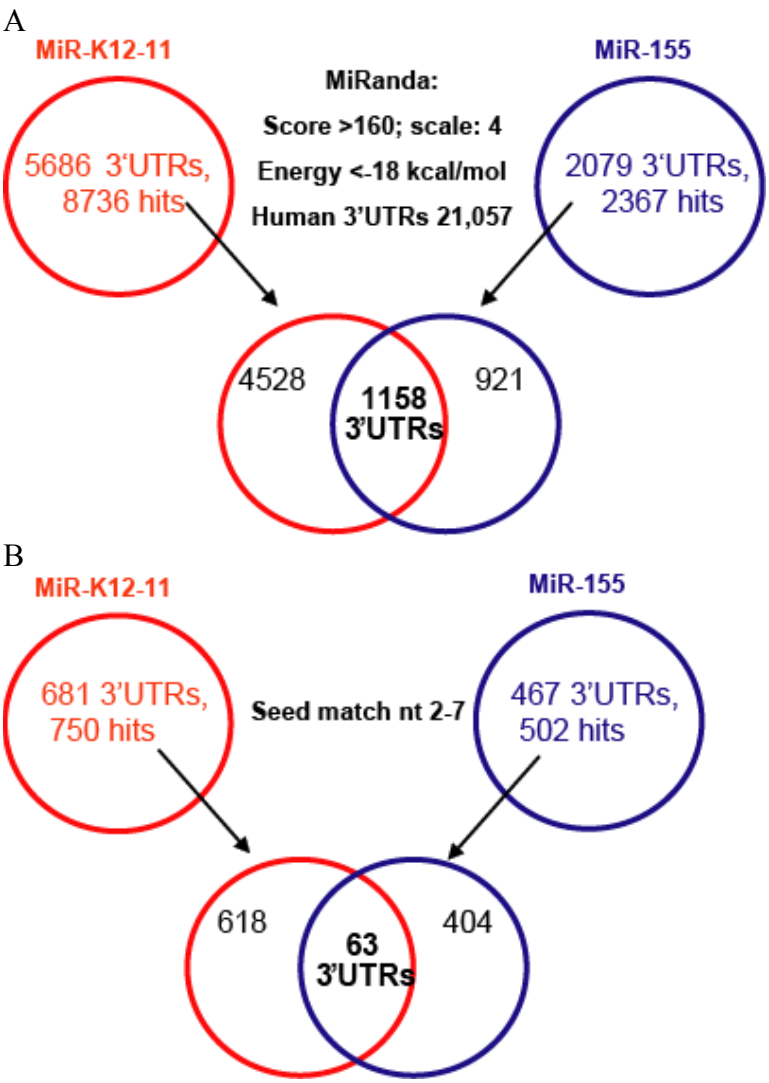

Figure 3-6. In silico, miR-155 and miR-K12-11 have overlapping cellular targets. MiRanda (Enright et al. 2004) was used to scan a library of >21,000 human 3'UTRs for putative miR-155 (blue) and miR-K12-11 (red) binding sites. A. 1158 overlapping 3'UTRs were predicted using parameters indicated. B. By restricting the analysis to 3'UTRs containing a seed match only, 63 3'UTRs were predicted as overlapping targets for both miRNAs.

A

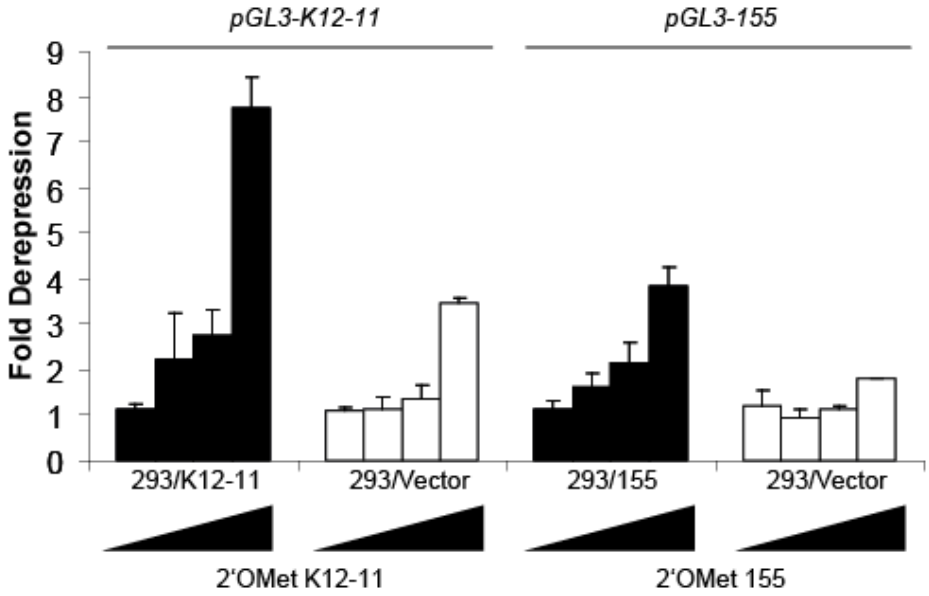

B

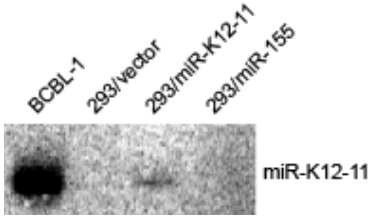

C

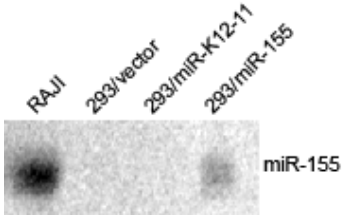

Figure 3-7. miRNA expression in stable cell lines. A. Luciferase de-repression assays were performed in 293/miR-K12-11, 293/miR-155, or 293/vector cells using 40 ng of indicated sensor vector and increasing amounts (20 to 80 pmol) of a 2'OMet antagomir specific to the miRNA of interest. 2'OMet K12-10 and 100 ng of pcDNA3.1 were used as filler. Light units are normalized to total protein by BCA (Pierce). B and C. Northern blot analysis of miRNA expression in stable cell lines. 30 μg of total RNA was loaded per lane and hybridized to a probe for either miR-K12-11 (B) or miR-155 (C). BCBL-1 and RAJI were used as positive controls.

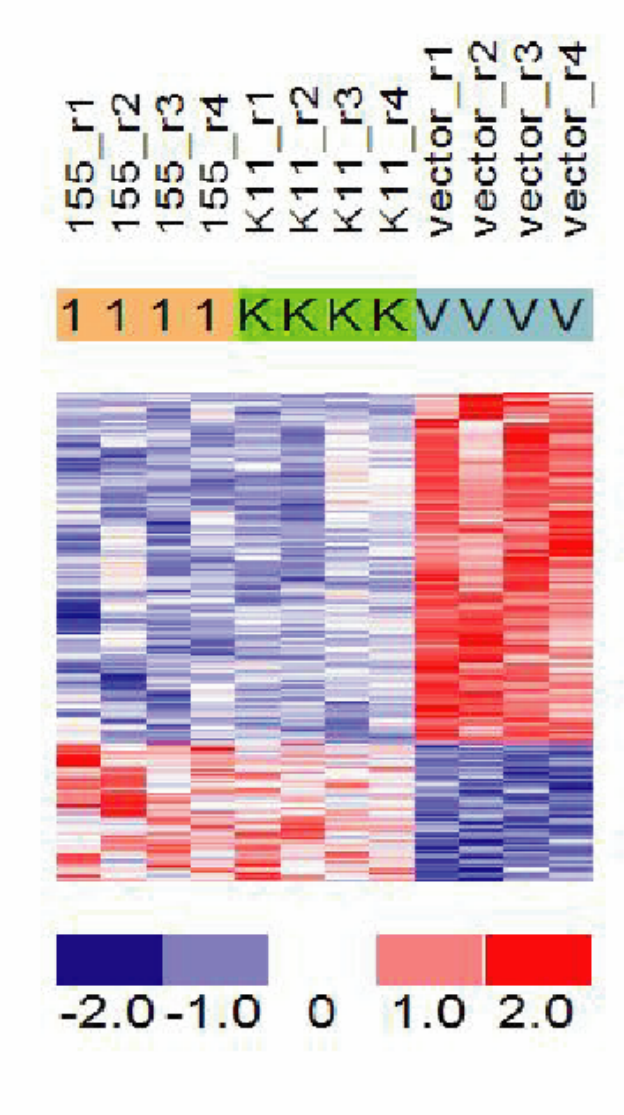

Figure 3-8. Genes are downregulated in response to miRNA expression. Colors represent changes in variance normalized gene expression differences for individual genes represented by the probe sets as indicated on the color scale. 4 samples were used for each cell line. 208 genes were changed in response to miRNA expression, 149 genes were down-regulated and 59 were up-regulated. 78 genes showed > 75% cross validation (CV).

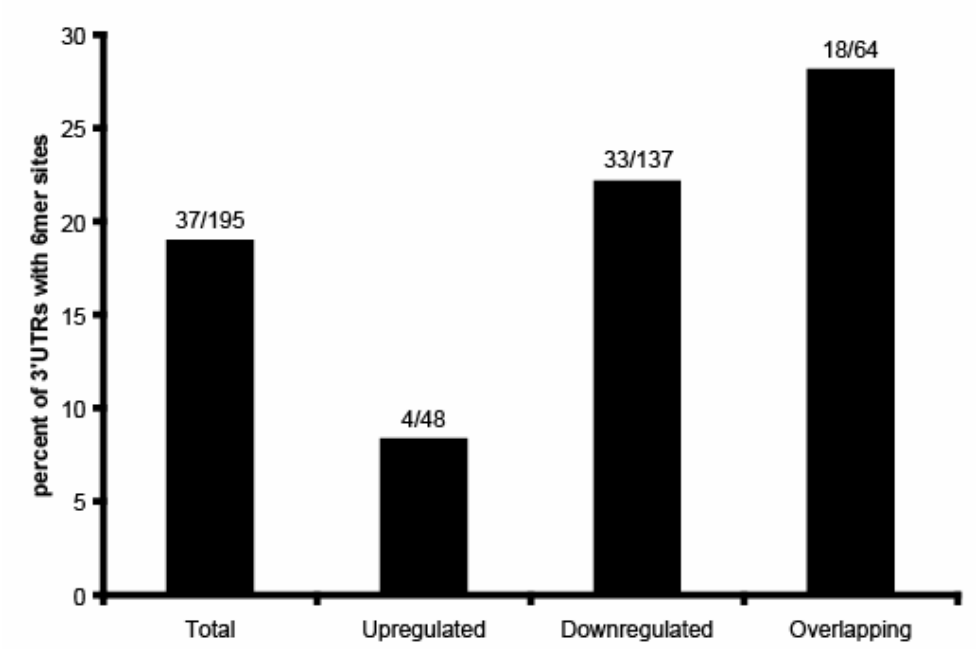

Figure 3-9. The 3'UTRs of downregulated genes are enriched for seed match sites. 3'UTRs of altered genes were scanned for seed match sites. Shown is the percent of 3'UTRs with seed match sites for either the total number of altered genes (total), upregulated or downregulated genes, or the 64 commonly downregulated genes (overlapping). 18 out of the 64 commonly downregulated genes contained seed match sites.

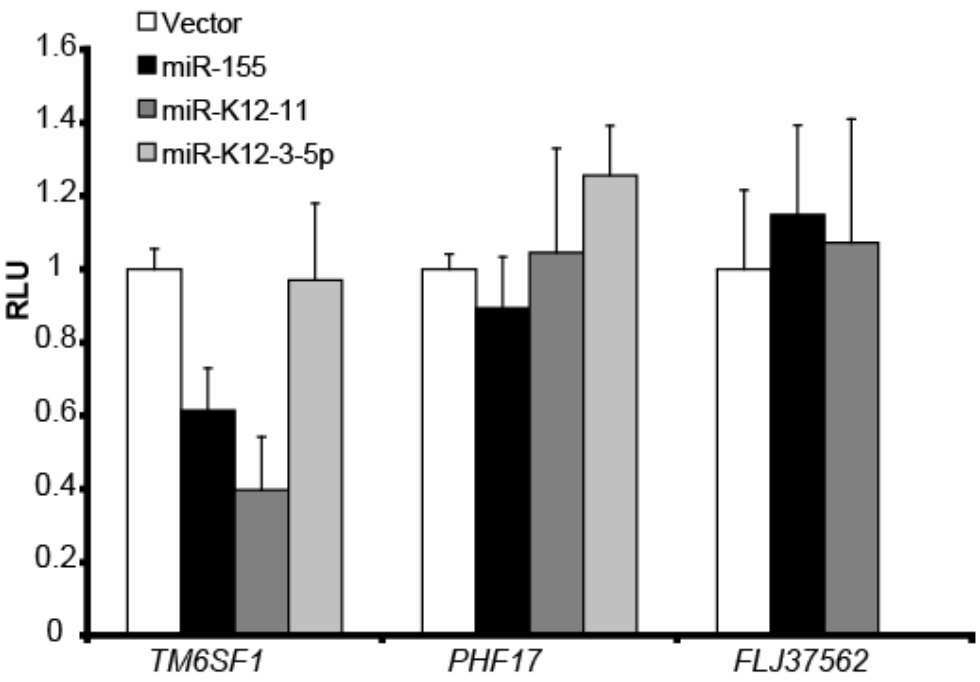

Figure 3-10. Validation of candidate target genes. 3'UTRs of downregulated genes were scanned for potential seed-match binding sites. The 3'UTRs of TM6SF1, PHF17, and FLJ37562 contained at least one seed-match site and were cloned into pGL3 downstream of luciferase. Luciferase reporters were co-transfected with pEF-RL (renilla), and pcDNA3.1 vector control or miRNA expression vector to determine miRNA-targeting. For TM6SF1, a 1.6 to 2.5 fold decrease in luciferase was observed with miR-155 and miR-K12-11.

Table 3-1 Primers

Gene or miRNA	Forward primer	Reverse primer
miR-155	ACAAACCAGGAAGGGGAATC	CAGGGTGACTCATGCTTCTTTGT
miR-K12-11	AAAAATTGCCGCCGTGAAGGTC	TAAAGCGGGCGTTCGTAAGC
BIC	ACCAGAGACCTTACCTGTCACCTT	GCACTCAGAGGATGAGGCATAAAG
B-ACTIN	AAATCTGGCACCACACCTTC	TCCATCACGATGCCAGTGGT
BACH-1 3'UTR	CAGGCTTTAAGCTACATTGGGA	GGCCGGCCTGTCATTTGTCTTCGGCAG
FLJ37562 3'UTR	TCTAGAGGAAAAGAGGGCCAGGTT	GGCCGGCCAATCTTTGACAATGGTGT
PHF17 3'UTR	GATATCTTAGAGAAGAAGATGC	GATATCGTGGTGATTGTGAGACAAAC
TM6SF1 3'UTR	TCTAGATTGATACATGCTGGAGGT	GGCCGGCCACCAATAAAACAAATG

Table 3-2 Primers for BACH-1 site-directed mutagenesis

Site	Primer
site 1	
fwd	CAT GAG TGA TTA CAC TGG CAC TCG AGT CTC AGG CTC CCT AGA ATC
rev	GAT TCT AGG GAG CCT GAG ACT CGA GTG CCA GTG TAA TCA CTC ATG
site 2	
fwd	TCT CTA CCT ATA AAC AGT TTA CTC GAG AGG GTT TCT ATT AAT GAC ACA
rev	TGT GTC ATT AAT AGA AAC CCT CTC GAG TAA ACT GTT TAT AGG TAG AGA
site 3	
fwd	GTA ATT TCT TAA AAT TTA CTC GAG CTT TAA ATA GCC AGC ATG
rev	CAT GCT GGC TAT TTA AAG CTC GAG TAA ATT TTA AGA AAT TAC
site 4	
fwd	GTA TAT TGC ATA CTC GAG CAC ATT TAT GCC
rev	GGC ATA AAT GTG CTC GAG TAT GCA ATA TAC

Table 3-3 64 Genes Downregulated in Response to miR-155 and miR-K12-11

Parametric p-value	t-value	% CV support	Geom mean of intensities in class 1 : Sample	Geom mean of intensities in class 2 : Vector	fold change	Probe set	Gene symbol
2.70E-06	-9.45	100	323.4	476.2	-1.4725	204454_at	LDOC1
6.60E-06	-8.55	100	5.6	61.9	-11.054	231628_s_at	SERPINB6
6.90E-06	-8.5	100	60.3	104.6	-1.7347	227101_at	LOC168850
8.60E-06	-8.29	100	112	250.4	-2.2357	1553107_s_at	FLJ37562
1.18E-05	-8	100	963	1649.8	-1.7132	224567_x_at	MALAT1
1.51E-05	-7.78	100	367.9	498	-1.3536	221485_at	B4GALT5
1.64E-05	-7.7	100	545.3	956.8	-1.7546	221839_s_at	UBAP2
2.53E-05	-7.32	100	339.9	555.5	-1.6343	212979_s_at	KIAA0738
4.36E-05	-6.87	100	548.5	880.5	-1.6053	224598_at	MGAT4B
4.44E-05	-6.85	100	34.4	48.1	-1.3983	242843_at	BCAN
4.72E-05	-6.8	100	47.2	73.7	-1.5614	205560_at	PCSK5
4.78E-05	-6.79	100	106.4	138.5	-1.3017	218935_at	EHD3
4.92E-05	-6.77	100	1158.2	1445.7	-1.2482	212453_at	KIAA1279
5.36E-05	-6.7	100	1084.2	1307.9	-1.2063	233080_s_at	FNBP3
5.76E-05	-6.64	100	6.1	14	-2.2951	217078_s_at	CD300A
5.92E-05	-6.62	100	529.6	782.3	-1.4772	227641_at	FBXL16
5.96E-05	-6.62	100	259.6	467.6	-1.8012	225820_at	PHF17
6.36E-05	-6.56	100	645.3	933.3	-1.4463	212055_at	C18orf10
6.58E-05	-6.54	100	44.8	80.8	-1.8036	211219_s_at	LHX2
6.76E-05	-6.52	100	147.4	219	-1.4858	204544_at	HPS5
6.78E-05	-6.51	100	46.5	77.1	-1.6581	211621_at	AR
7.52E-05	-6.43	100	617.7	823.4	-1.333	203119_at	MGC2574
8.07E-05	-6.38	100	576.4	913	-1.584	201101_s_at	BCLAF1
8.33E-05	-6.35	100	1570.6	1921.6	-1.2235	200999_s_at	CKAP4
8.69E-05	-6.32	100	265.2	342	-1.2896	203846_at	TRIM32
9.14E-05	-6.28	100	115.3	167	-1.4484	203147_s_at	TRIM14
9.49E-05	-6.25	100	892.7	997.6	-1.1175	212120_at	RHOQ
9.91E-05	-6.22	100	186.2	260.9	-1.4012	201604_s_at	PPP1R12A
0.0001122	-6.12	100	669.5	808.7	-1.2079	226233_at	B3GALNT2
0.0001271	-6.03	100	57.7	85.6	-1.4835	221528_s_at	ELMO2
0.0001274	-6.03	100	762.1	1219.3	-1.5999	229949_at	TRIM50A
0.0001323	-6	100	202.2	297.8	-1.4728	214212_x_at	PLEKHC1
0.0001336	-5.99	100	152	233.4	-1.5355	212758_s_at	TCF8
0.0001455	-5.93	100	65.5	106.1	-1.6198	231297_at	DOT1L
0.0001462	-5.92	100	1126.8	1432.2	-1.271	227522_at	LOC134147
0.0001469	-5.92	100	20.7	27.6	-1.3333	211067_s_at	GAS7
0.0001498	-5.91	100	314.2	511.7	-1.6286	226010_at	SLC25A23
0.000156	-5.88	100	1020.5	1254	-1.2288	201948_at	GNL2
0.0001609	-5.85	100	13.5	25.2	-1.8667	204388_s_at	MAOA
0.0001706	-5.81	100	131	190.8	-1.4565	217974_at	TM7SF3
0.0001766	-5.78	100	849.6	982.7	-1.1567	226287_at	NY-REN-41
0.0001797	-5.77	100	219.8	377.9	-1.7193	1553993_s_at	MED25
0.0001801	-5.77	100	32.5	56.9	-1.7508	228311_at	BCL6B
0.0001853	-5.75	92	1079.1	1292.6	-1.1979	218106_s_at	MRPS10
0.0001864	-5.75	92	58	80.3	-1.3845	210214_s_at	BMPR2
0.0001879	-5.74	92	306.6	370.6	-1.2087	31845_at	ELF4

Table 3-3 continued

0.0001932	-5.72	83	258.6	390.9	-1.5116	216038_x_at	DAXX
0.0001976	-5.7	83	615.4	1780.9	-2.8939	200799_at	HSPA1A
0.0002066	-5.67	83	394.9	597.5	-1.513	210616_s_at	SEC31L1
0.0002077	-5.67	92	483.4	542.5	-1.1223	209188_x_at	DR1
0.0002078	-5.67	92	748.1	908.4	-1.2143	209489_at	CUGBP1
0.0002146	-5.64	92	116.3	171.8	-1.4772	214852_x_at	VPS13A
0.0002291	-5.6	92	23.9	33.7	-1.41	225597_at	SLC45A4
0.0002379	-5.57	83	84.9	112.5	-1.3251	218029_at	FAM65A
0.00024	-5.56	83	1731.3	2046.7	-1.1822	217869_at	HSD17B12
0.0002429	-5.55	92	97	127.9	-1.3186	1553162_x_at	LOC148137
0.0002438	-5.55	83	224.1	374.9	-1.6729	41047_at	C9orf16
0.0002639	-5.49	83	82.8	123.6	-1.4928	235058_at	FLJ10349
0.0002652	-5.49	83	1500.6	1756.1	-1.1703	218224_at	PNMA1
0.0003203	-5.36	83	646.7	897.7	-1.3881	225098_at	ABI2
0.0003408	-5.31	83	323.4	414.3	-1.2811	40225_at	GAK
0.0003967	-5.21	83	99.1	140.5	-1.4178	239433_at	LRRC8E
0.000293	-5.42	75	258.5	386.8	-1.4963	244523_at	MMD
0.0002137	-5.65	75	294.7	481.6	-1.6342	1558102_at	TM6SF1

CHAPTER 4
KSHV-ENCODED MIRNAS TARGET CELLULAR GENES

Abstract

Recently, 12 miRNA genes have been identified in Kaposi's sarcoma-associated herpesvirus; however, the functions of these miRNAs are relatively uncharacterized as to whether they target viral and/or cellular transcripts. To identify cellular genes targeted by KSHV miRNAs, we performed gene expression profiling on cells which stably express the KLAR miRNA cluster. 65 genes were found significantly downregulated in response to KSHV miRNAs, several of which were confirmed by qRT-PCR. Additional bioinformatics analysis in combination with reporter assays showed that THBS1, a potent regulator of angiogenesis, was targeted by KSHV miRNAs. Multiple KSHV miRNAs were found to target the THBS1 3'UTR, suggesting the importance of downregulating this protein in KSHV tumorigenesis. To identify viral genes that could potentially be targeted by KSHV miRNAs, we performed genome-wide quantitative real-time PCR analyis on latently infected BCBL-1 cells transfected with antagomirs to inhibit viral miRNA activity. No significant differences were observed in the abundance of viral transcripts expressed in control BCBL-1 cells compared to miRNA-inhibited BCBL-1 cells. Together, these data suggest that the primary function of KSHV miRNAs is to target cellular genes, creating a host cellular environment conducive to persistent viral infection, and potentially contributing to viral pathogenesis.

Functions Of KSHV MiRNAs

Data presented in Chapters 2 and 3 are accepted for publication or in the process of being submitted. In this chapter, I will describe some of the work I did in collaboration with Dr. Mark Samols, a former graduate student in the lab, which has now been published, as well as some of my additional work.

Cellular genes targeted by KSHV-encoded miRNAs. Cellular target genes for a single KSHV miRNA, miR-K12-11, have been described in Chapter three. In order to further elucidate the roles of these novel regulators in KSHV-associated pathogenesis, we sought to identify cellular genes targeted by miRNAs encoded within the KSHV miRNA cluster.

To first examine potential cellular targets *in silico,* I used the open-source version of miRanda (Enright et al. 2003) (www.microrna.org) to scan for KSHV miRNA binding sites within a library of >21,000 annotated human 3'UTRs from chromosomes 1 through 22 (www.ensembl.org). The number of predicted target genes ranged from 214 to 1134 amongst various miRNAs (Table 4-1), providing us with a daunting list of potential cellular targets, but also gave us the first indication that KSHV miRNAs might target cellular transcripts.

Next, we experimentally investigated targets using gene expression profiling to observe cellular mRNAs downregulated in response to ectopic KSHV miRNA expression. While some miRNAs, such as *lin-4*, were first thought to interfere predominantly with translation (Lee et al. 1993), it is now known that most miRNAs, including *lin-4,* directly affect mRNA levels (Bartel 2004; Bagga et al. 2005), making gene expression profiling a practical experimental approach to identify targets. 293 cells were generated which stably express miRNAs encoded within the KSHV miRNA cluster (293/pmiRNA) or the vector backbone (293/pcDNA3.1). miRNA sensor vectors containing two antisense complementary binding sites to each miRNA of interest were designed in order to validate miRNA expression in these cells (Fig. 4-1A). Reporter assays and Northern blot analysis confirmed miRNA expression within 293/pmiRNA (Fig. 4-1B and C).

Using Affymetrix-based microarray gene expression profiling, we identified 65 out of 81 significantly altered cellular genes that were downregulated in 293/pmiRNA cells in response to KSHV miRNA expression. Several of the 65 downregulated genes that exhibited high fold

changes, over four-fold, were confirmed by quantitative RT-PCR analysis (Table 4-2). Interestingly, five of these genes have roles in cell proliferation, cell survival, immune modulation, and angiogenesis.

Using an *ad hoc* scanning algorithm created by Dr. Alberto Riva in the Department of Molecular Genetics and Microbiology at the University of Florida, we scanned the 3'UTRs of altered genes for potential miRNA binding sites by looking for 7-mer (nt 2-8) seed match sites. A similar method has been successfully utilized to correlate tissue-specific miRNA expression with low levels of miRNA target genes within those tissues (Sood et al. 2006). We found a significant enrichment for KSHV miRNA binding sites within the 3'UTRs of downregulated genes, further indicating these genes are targeted by KSHV miRNAs (not shown). Using miRanda (Enright et al. 2003), we further investigated potential miRNA binding sites within the 3'UTRs of *SPP1, PRG1, ITM2A, S100A2, RAB27A,* and *THBS1* (Table 4-3). *THBS1* 3'UTR was found to contain at least 34 high probability binding sites for the 11 KSHV miRNA genes tested, strongly suggesting that multiple KSHV miRNAs could target this 3'UTR.

KSHV miRNAs target Thrombospondin-1. Western blot analysis of *THBS1* showed that the protein levels were decreased in KSHV-miRNA expressing cells (not shown), and luciferase reporter assays using antagomirs to specific miRNAs indicated that multiple KSHV miRNAs could target the *THBS1* 3'UTR (Fig. 4-2A). Concomitant targeting of a single 3'UTR by multiple miRNAs has been observed for other miRNAs such as the *let-7* family members and *Ras* (Johnson et al. 2005).

THBS1, known as thrombospondin 1, is a matricellular glycoprotein with cell-cell and cell-matrix adhesion functions as well as strong anti-angiogenic and anti-proliferative activity (de Fraipont et al. 2001; Lawler 2002). Decreased levels of THBS1 have been reported in

KSHV-infected endothelial derived KS tumors (Taraboletti et al. 1999). Additionally, within latently infected TIVE cells, THBS1 levels are downregulated 7-fold as previously published (An et al. 2006) and shown by qRT-PCR (Fig. 4-2B). Thus, downregulation of THBS1 by KSHV miRNAs could contribute significantly to angiogenesis, particularly in KS tumors which are highly vascular (Arasteh and Hannah 2000).

THBS1 can bind directly to and activate TGF-β (Lawler 2002). To determine whether reduced THBS1 levels affected TGF-β signaling, we transfected 293/pmiRNA cells with two different TGF-β responsive reporters. SBE4 contains four Smad-binding elements to which Smad3 can bind within the promoter region while MMP9 contains the matrix-metalloprotease 9 promoter upstream of luciferase and is also responsive to active TGF-β (Chou et al. 2006). We observed decreased activity from both reporters in 293/miRNA cells compared to control cells (Fig. 4-2C). Importantly, the transcript levels of TGF-β and Smad3 were not altered as determined from the gene expression profiling, thus the decrease in TGF-β activity can be accounted for in part by aberrant levels of THBS1. These data indicate that KSHV miRNA target THBS1 and can influence TGF-β signaling, potentially contributing to angiogenesis. This work was published in May 2007.

Samols, M.A., Skalsky, R.L., Maldonado, A.M., Riva, A., Lopez, M.C., Baker, H.V., and R. Renne. (2007). Identification of cellular genes targeted by KSHV-encoded microRNAs. PLOS Pathog 3(5): e65.

293/pmiRNA cells exhibit accelerated growth rates. Many of the genes identified in the gene expression profile of KSHV miRNA expressing cells have roles in cell proliferation and cell survival. For example, SPP1, a glyco-phosphoprotein also known as osteopontin, has anti-proliferative activity in rotavirus-infected mucosal epithelial cells (Rollo et al. 2005) and has

roles in regulating cell adhesion, cell survival, and cell-matrix interactions through binding to integrins (Rangaswami et al. 2006).

To determine the effects of KSHV miRNAs on cell proliferation, I measured the growth rates of 293/pmiRNA cells in comparison to 293/pcDNA3.1 control cells. Cells were plated in 6-well plates and counted using a Coulter counter (Beckman) each day for a period of 6 days. I found that 293/pmiRNA cells grow 1.5 times faster than control cells (Fig. 4-3). In order to verify that this accelerated growth rate is due to KSHV miRNAs, these experiments must be repeated in the presence of antagomirs which specifically inhibit miRNA activity and should presumably restore the growth rate of 293/pmiRNA cells to control cell levels. Additionally, cell proliferation should be monitored by another independent method such as assaying for BrdU incorporation or performing cell cycle analysis using flow cytometry techniques.

To determine whether 293/pmiRNA cells might also be resistant to apoptosis, I attempted to induce Fas-mediated apoptosis using anti-CD95 antibodies. 293 cells are reported to express the Fas-ligand receptor (CD95) and will undergo apoptosis when incubated with the Fas ligand (Larregina et al. 1998). Briefly, 2.5 x 10^4 293/pmiRNA or 293/pcDNA3.1 control cells were plated per well in a 12-well plate and 1 μg/ml anti-CD95 (clone CH11) in media containing 1% FBS was added per well. Cells were incubated for 20 hrs, harvested, and fixed in 70% ethanol. DNA content was stained with propidium iodide and assayed by flow cytometry. Both 293/pmiRNA and 293/pcDNA3.1 cells exhibited between 2% and 6% apoptotic cells (not shown), which is the background level reported for untreated cells (Larregina et al. 1998).

While I was unable to induce apoptosis using this method, further studies are certainly warranted. This protocol can be adapted to Jurkat cells which are highly inducible by the CH11 anti-CD95 antibody. Jurkat cells can be transfected with the miRNA-expressing vector prior to

apoptosis induction and apoptosis can be measured both by propidium iodide staining as well as caspase-8 activation using the Caspase-8 Glo kit (Promega) and a 96-well plate reader.

KSHV miRNAs do not possess transforming activity in mouse fibroblasts as determined by colony formation assays. Overexpression of murine miR-155 in transgenic mice results in splenomegaly and high grade B cell lymphomas (Costinean et al. 2006). Similarly, in a mouse B-cell lymphoma model, expression of the miR-17-92 cluster significantly accelerates lymphoma development (He et al. 2005). Since KSHV is linked to human malignanices including Kaposi's sarcoma and primary effusion lymphoma, we sought to determine whether KSHV miRNAs might possess transforming activity.

NIH3T3 mouse fibroblasts were transfected with pcDNA3.1, pmiRNA, pmiR-155, or pmiRK12-11 and placed under G418 selection for 4 weeks to obtain stable cell lines. miRNA expression was validated by derepression assays using sensor vectors and antagomirs to individual miRNAs (Fig. 4-4A and B). To measure transforming potential, colony formation assays in soft-agar were performed.

Briefly, 10,000 cells were seeded in 0.5% agar and modified eagle's medium (MEM) containing 1% FBS and poured over a 1% agar base layer in 6-well plates. Cells were incubated for over 10 days, and stained with crystal violet to visualize colonies. While we observed colonies growing in wells containing 293 cells (Fig. 4-4C), no colonies were observed from wells containing NIH3T3 cells transfected with the vector control or stably expressing the KSHV miRNA cluster, miR-K12-11, or miR-155. Thus, these miRNAs by themselves do not induce transformation of mouse fibroblasts. One explanation for this result is that these miRNAs might require additional oncogenic stress in order to induce or enhance cellular transformation. This has been observed for the miR-17-92 cluster which enhances tumorigenesis when expressed in

the presence of *Ras* (He et al. 2005; Dews et al. 2006) as well as miR-372 and miR-373 which enhance *Ras*-induced testicular germ cell tumors (Voorhoeve et al. 2006).

KSHV miRNAs likely target cellular mRNAs and not viral mRNAs. Our studies using Affymetrix gene expression profiling to examine cellular mRNAs altered in the presence of KSHV miRNAs provided us with an extensive list of potential cellular genes targeted directly by KSHV miRNAs. EBV, another member of the gamma-herpesvirus family, has been shown to encode a number of miRNAs, one of which, EBV BART2, exhibits complementarity to a region within the EBV genome. It has been proposed that this EBV miRNA directs cleavage of the BALF5 mRNA, possibly during lytic replication (Pfeffer et al. 2004). Another DNA tumor virus, SV40 polyomavirus, has been reported to encode two miRNAs that target the SV40 large T antigen to downregulate the highly antigenic viral protein during persistent infection, potentially as an immune evasion mechanism (Sullivan et al. 2005).

To determine whether KSHV miRNAs might target viral genes, we first examined the viral genome for regions of miRNA complementarity. A total of 30 seed matches (representing the 11 miRNAs cloned by (Samols et al. 2005)) were found antisense to KSHV ORFs (not shown; Cai et al. 2005). A limited number of these seed match sites are predicted to be within 3'UTRs; however, KSHV transcripts are quite complex and many have non-annotated 3'UTRs.

To determine the impact KSHV miRNAs might have on viral gene expression during latent infection, we chose to inhibit miRNA activity in latently infected BCBL-1 cells using antagomirs directed against the KSHV miRNAs. BCBL-1 cells were co-transfected with 100 pmol FITC-labeled control RNAi duplex (Mirus, inc.) and either 30 pmol each of 10 different antagomirs, 300 pmol of the miR-K12-5 antagomir, or 300 pmol of the miR-K12-11 antagomir. As control, cells were transfected with 300 pmol of FITC-RNAi alone. All transfections were

performed in duplicate. 20 hrs post-transfection, cells were FAC-sorted for FITC expression to eliminate the majority of untransfected cells from the populations (Fig. 4-5). Total RNA was harvested 48 hrs later and sent to Dr. Dirk Dittmer's laboratory at the University of North Carolina, Chapel Hill for KSHV genome-wide qRT-PCR analysis.

The PCR genome array designed by the Dittmer laboratory contains primers for every open reading frame within KSHV (Fakhari and Dittmer 2002). The method allows for genome-wide transcript analysis in a highly sensitive, high-throughput manner and has been successfully used to detect minor expression differences from tumors derived from latently-infected endothelial cells transplanted into mice (An et al. 2006).

No differences in viral gene expression were observed between the four samples tested (data not shown). This data indicates that KSHV miRNAs do not likely target viral transcripts, at least during latent infection. It is possible that KSHV miRNAs influence lytic viral gene expression; however, it is not yet determined whether miRNAs are expressed during the early stages of viral infection. Initial experiments to investigate viral miRNA expression during *de novo* infection are currently in progress.

In summary, these data indicate that the major function of KSHV miRNAs is to target cellular genes, some of which such as THBS1, have potential roles in KS biology. Experiments to further investigate the effects of KSHV miRNAs on cellular gene expression and the biological consequences associated with this type of post-transcriptional regulation are currently ongoing in the laboratory. Such experiments will hopefully answer whether KSHV miRNAs contribute directly to pathogenesis within the infected host.

A

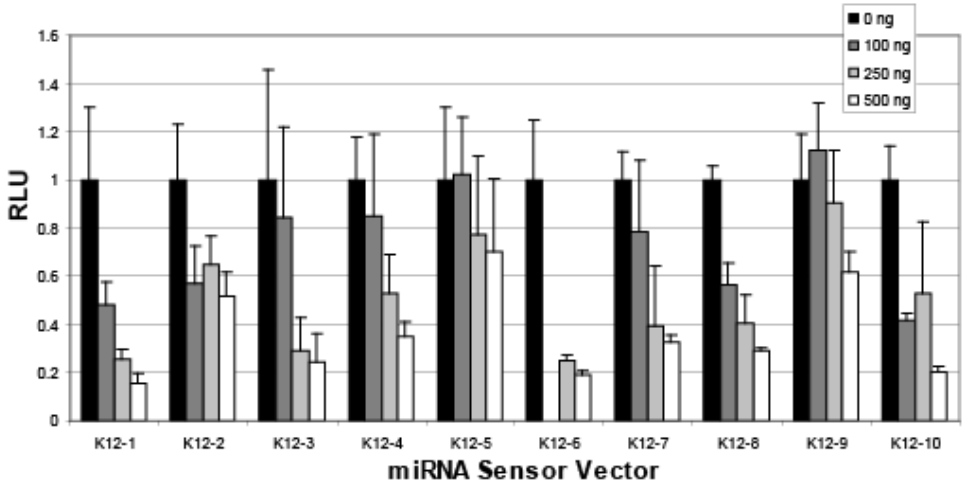

B

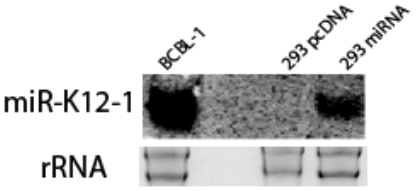

C

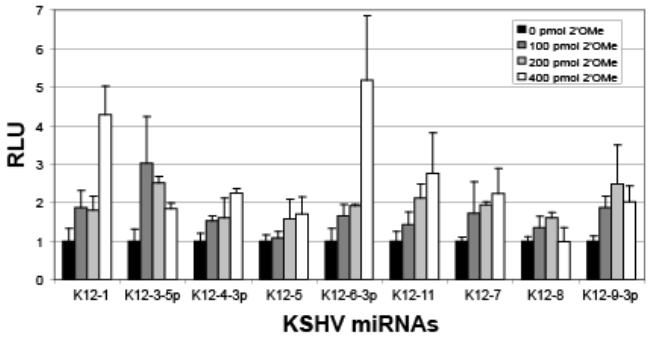

Figure 4-1. Validation of miRNA expression in 293 cells. A. Luciferase assays with all miRNA sensor vectors and miRNA expression vectors. 293 cells were transfectged with 40 ng sensor vector and increasing amounts of miRNA expression vector (0 to 500 ng). B. Luciferase de-repression assays show expression of all miRNAs within the cloned cluster in 293 pmiRNA cluster cells. The level of 2'OMe RNA was kept constant at 400 pmol with filler 2'OMe targeting miR-K12-10, a KSHV miRNA not represented in the cluster. 200 ng of luciferase sensor was transfected along with the noted amounts of 2'OMe RNA specific to that miRNA. Transient transfection assays were done twice in triplicate and luciferase activity was normalized to total protein concentration. C. Northern blot analysis of KSHV miRNAs in 293 pmiRNA cluster cells versus 293 pcDNA control cells and BCBL-1 cells. 30 μg of total RNA was loaded and hybridized to a probe for miR-K12-1. Ribosomal RNA shown as a loading control.

A

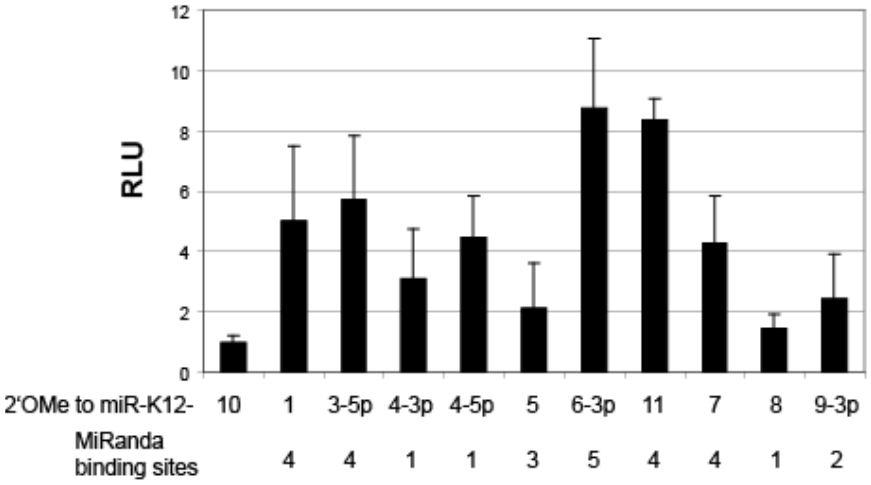

B

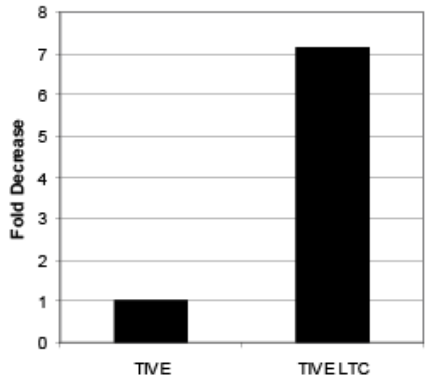

C

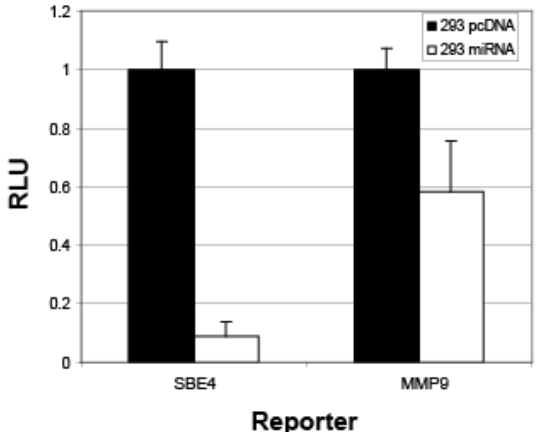

Figure 4-2. KSHV miRNAs target thrombospondin 1. A. Multiple KSHV miRNAs can target the THBS1 3'UTR. 293/pmiRNA cells were transfected with pGL3-THBS1, containing 2 kb of the THBS1 3'UTR downstream of luciferase, and the antagomir indicated. 72 hrs post-transfection, lysates were assayed for luciferase expression (Promega). Light units are normalized to total protein determined by BCA (Pierce). Data is normalized to the control antagomir, 2'OMe-K12-10. B. THBS1 is downregulated in KSHV latently infected endothelial cells (TIVE LTC). Total RNA was harvested from uninfected TIVE and long-term infected TIVE-LTC cells, reverse transcribed, and analyzed by quantitative PCR for levels of THBS1. A 7-fold decrease in THBS1 levels was observed in TIVE-LTCs. C. Decreased THBS1 levels in 293/miRNA cells result in reduced TGF-β activity. 293/pmiRNA or 293/pcDNA3.1 control cells were transfected with two TGF-β responsive luciferase

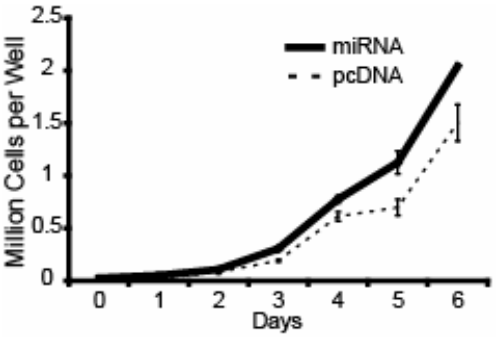

Figure 4-3. 293/pmiRNA cells exhibit an accelerated growth rate. 293-miRNA or 293-pcDNA cells were plated at 3x10^4 cells per well in a 6-well plate. Cells were trypsinized and counted at days indicated. Curves represent the average of two experiments performed in triplicate.

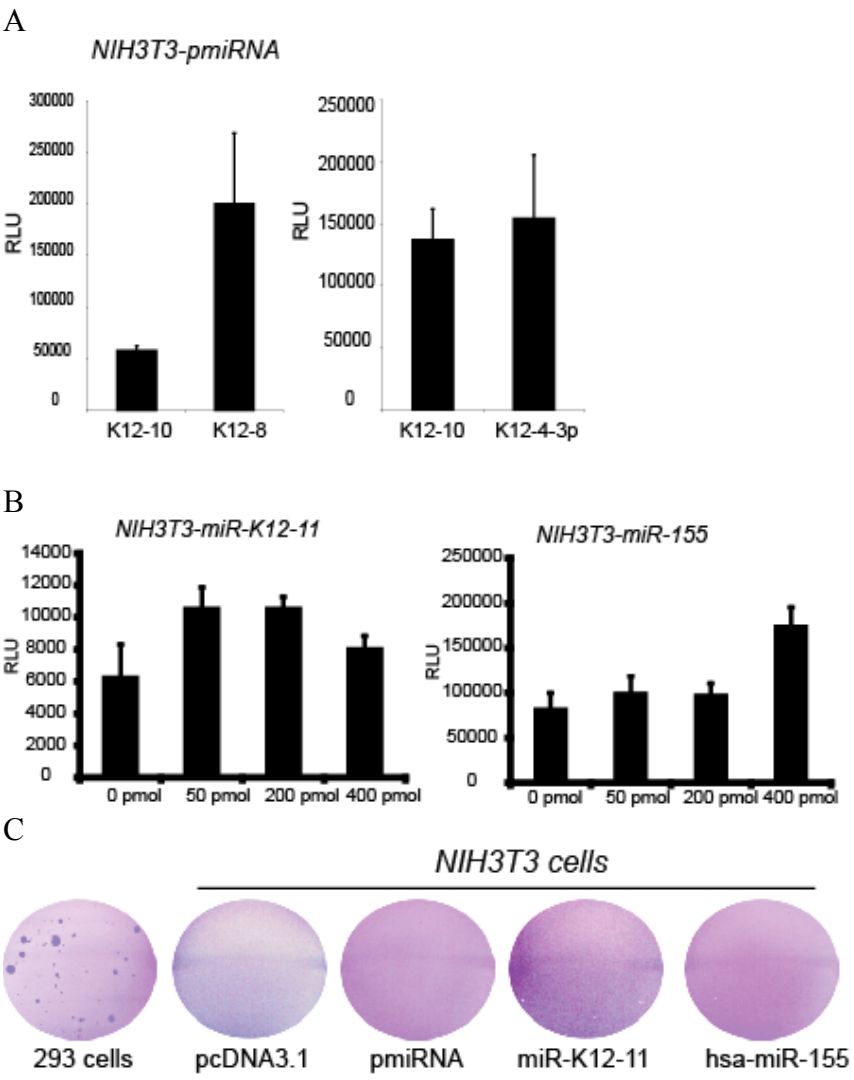

Figure 4-4. KSHV miRNAs do not possess transforming activity. NIH3T3 cells were transfected (Lipofectamine 2000, Invitrogen) with pcDNA3.1, pmiRNA, pmiR-K12-11, or pmiR-155 and selected with G418 for >3.5 wks. A. To test for miRNA expression, a miRNA-specific sensor vector and 400 pmol of antagomir corresponding to either miR-K12-8 or miR-K12-4-3p was transfected into NIH3T3/pmiRNA cells. 400 pmol of miR-K12-10 antagomir was used as control. B. Sensor vectors and increasing amount of antagomirs specific to miR-155 or miR-K12-11 were used to validate miRNA expression in NIH3T3/K12-11 and NIH3T3/155 cells. K12-10 antagomir was used as filler. All transfections were performed in triplicate. Cell lysates were harvested at 48 hrs. Light units are relative to total protein determined by BCA (Pierce). C. NIH3T3 cells expressing KSHV miRNAs or hsa-miR-155 do not form colonies in soft agar. Colonies were stained with crystal violet >14 days after plating.

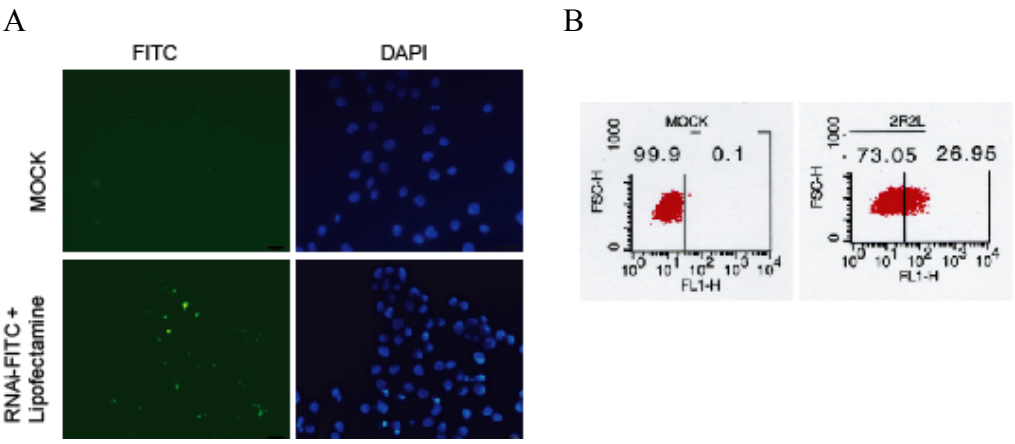

Figure 4-5. FACS of BCBL-1 cells transfected with RNAi-FITC. A. BCBL-1 cells were transfected with 100 pmol FITC-RNAi duplex (Mirus) using Lipofectamine 2000 according to manufacturer's instructions (Invitrogen). Mock indicates 100 pmol FITC-RNAi, but no transfection reagent. B. 24 hrs post-transfection, cells were analyzed for FITC-expression by flow cytometry.

Table 4-1 Target predictions for KSHV miRNAs

KSHV miRNA	**# hits (top 5%)**	**# Genes (top 5%)**
K12-1	301	214
K12-3-5p	1605	1134
K12-4-3p	607	443
K12-11	531	390
K12-9	836	633

Table 4-2 qRT-PCR confirmation of select downregulated genes

Gene	Microarray %CV support	Microarray Fold Change	Microarray p-value	qRT-PCR fold change	qRT-PCR p-value
SPP1	100	-20.44	1.00E-06	-93.31	0.005
THBS1	100	-6.10	3.20E-05	-6.83	0.005
S100A2	100	-5.03	2.00E-06	-16.18	0.005
PRG1	100	-4.27	1.00E-06	-8.82	0.005
ITM2A	100	-4.06	1.76E-04	-4.54	0.1
RAB27A	100	-1.35	3.11E-04	-1.22	0.5

Table 4-3 Predicted binding sites within 3'UTRs of select genes

Gene	# potential binding sites	Targeting miRNAs
SPP1	4	10a, 1, 6-3p, 4-3p
S100A2	10	9-5p, 7, 6-5p, 6-3p, 5, 4-3p, 3-5p, 3-3p,
THBS1	34	10a, 10b, 11, 1, 2, 9-3p, 8, 7, 6-5p, 6-3p, 5, 4-5p, 4-3p, 3-5p, 3-3p
ITM2A	3	1, 6-5p, 4-3p
RAB27A	28	10a, 10b, 11, 1, 2, 9-5p, 9-3p, 8, 6-5p, 6-3p, 5, 4-5p, 4-3p, 3-5p, 3-3p
PRG1	7	10a, 10b, 11, 1, 2, 9-3p, 3-5p

CHAPTER 5
CONCLUSIONS AND FUTURE DIRECTIONS

LANA is a multifunctional protein, encoded by ORF73 within the KSHV latency-associated region (KLAR), required for the maintenance of viral episomes during latent infection. Latent episome maintenance is a two-step process, involving both viral DNA replication and partitioning of episomes to daughter cells. My studies in Chapter two focused on the early events mediated by LANA contributing to the establishment of episome maintenance. Additionally, I investigated the *cis*-elements involved in episome partitioning. These experimental results directly contribute to our understanding of LANA-mediated episome maintenance which lies at the core of KSHV latency.

Important for latency are transcripts expressed from the KLAR (Fig. 1-5). 12 recently identified miRNAs are also encoded within this region. My studies presented in Chapters three and four investigate the regulatory targets of these miRNAs. I focused on a single viral miRNA, miR-K12-11, which has seed sequence homology to the human oncogenic miR-155, and demonstrated that these two miRNAs can regulate a common set of cellular genes. In collaboration with Dr. Mark Samols, we identified several cellular genes targeted by the KSHV miRNA cluster, which have roles in angiogenesis and cell proliferation. Together, these data show that KSHV miRNAs modulate the host cellular environment and potentially, contribute to pathogenesis and possibly, tumorigenesis.

LANA Significantly Enhances KSHV Replicon Retention

Using KSHV GFP-reporter replicons and short-term maintenance assays, we observed that LANA significantly enhances replicon retention when provided *in cis* or *in trans* (Fig. 2-2). More importantly, we were able to quantitatively analyze these events at early time points after introduction of the DNA into cells during the first few cell divisions. These experiments

highlighted that early events mediated by LANA are crucial in determining the efficiency by which episomes are established and stably maintained. Additionally, we were able to observe stable, long-term replicon maintenance in transfected cells for the first time under non-selective conditions (Fig. 2-5). Our data is in contrast to that of Grundhoff and Ganem (Grundhoff and Ganem 2004) who utilized a similar GFP-reporter replicon system but did not observe any differences in KSHV replicon maintenance in the presence or absence of LANA.

A number of key differences between our assay system and that utilized by Grundhoff and Ganem are likely responsible for these discrepancies. To look for stable replicon maintenance under non-selective conditions, Grundhoff and Ganem analyzed batch-sorted populations and found that LANA-expressing cells completely lost TR-plasmids, as determined from GFP-expression and Southern blot analysis, in as little as two weeks. Under these conditions, we too have observed rapid loss of GFP expression from LANA-positive populations within two weeks (not shown); however, these results suggested to us that the frequency of events resulting in stable episome maintenance may be too low to measure using a population-based assay. Further evidence of this comes from the fact that TR-plasmids can be maintained in the rare cells which arise following antibiotic selection (Ballestas et al. 1999; Grundhoff and Ganem 2004). Additionally, a few cases in which cells of endothelial origin (TIVE and SLK) support stable latency following *de novo* infection have been reported (Bechtel et al. 2003; Grundhoff and Ganem 2004; An et al. 2006), indicating that establishment of latent viral episomes is achievable *in vitro*.

In order to focus on the potentially very small number of maintenance events, we performed a clonal analysis, and FAC-sorted GFP-positive cells into 96-well plates immediately following transfection. Examination of individual clones in the two months that followed

showed that TR-plasmids could indeed be maintained as episomes in a LANA-dependent manner at a low frequency under non-selective conditions. Interestingly, the percent of GFP-expressing cells within the individual clonal populations that arose ranged from 16.3% to 55.3% (Fig. 2-5) which, if taken within the context of the entire originally transfected population, translates to ~1% GFP-positive, which is the background levels of GFP-expression seen both by us (not shown) and Grundhoff and Ganem in a population-based assay.

To investigate replicon kinetics at early times after transfection, we implemented a new method of transfection (amaxa, inc.) which preserved cell viability for FAC-sorting and enabled us to drastically reduce the number of plasmid molecules transfected to an optimized 5,000 copies per cell (~200 ng or 0.04 fmoles). These transfection conditions are in contrast to the experiment mentioned above in which 15 μg of plasmid DNA was used, which also induced cell death in >30% of cells. Rapid GFP expression, which occurs within three to six hours with this new transfection method (not shown), allowed us to measure replicon kinetics within the first cell divisions.

Using these optimized conditions, we found that, when provided *in cis*, LANA enhances TR-plasmid retention two-fold, and *in trans*, four-fold (Fig. 2-2). This system allowed us also for the first time to observe LANA-mediated partitioning events in the absence of DNA replication. We found that plasmids containing LBS1/2 alone could be retained short-term in the presence of LANA (Fig. 2-6), indicating that episomes can be stabilized and tethered independently of replication.

The replicon system described here has numerous applications. For instance, this system can be used to evaluate potential therapeutic agents that might disrupt or alter the establishment of episomes from either the replication aspect or the partitioning process. Replicon kinetics can

be measured in the presence of candidate drugs targeted either at LANA or at cellular proteins involved to determine whether such agents influence episome retention. Given that the ultimate therapeutic agent would target latently infected cells which maintain stable viral episomes, such agents could also be applied to stably maintaining GFP positive clonal populations and cells could be monitored for the loss of replicons either by loss of GFP expression or loss of DNA by Southern blot. To this point, I have treated three clonal populations (L-A3, L-C3, and L-C4) with hydroxyurea, an agent that alters Parp1 activity (Ohsaki et al. 2004) and induces EBV episome loss in certain Burkitt's lymphoma cell lines (Takada and Ono 1989), but was unable to observe any loss of replicons (not shown). These very preliminary experiments need to be repeated using our newly refined replicon system.

LBS1/2 Function As A *Cis*-partitioning Element

EBV oriP contains two distinct elements: a replication origin in DS and multiple EBNA-1 binding sites within FR for episome partitioning. While the minimal sequence requirements for latent KSHV replication have been defined (Hu et al. 2002; Hu and Renne 2005), sequences for DNA partitioning have not been formally determined. A single TR confers DNA replication with the same efficiency as two TRs in short-term replication assays (Hu et al. 2002). For long-term maintenance, a single TR is reported to be inefficient while two copies of TR convey efficient maintenance (Ballestas et al. 1999; Ballestas and Kaye 2001). We quantified the contribution of multiple TRs to episome maintenance and found that four TRs were twice as efficient as two TRs which were twice as efficient as a single TR (Fig. 2-7 and 2-9). This enhanced maintenance with additional TRs was not surprising given that KSHV genomes contain an average of 35 to 45 copies of TR, each with a pair of LANA binding sites. Whether all TRs are utilized for partitioning in the context of the viral genome is not known, and it is possible that the multiple TRs coordinate with LANA and cellular proteins to form a higher

order structure during stable episome maintenance. Such a question might be examined using a KSHV Bacmid with variable numbers of TRs or a mixture of TRs that lack LBS1/2 and other *cis*-elements, such as the replication element (RE), known to be important in episome replication and partitioning.

To dissect the replication and partitioning elements of KSHV, we generated hybrid origins and demonstrated that partitioning could be conferred by multiple LBS1/2 within consecutive copies of TR, forming an array of LANA binding sites analogous to the multiple EBNA-1 sites within FR (Fig. 2-7). Interestingly, these experiments also revealed that LBS1/2 was less efficient at maintenance than a full length TR (Fig. 2-7). There are many possible explanations for this observation as mentioned in Chapter two; however, the two most plausible explanations are either that cellular proteins that bind TR outside of LBS1/2 contribute to maintenance and thus no longer have an affect in the absence of surrounding TR sequences, or that the TR assumes a favorable epigenetic structure which is disrupted when only LBS1/2 are present.

Future Directions For Episome Maintenance Studies

Tethering and a mechanism for non-random partitioning. While we have shown that LBS1/2 function as a *cis*-partitioning element, several unanswered questions still remain regarding episome tethering and partitioning. Replication deficient plasmids are retained short-term in the presence of LANA. This data indicates that plasmids can be tethered to chromosomes independently of replication. Determining whether this is truly the case can only be addressed by single-cell techniques such as fluorescent *in situ* hybridization (FISH). Using microscopic and flow-cytometry based techniques, additional questions regarding the non-random nature of episome partitioning can also be addressed.

To this purpose, I have generated full length LANA and LANA-C terminus fusion proteins containing an N-terminally linked red fluorescent protein (RFP) to observe LANA bound to viral

genomes or potentially, TR DNA, *in situ* (Fig. 5-1). In collaboration with Dacia Kwiatkowski (IDP student), we used these fluorescent proteins to ask whether KSHV latently infected endothelial cells harbored stable episome copy numbers. We transfected pLANA-RFP or pLANA-C-RFP into latently infected SLK KSHV+ or TIVE-LTC cells and examined individual nuclei by confocal microscopy. Assuming that each concentrated fluorescent LANA speckle correlated with a single viral episome, we enumerated the viral copy number per cell and found an average of 21 viral genomes per SLK KSHV+ nucleus. Quantitative PCR and genomic Southern blot analysis further validated these results (Fig. 5-1). These data show that fluorescent-tagged LANA proteins bind to viral genomes *in vivo* and can be used as a tool to study episome tethering. Additionally, these results indicate that once established, viral copy number is stable within *de novo* infected endothelial cells as is observed in PEL-derived cell lines. A similar observation has been made using a high-throughput single cell analysis of immunofluorescent stained infected cells (Adang et al. 2006) which further supports the idea that episome partitioning for KSHV is non-random.

To test tethering by FISH, concatamerized TR plasmid such as the Z6 cosmid (Ballestas et al. 1999) or one containing multiple sets of LBS1/2 (>10) can be generated and co-transfected with LANA-RFP or introduced into a cell line that stably expresses LANA-RFP. Alternatively, in order to concentrate enough LANA molecules for visualization, LANA or N-terminal LANA, which is important for chromosome binding, could be fused to a Gal-4 DNA binding domain and used together with a plasmid containing multiple Gal-4 binding sites. Combining this with high throughput single cell imaging such as multispectral imaging flow cytometry (MIFC) (Adang et al. 2006) could be very powerful in determining (i) when tethering occurs- i.e. upon immediate introduction of the DNA into the nucleus or during a specific stage of the cell cycle such as prior

to replication, (ii) whether tethering occurs independently of replication as indicated by our data (Fig. 2-6), and (ii) whether cellular factors either ectopically expressed or knocked down via siRNA increase or inhibit tethering.

To explore the mechanism of faithful episome segregation, infected, transfected, or microinjected cells can be synchronized. FISH can be used to analyze viral genome localization over the course of the cell cycle. Given that the foundation for appropriate chromatid separation is set forth during late telophase, coinciding with pre-RC assembly (Nasmyth 2001; Sasaki and Gilbert 2007), I would predict that the foundation for faithful tethering is also developed during this time and thus newly synthesized viral genomes would become tethered symmetrically to opposite arms of the sister chromatids in synchrony with chromosome replication, thus preserving the viral copy number. Likely, the predicted symmetrical pairs of episomes would become more apparent as chromatin condensation ensues in mitosis. Using replication-deficient plasmids, we can also ask whether replication of the viral DNA itself or the cellular microenvironment where replication takes places might contribute to faithful episome segregation. Interestingly, one study has found that exogenous plasmids when nuclear injected into cells during early S-phase assemble into transcriptionally competent, hyperacetylated chromatin which is preserved even after cell division while those injected in late S phase assemble into transcriptionally repressed, inactive chromatin (Zhang et al. 2002).

Thus, the cellular environment within a specific cell cycle phase, such as S phase, appears to be tightly linked to the type of epigenetic factors available and chromatin structure established. Additionally, early S phase seems to be when heritable DNA modifications are set forth. Given that LANA itself promotes S-phase entry by interactions with Rb and GSK3β (Radkov et al. 2000; Fujimuro et al. 2003), it is likely that LANA also influences

epigenetic modifications which occur to the viral episome during and/or prior to replication and tethering.

Epigenetic factors influencing episome stability. The mechanisms underlying faithful episome partitioning are likely tightly linked to cellular epigenetic factors. Indeed, the cohesin complex itself, responsible for proper chromosome segregation, is actually loaded onto DNA by the SWI/SNF2 chromatin remodeling complex and the state of DNA methylation can influence cohesin loading (Hakimi et al. 2002). Both our own experiments designed to investigate the role of LANA in episome establishment as well as reports from several other labs (Leight and Sugden 2001; Grundhoff and Ganem 2004; Stedman et al. 2004) indicate that epigenetic factors play a role in mediating episome stability, thus contributing to the establishment and maintenance of viral episomes. Evidence of this comes largely from the fact that established, stable replicons within drug-resistant cells remain genetically intact, thus are not altered in any way at the DNA sequence level (Chapter 2; (Leight and Sugden 2001; Grundhoff and Ganem 2004).

The epigenetic determinants involved specifically in viral episome stability following *de novo* infection remain to be defined. Studies of HSV-1 show that HSV-1 genomes lack nucleosome structure within virions and become assembled around histones early after infection, taking on a chromatin structure characteristic of active transcription (euchromatin) with enriched histone acetylation and lack of histone methylation (Kent et al. 2004). During latent infection, the genome becomes organized into transcriptionally permissive and transcriptionally silent regions which correlate with the major latency-associated transcript (LAT) and lytic genes, respectively (Kubat et al. 2004b; Kubat et al. 2004a). EBV latent genomes are also tightly regulated by epigenetic modifications. DNA methylation, for example, regulates both the Wp and Cp promoters which express EBNA-1 (Robertson et al. 1996; Robertson and Ambinder

1997; Tao et al. 1998; Tao et al. 1999) as well as LMP promoters (Falk et al. 1998). Additionally, distinct patterns of histone modifications control expression of EBNA-2 and LMP1 during latency (Chau and Lieberman 2004). Classic studies have shown that introduction of plasmid DNA such as SV40 DNA into the nucleus results in the immediate development of chromatin structure which is detectable as ladders by micrococcal nuclease treatment within 36 to 80 hours post-transfection (Cereghini and Yaniv 1984) and such plasmid DNA associates with nuclear structures such as the nuclear matrix thus allowing the DNA to become transcriptionally competent (Jeong and Stein 1994). While these observations indicate that chromatin assembly is an inherent process, it is likely that virally encoded origin binding proteins such as LANA help regulate the organization, preservation, and modifications of chromatin architecture to stabilize latent viral episomes.

For KSHV, the majority of lytic genes, such as ORF50, are suppressed both by DNA methylation and histone modifications. Evidence of this comes from the fact that lytic gene expression can be induced by treating latently infected cells with histone deacetylase (HDAC) inhibitors such as trichostatin A (TSA) or NaB (Lu et al. 2003). Examination of the CpG suppression status of herpesvirus genomes showed that γ-herpesviruses in general show CpG suppression whereas α- and β- herpesviruses exhibit a relatively normal CpG status (Chen et al. 2001). Additionally, the ORF50 promoter is highly methylated in latently infected PEL cells which can also be reactivated by treatment with 5'azacytidine, a DNA methyltransferase inhibitor (Chen et al. 2001).

During latent DNA replication, the chromatin architecture surrounding the origin within KSHV TR is extensively remodeled. Histone modifications occur in a cell cycle dependent manner- histone H3 is acetylated and methylated at Lys4 in S phase- likely creating a more open

DNA structure to permit accessibility of the cellular replication machinery (Stedman et al. 2004). Recently identified TR-interacting proteins include BRG1 (Si et al. 2006), a known member of the ATP-dependent chromatin remodeling complexes that also include SNF2 which alter nucleosome positioning and DNA accessibility during replication (Becker and Horz 2002). S phase is also the time when new histones are deposited onto newly replicated DNA (Mello and Almouzni 2001). Additionally, a number of replication and epigenetic factors such as proliferating cell nuclear antigen (PCNA) and DNA methyltransferase 1 (DNMT1) interact and localize to distinct replication foci to preserve the epigenetic state of the DNA which is inherited into the next generation (Shibahara and Stillman 1999; Zhang et al. 2000; Iida et al. 2002). EBNA-1 has been reported to co-localize with these replication foci (Ito and Yanagi 2003); however, similar studies for KSHV have not yet been done.

The refinement of our KSHV GFP-reporter replicon system allows us now to address the timing and nature of chromatin assembly on newly introduced replicons. To look at histone modifications at various times leading to the establishment and stabilization of episomes, chromatin immunoprecipitation (ChIP) studies can be performed in the presence and absence of LANA using antibodies to methylated or acetylated histones. Such studies could potentially answer whether LANA itself contributes to or alters chromatin assembly as has been proposed for EBNA-1 (Chau and Lieberman 2004). Our data in Chapter 2 indicates that replication and partitioning are independent processes for KSHV, and plasmids containing the *cis*-partitioning element LBS1/2 alone can be stabilized by LANA. Using this system in conjunction with ChIP assays, we can now ask whether there are distinct epigenetic states determined by active replication or simply tethering by itself.

Epigenetic modifications include not only histone modifications but also DNA methylation. In mammalian cells, DNA methylation is a heritable modification mediated by DNA methyltransferases (DNMTs). These enzymes covalently modify cytosine residues by adding a methyl group, creating 5' methyl cytosines. Methyl-cytosine binding proteins can bind methylated CpGs and recruit histone deacetylases, resulting in a highly condensed state of chromatin and transcriptional repression (Nan et al. 1998; Fuks et al. 2003). Interestingly, LANA is known to interact with MeCP2 and SUV39H1, a histone methyltransferase (Krithivas et al. 2002; Sakakibara et al. 2004). Additionally, heterochromatin components such as HP1α and methylated histone H3 are found associated with TR in a LANA-dependent manner (Sakakibara et al. 2004). MeCP2 and heterochromatin protein 1 (HP1) have been found co-localized with a DNA methyltransferase, DNMT3a, at sites of pericentromeric heterochromatin in mouse embryonic fibroblasts (Bachman et al. 2001). DNMT3a facilitates *de novo* methylation of DNA while DNMT1 preserves DNA methylation patterns during cellular replication (Okano et al. 1999; Grace Goll and Bestor 2005). Recently, LANA has been shown to interact directly with DNMT3a, an association that has been linked to transcriptional repression of several cellular promoters (Shamay et al. 2006). We propose this interaction may also contribute to the establishment and stability of viral episomes.

Within this context, we have examined the maintenance of *in vitro* methylated TR-plasmids in the presence of LANA and have observed that this type of modification inhibits plasmid maintenance (Fig. 2-11). It is possible that *in vitro* methylated plasmids do not replicate efficiently. This can easily be tested using *DpnI*-based short term replication assays previously described (Hu et al. 2002). Alternatively, it is possible that methylation disrupts the binding of DNMT3a and other chromatin factors to newly introduced TR-plasmids and therefore, such

plasmids are no longer stabilized. This can be addressed by co-transfecting KSHV replicons with DNMT3a and examining not only their retention kinetics, but also their methylation status either by restriction enzyme analysis or bisulfite sequencing analysis at time points following transfections.

In conclusion, LANA interacts with many chromatin-associated proteins, but where these interactions take place, either on viral or cellular chromatin or both, is still unknown. Understanding these molecular interactions will further define our model of how cellular and viral proteins coordinate to stabilize and maintain viral episomes. Additionally, a number of viral proteins as well as miRNAs encoded within KLAR modulate the host cell environment which may also contribute to the establishment and maintenance of viral latency.

KSHV MiR-K12-11 Is A Member Of The MiR-155 MiRNA Family

KSHV miRNAs lack sequence homology with the majority of metazoan miRNAs (Samols et al. 2005). To determine whether seed sequences, shown to be important for target recognition, might be conserved, we aligned the sequences of herpesvirus-encoded miRNAs against the human miRNA database. KSHV miR-K12-11 exhibits 100% seed sequence identity with miR-155, an oncogenic miRNA (Fig. 3-1). Analysis of miR-K12-11 and miR-155 showed that both miRNAs could target a common set of genes which was due in part to the observed seed sequence identity (Fig. 3-8 and 3-9).

Bioinformatics tools predicted BACH-1 as a potential target for both miRNAs. Using luciferase reporter assays, we showed that specific seed match sites within the BACH-1 3'UTR are targeted by both miR-K12-11 and miR-155 (Fig. 3-4). Additionally, gene expression profiling studies and seed sequence analysis identified TM6SF1, a protein with no known function, as a common target, which was verified by luciferase assays (Fig. 3-10). We have recently identified a number of cellular genes targeted by multiple miRNAs encoded within the

KSHV miRNA cluster (Samols 2007). The list of genes targeted by miR-K12-11 represents the first cellular genes targeted by a single, specific KSHV miRNA. To the best of our knowledge, this is also the first viral miRNA demonstrated to have a cellular ortholog and target a common set of genes.

The identification of common genes downregulated in response to both miR-K12-11 and miR-155 now provides us with a unique opportunity to analyze the contribution of the 3' region of each miRNA to target recognition. We are currently in the process of cloning seven additional 3'UTRs (*TRIM32, MMD, LDOC1, MALAT1, MATR3, BCL6B, and NFAT2CIP)* identified as potential targets by expression profiling and bioinformatics tools, and performing luciferase assays to confirm miRNA-dependent targeting of these genes. Once additional targets have been validated, we can perform extensive mutational analysis on these 3'UTRs as has been done for BACH-1 (Fig. 3-4). While the 5'seed sequence is known to be critically important (Lewis et al. 2003; Stark et al. 2003; Lewis et al. 2005), the 3' end of the miRNA can help determine target specificity and target site selection (Brennecke et al. 2005). A greater understanding of the pairing between a miRNA and its targets will certainly aid in refining target prediction criteria.

We found that six viral miRNAs exhibited seed sequence homology to human miRNAs, some with known tumor suppressor or oncogenic activity. Thus, herpesviruses, through co-evolution with their human hosts, have pirated miRNA genes in addition to genes such as v-Bcl-2, v-IRF, and v-IL-6, which all have cellular counterparts (Russo et al. 1996; Neipel et al. 1997), in order to modulate the host cell environment. Sequence analysis of miRNAs from additional non-human herpesviruses such as RRV, MHV68, and MDV, as well as polyomaviruses, may further support this observation.

Sequence alignments of human herpesvirus miRNAs against the human database showed not only 5'seed sequence homology for six viral miRNAs, but also homology within the 3'end of the miRNA; notably, EBV-BART3-5p with hsa-miR-652 and EBV-BART8-5p with hsa-let-7g (Fig. 3-1). 3'compensatory binding sites have been reported (Brennecke et al. 2005), and it is possible that miRNAs with 3'sequence homology may also share a limited set of common targets. The let-7 family has reported tumor suppressor activity, and negatively targets Ras and Myc oncogenes (Johnson et al. 2005). EBV, in contrast, is linked to human malignancies such as Burkitt's lymphoma (Liebowitz and Kieff 1993). It is possible that EBV-BART8-5p could interfere with let-7 dependent regulation by mimicking let-7, and indirectly contribute to tumorigenesis. Recently, the loss of let-7 regulation of Hmg2a, a chromatin-modifying protein with oncogenic activity, has been shown to promote cellular transformation (Mayr et al. 2007). Thus, disruption of cellular miRNA-dependent regulation of protein expression potentially by viral miRNAs could have adverse biological consequences.

KSHV MiRNAs Target Cellular Genes

To experimentally determine cellular genes targeted by the KSHV miRNA cluster, we performed gene expression profiling, and identified a set of 65 genes downregulated in response to KSHV miRNAs. The 3'UTRs for several of these genes were significantly enriched for KSHV miRNA seed-match binding sites, indicating that these genes could be targeted directly by KSHV miRNAs.

Based on this data, we chose several genes for additional analysis. Five genes, which were confirmed by qRT-PCR, have roles in cell proliferation (*SPP1, THBS1*), cell survival (*PRG1, S100A2*), angiogenesis (*THBS1*), and immune modulation (*SPP1, ITM2A*), all cellular pathways which are often altered in cancers. Interestingly, I also observed an increased growth rate of

293/pmiRNA cells (Fig. 4-3), suggesting that one consequence of KSHV miRNA-dependent regulation is to aid cell proliferation.

Luciferase reporter assays showed that multiple KSHV miRNAs could target the 3'UTR of thrombospondin 1 (THBS-1) both in 293 cells (Fig. 4-2) and in a Burkitt's lymphoma B cell line (Samols 2007). THBS-1 is a potent regulator of angiogenesis (Lawler 2002) and has been shown to be regulated also by the miR-17-92 cluster, in particular miR-19 (Dews et al. 2006). Additionally, knockdown of Dicer and Drosha in endothelial cells increases levels of THBS-1 and impairs angiogenesis *in vitro* ((Kuehbacher et al. 2007), indicating that THBS-1 may be tightly regulated by additional cellular miRNAs. It will be interesting to determine in the future whether KSHV miRNAs influence the targeting of cellular miRNAs on the THBS-1 3'UTR. This could be investigated by direct target cloning techniques as first demonstrated by Vatolin et. al. (Vatolin et al. 2006). RNA from cytoplasmic extracts enriched for RISC-bound mRNAs from cells expressing KSHV miRNAs can be used to generate a cDNA pool. miRNAs bound to their corresponding targets can be used directly as primers for the first round of DNA synthesis. Using nested PCR in combination with TA-cloning, a miRNA-target library can then be generated. By comparing miRNA-target libraries of KSHV miRNA expressing cells to control cells, we will be able to determine whether KSHV miRNAs affect cellular miRNA targeting of 3'UTRs such as THBS-1.

We found that the downregulation of THBS-1 directly affected TGF-β activity in 293/pmiRNA cells (Fig. 4-2). Interestingly, another member of the herpesvirus family, HSV-1, encodes miR-LAT which downregulates TGF-β and Smad3, consequently producing an anti-apoptotic phenotype (Gupta et al. 2006). Although I was unable to measure apoptosis in 293 cells expressing the KSHV miRNA cluster (Chapter 4), it is likely that the downregulation of

THBS-1 and thus TGF-β activity, affects apoptosis. Additionally, we found that both Bim and Btf, two pro-apoptotic Bcl-2 family members, were downregulated in 293/miR-K12-11 cells (Chapter 3), and thus, might also contribute to a pro-survival phenotype. These pathways need to be further investigated by performing apoptosis assays in KSHV miRNA-expressing cells. Experiments to test THBS-1 effects on cell migration in response to KSHV miRNAs using matrigel-based assays with primary endothelial cells are also planned in the laboratory. Investigating the consequences of THBS-1 downregulation by KSHV miRNAs will put us in the direction of determining whether targeting this pathway could be used as a valuable therapeutic tool.

Future Directions For KSHV MiRNAs

KSHV miR-K12-11 in B cells. The recent link of miR-155 to normal B cell development (Rodriguez et al. 2007; Thai et al. 2007) suggests that miR-K12-11 may also regulate B-cell specific genes. miR-155 is expressed within B and T lymphocytes following activation, but absent from progenitor and resting cells, and has a critical role in regulation of the germinal center reaction during B cell development (Thai et al. 2007). Abnormal high levels of miR-155 have been observed in many B cell lymphomas representing several stages of B cell development (van den Berg et al. 2003; Eis et al. 2005; Lawrie et al. 2007). Interestingly, we found that KSHV-infected PEL-derived cells do not express miR-155, but do express the KSHV ortholog, miR-K12-11 (Fig. 3-2). PEL cells have a transformed plasma cell phenotype (Jenner et al. 2003) and have undergone somatic hypermutation evident from rearranged immunoglobulin genes (Matolcsy et al. 1998; Fais et al. 1999). The progression to this late stage of B cell development is due in part to precise regulation of miR-155 expression (Thai et al. 2007).

We have demonstrated that miR-155 and miR-K12-11 can target a common set of cellular genes in 293 cells (Chapter 3). Given that PEL cells highly express miR-K12-11, it is possible that miR-K12-11 continues to regulate a set of miR-155 targets within B cells following miR-155 downregulation, thus contributing to dysregulated B cell proliferation and lymphomagenesis. To test this, miRNA targets within primary B cells can be examined both in tissue culture and in animal models. MiR-155 or miR-K12-11 can be introduced into primary B cells and cells can be assayed for cell growth, as well as the presence of cell surface markers using flow cytometry.

Overexpression of miR-155 in transgenic mice results in splenomegaly and high grade B cell lymphomas (Costinean et al. 2006). To test whether miR-K12-11 might also produce lymphomas within an animal model, Isaac Boss, a graduate student in the lab, is cloning miR-155 and miR-K12-11 into retroviral vectors to transduce human CD34+ cells which will be grafted into transgenic NOD/SCID mice. These mice lack functional murine B and T cells due to a defect in V(D)J recombination (Chang et al. 1995) and thus can not reject human cells (Greiner et al. 1998). Following engraftment with human CD34+ cells, these mice will have reconstituted human B cells which will express either miR-155 or miR-K12-11. A detailed phenotypic analysis of the lymphocyte populations will reveal whether expression of miR-155 or miR-K12-11 has consequences for hematopoiesis. In addition, mice will be followed and carefully analyzed for potential tumor formation.

To take this one step further, the Cre/loxP system could be used with miR-K12-11 to temporally express this miRNA, for example, just prior to or at the same time as endogenous miR-155 induction, thus recapitulating a miRNA expression pattern more close to that of KSHV infection.

Do KSHV miRNAs target viral genes? Do KSHV miRNAs influence cellular miRNA expression? Do miRNAs contribute to the establishment of latency? The list of KSHV miRNA cellular targets is slowly growing (Samols 2007) (Chapter three). While it is now known that KSHV miRNAs can target host genes, it remains to be determined whether these novel regulators also target viral genes. Using antagomirs, I examined the consequences of inhibiting viral miRNAs in latently infected BCBL-1 cells. Genome-wide transcript analysis showed that inhibition of the KSHV miRNAs had no significant effect on viral gene expression (Chapter 4). Although we have not yet demonstrated knockdown of viral miRNA expression in BCBL-1 cells, using similar amounts of antagomirs effectively inhibited miRNA activity as shown by reporter assays in 293/pmiRNA cells which express comparable amount of KSHV miRNAs (Fig. 4-1).

Using this method, we have tested only latently infected cells, and it may be possible that the KSHV miRNAs do target viral genes during *de novo* infection and the establishment of latency. On the other hand, given the fact that KSHV miRNAs were originally cloned from latently infected cells and are expressed during latent infection (Cai et al. 2005; Pfeffer et al. 2005; Samols et al. 2005), it is entirely possible that the negative result we observed is indeed real and KSHV miRNAs do not target viral genes.

Within this context, it will be important to know when KSHV miRNAs are expressed following *de novo* infection. Studies to investigate the expression of viral miRNAs following infection of endothelial cells have been initiated by Karlie Plaisance, a graduate student in the lab. Total RNA isolated from infected TIVE cells (An et al. 2006) at select time points following infection will be sent to Dr. Denise Whitby's laboratory for microRNA profiling using a microarray platform that probes for all known viral miRNAs in addition to human miRNAs

(Wang et al. 2007). Using this technology, we will be able to determine (i) when miRNAs are expressed, (ii) the levels of each KSHV miRNA expressed, and (ii) whether KSHV infection influences the levels of cellular miRNAs. Arguably, KSHV miRNA expression could interfere with cellular miRNA expression by competing for access to the Exportin V/Ran GTPase nuclear export machinery and other components of the miRNA biogenesis pathway (Fig. 1-7) as has been observed for the adenovirus VA1 non-coding RNA (Lu and Cullen 2004).

We have also sent to Dr. Whitby total RNA isolated from four PEL-derived cell lines, as well as a latently-infected KSHV endothelial cell line and the isogeneic control (An et al. 2006), to determine, in addition to the abundance of KSHV and cellular miRNAs, whether KSHV miRNAs have a cell specific expression profile. To date, it is not known whether KSHV-infected endothelial cells actually express KSHV miRNAs. Infected-TIVE-LTCs were included as part of the original KSHV miRNA cloning protocol; however, while we cloned cellular miRNAs from these cells, no KSHV miRNAs were cloned (Samols et al. 2005). Additionally, I have probed for miR-K12-11 in both infected TIVE-LTCs and KSHV-positive SLK endothelial cells by Northern blot, but could not detect expression (not shown). These negative results do not rule out KSHV miRNA expression within infected endothelial cells; rather, these results suggest that KSHV miRNAs may be expressed at very low levels in these cells and thus, may only be detectable via microRNA profiling or high-throughput pyrosequencing methods such as 454 sequencing (Ruby et al. 2006).

To further examine the influence of KSHV miRNAs on the establishment of latency, we are collaborating with Dr. Greg Pari whose lab has generated a KSHV Bacmid with a deletion in the region encompassing oriLyt(R), between nt 118,108 and 122,139 (Xu et al. 2006). This region also encompasses the KSHV miRNA cluster (Fig. 1-5). The recombinant virus undergoes

efficient lytic replication in tissue culture; however, whether it can establish latency has not yet been determined. This recombinant virus can be introduced into cell types susceptible to KSHV infection such as endothelial, epithelial, and lymphoid cells, and assayed for the establishment of latent infection by examination of latent protein expression (LANA) and the presence of maintained circular episomes by Gardella gel and Southern blot analysis. These experiments together with the microRNA profiling described above should determine whether KSHV miRNAs contribute to events leading to the establishment of latent episomes.

DNA tumor viruses encode a new class of potentially oncogenic miRNAs. Metazoan miRNAs regulate many biological processes including developmental timing, cell growth and differentiation, apoptosis, and most recently, have been implicated in cancer. Recent gene expression profiling studies have shown that tumors display unique miRNA profiles which may be useful as biomarkers for cancer initiation/progression (Calin and Croce 2006). For example, chronic lymphocyte leukemias (CLL) have unique miRNA signatures corresponding to disease progression and prognosis (Calin et al. 2005). The progression of CLL has been linked in part to the absence of two miRNAs, miR-15a and miR-16, with reported tumor suppressor activity (Cimmino et al. 2005). The miR-15a-miR-16-1 cluster lies within a region on chromosome 13 deleted in CLL, multiple myeloma, and some prostate cancers (Calin et al. 2002). Both these miRNAs are proposed to target Bcl-2, an anti-apoptotic protein that promotes cell growth and survival. Indeed, overexpression of miR-15a and miR-16 in a leukemic cell line results in apoptosis due to negative regulation of Bcl-2 (Cimmino et al. 2005).

We identified one KSHV miRNA, miR-K12-6-5p, which shares nt 3 to 10 with both miR-15a and miR-16. It is difficult to imagine that a herpesvirus would encode miRNAs with tumor suppressor activity and potentially, contribute to apopotosis by targeting Bcl-2; however, KSHV

encodes a Bcl-2 homolog (ORF16) (Cheng et al. 1997; Sarid et al. 1997) that is an early viral transcript (Fig. 1-1) and is detectable in KS lesions as well as PEL-derived cell lines during latent infection (Sarid et al. 1997). Thus, one might speculate that miR-K12-6-5p and v-Bcl-2 may have a synergistic effect: miR-K12-6-5p downregulates the cellular Bcl-2 while v-Bcl-2 promotes cell survival to benefit the viral life cycle. This hypothesis could be tested by looking at cell survival following transfection of Bax, a Bcl-2 inhibitor, in cells expressing miR-K12-6-5p, v-Bcl-2, or both together. Additionally, the levels of cellular Bcl-2 could be investigated following expression of miR-K12-6-5p.

The fact that oncogenic viruses encode miRNAs suggests that virally-encoded miRNAs might directly influence transformation and act as oncogenes themselves. We identified two γ-herpesvirus miRNAs that have seed sequence homology to human oncogenic miRNAs: (i) KSHV-miR-K12-1 and miR-155 and (ii) EBV-BART5 and miR-18. The miR-17-92 cluster, which includes miR-18, is highly expressed in several human malignancies (He et al. 2005).

We have examined the transforming potential of the KSHV miRNA cluster and two individual miRNAs, miR-K12-11 and miR-155, by soft-agar asays using mouse fibroblasts, and were unable to observe colony formation with overexpression of these miRNAs (Fig. 4-4). While it may be possible that KSHV miRNAs in general do not target mouse mRNAs, hsa-miR-155 should target mouse transcripts, since murine and human miR-155 are highly conserved, differing by only 1 nt (Lagos-Quintana et al. 2002). Additionally, I have tested NIH3T3 cells by RT-PCR and found they express murine *bic*, thus likely also produce the mature mmu-miR-155 and express mmu-miR-155 targets (not shown). Given that the nucleotide variation between the murine and human miR-155 does not occur within the seed sequence, we would also predict that miR-K12-11 could target similar 3'UTRs as the miR-155 family (Chapter 3).

A more plausible explanation is that KSHV miRNAs might require additional oncogenic stress such as has been observed for the miR-17-92 cluster which augments Myc-induced lymphomagenesis (He et al. 2005) or miR-372 and miR-373 which collaborate with Ras (Voorhoeve et al. 2006). This requirement has also been observed for other KSHV proteins such as LANA. Expression of LANA in primary endothelial cells enhances cell proliferation but does not induce transformation as determined by lack of anchorage-independent growth in soft-agar or tumor formation in nude mice (Watanabe et al. 2003). Additionally, over-expression of LANA from its own B-cell specific promoter in transgenic mice induces B cell hyperplasia which predisposes the animals to lymphoma formation (Fakhari et al. 2006). LANA, in cooperation with Ras, has been shown to transform primary rat cells and potentially contribute to oncogenesis by influencing the Rb/E2F pathway (Radkov et al. 2000). Recently, transformation following *de novo* KSHV infection of endothelial cells has been demonstrated and these latently-infected cells form tumors when injected into mice (An et al. 2006).

Given these observations, it is very possible that KSHV miRNAs and LANA could cooperate together and induce transformation. Interestingly, it is important to note that KSHV encodes a variety of other proteins, such as vGPCR and vIRF, that have been shown to transform cells in cooperation with cellular oncogenes (Arvanitakis et al. 1997; Nicholas 2007). This idea can be first tested by expressing LANA or cellular oncogenes such as Myc or Ras in the NIH3T3 cell lines which stably express KSHV miRNAs (Fig. 4-4) and assaying for anchorage-independent growth and colony formation in soft agar. Similar assays can be performed in cell types more relevant to KSHV biology such as primary endothelial cells. These studies would show whether viral miRNAs, like their metazoan counterparts, have a role in tumorigenesis.

LANA And KSHV MiRNAs: A Model

For the establishment and maintenance of latent KSHV episomes following *de novo* infection, several steps must be accomplished. First, at the transcriptional level, lytic gene expression must be suppressed and latent gene products must be upregulated. Studies on the kinetics of viral gene expression following infection of primary endothelial cells show ORF50 levels rise sharply within 2 hrs, then rapidly decline as LANA is expressed and reaches steady state levels (Krishnan et al. 2004). Within 8 to 24 hrs post-infection, nearly all lytic genes are absent and only latent genes such as ORF72, ORF73, and K13 are detectable (Krishnan et al. 2004). The downregulation of Rta/ORF50 has been linked, in part, to the transcriptional repressor function of LANA which inhibits the ORF50 promoter (Lan et al. 2004). Additionally, immunoprecipitation experiments showed that LANA can interact directly with Rta, potentially inhibiting the transactivator function of Rta (Lan et al. 2004). Recent experiments examining the methylation status of plasmids containing the ORF50 promoter in the presence of LANA and DNMT3a indicated that LANA and DNMT3a coordinate together to induce *de novo* methylation of ORF50 (Shamay et al. 2006). These events likely take place over the course of several cell divisions. Thus, the suppression of lytic gene expression by LANA, DNA methylation, and histone modifications plays an important role in stabilizing episomes from the epigenetic standpoint.

During this time, the cellular environment is also altered to prevent apoptosis and promote cell cycle progression. KLAR gene products have critical roles in exploiting these processes (Fig. 5-2). Both LANA and v-cyclin promote S phase entry. V-cyclin is a homolog of cyclin D and interacts with cdk6 to phosphorylate Rb, thereby overcoming a cell cycle checkpoint control (Godden-Kent et al. 1997; Li et al. 1997). The phosphorylation of Rb results in the release of E2F, a transcription factor that promotes expression of genes involved in DNA

synthesis. LANA also disrupts the Rb/E2F interaction (Radkov et al. 2000). Additionally, LANA dysregulates GSK3β, leading to the stabilization of β-catenin and expression of β-catenin responsive genes (Fujimuro et al. 2003) such as c-myc and cyclin D1; consequently, cell cycle progression ensues. These functions of LANA, in particular, potentially allow access of the virus to the cellular replication machinery which is important for latent DNA replication.

vFLIP and v-cyclin both have roles in promoting cell survival. vFLIP inhibits Fas-mediated apoptosis by preventing caspase 8 activation (Bertin et al. 1997). V-cyclin directs cdk6 to phosphorylate Bcl-2, resulting in the instability and degradation of Bcl-2 (Ojala et al. 2000). Normally, this would lead to cell death; however, KSHV encodes v-Bcl-2, which is not phosphorylated by cdk6, to compensate for this activity, and thus promotes cell survival (Ojala et al. 2000). Interestingly, our data indicates that miRNAs, such as the potential targeting Bim and Btf by miR-K12-11 or targeting of THBS-1 by the KSHV miRNA cluster and consequent downregulation of TGF-β, may also have roles in promoting cell survival (Fig. 5-2). Thus, latent proteins and viral miRNAs seem to work concomitantly to promote a cellular environment conducive to latency.

Crucial steps in the establishment of latency are the hijacking of the cellular replication machinery and tethering of episomes to cellular chromosomes by LANA. Our data shows that replication and partitioning of episomes are independent processes. Both processes are tightly linked to cell cycle progression and the availability of replication and chromatin factors, which are facilitated, in part, by LANA (Fig. 5-3).

The targeting of cellular genes by KSHV miRNAs may further influence the availability of chromatin remodeling factors responsible for episome stabilization or the accessibility of replication licensing machinery for latent DNA replication (Fig. 5-3). Thus, KSHV miRNAs,

like LANA, may also contribute to early events after *de novo* infection for the establishment and maintenance of viral episomes. Additionally, LANA may indirectly influence the cellular miRNA profile within an infected cell through its interactions with transcriptional regulatory proteins such as the mSin3 corepressor complex, DNMT3a, GSK3β, p53, and Rb (Friborg et al. 1999; Krithivas et al. 2000; Radkov et al. 2000; Fujimuro et al. 2003; An et al. 2005; Shamay et al. 2006), further contributing to the establishment and maintenance of latent episomes.

While so far this model strictly focuses on intracellular events, it is important to note that interactions of virally-infected cells and surrounding cells in the context of the infected host are crucial for viral biology. In that context, our findings that virally-encoded miRNAs also inhibit anti-angiogenic factors such as THBS-1 and proteins such as PRG1 and SPP1 (Table 4-1), which play a role in regulating immune surveillance and apoptosis, further supports our hypothesis that the KLAR region of KSHV modulates many host cellular processes both through the expression of viral proteins and miRNAs. To integrate these complex host/virus interactions, it will be necessary to study γ-herpesvirus systems that are more amenable to *in vivo* experiments such as MHV68 or RRV as well as KSHV in the context of the NOD/SCID mouse system.

Elucidating the combinatory roles of these latent proteins and viral miRNAs in the future will greatly enhance our understanding of how human γ-herpesviruses establish and maintain latency, an important prerequisite for tumorigenesis.

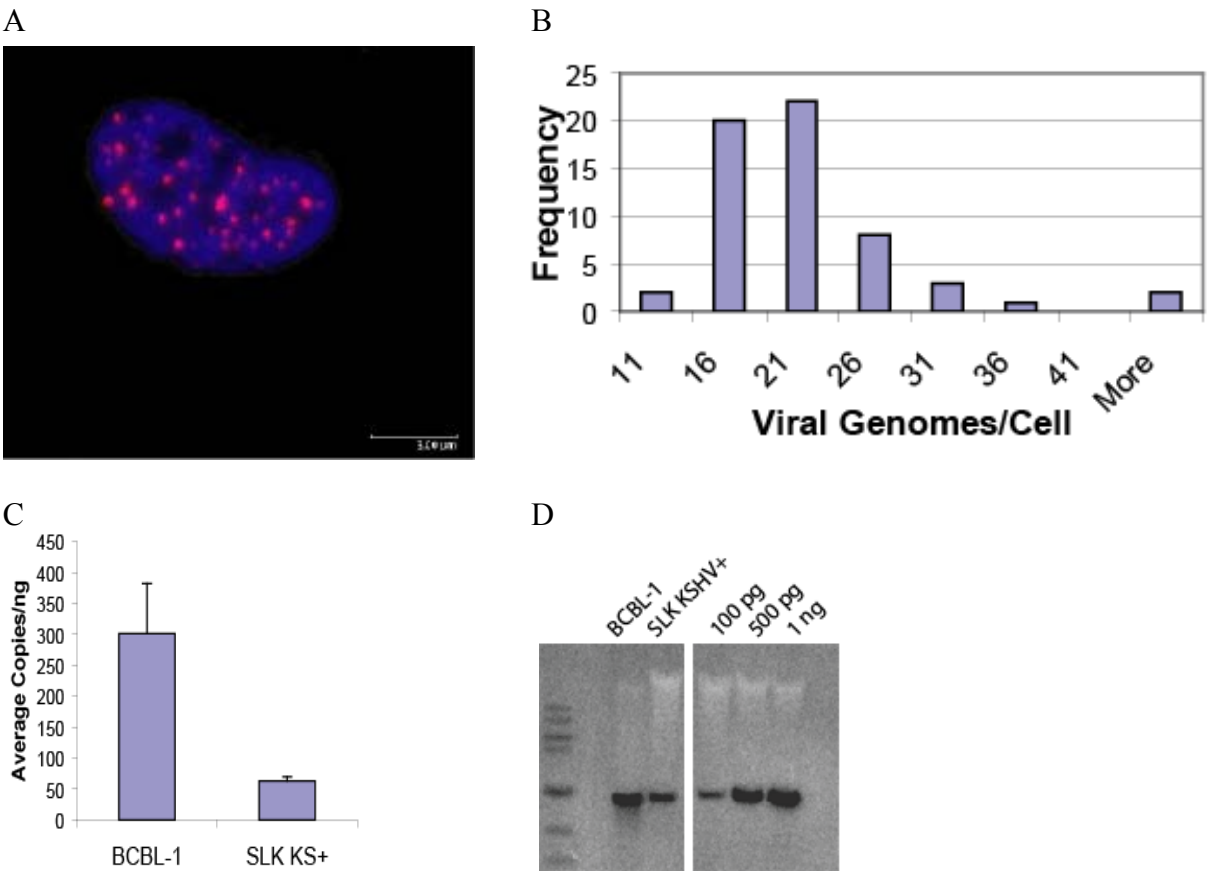

Figure 5-1. Episomes are maintained at stable copy numbers following de novo infection. A. Confocal microscopy analysis of SLK KSHV+ endothelial cells transfected with pLANA-C-RFP. Red indicates LANA-C-RFP bound to KSHV episomes; blue is DAPI staining of the nucleus. B. Frequency distribution of the number of viral episomes (determined from each red speckle) per cell nucleus. The average viral copy number per cell was 20.3. C. Quantitative PCR analysis of viral copy number using LANA-specific primers in BCBL-1 and SLK KSHV+ cells. BCBL-1 cells contain 80 viral episomes per cell. D. Genomic southern blot analysis of BCBL-1 and SLK KSHV+ cells. 25 μg of genomic DNA, digested overnight with BamHI, was loaded per lane. Blots were probed for the BamHI N-terminal fragment of LANA. Increasing amounts of pLANA-2TR-GFP are shown at right for comparison.

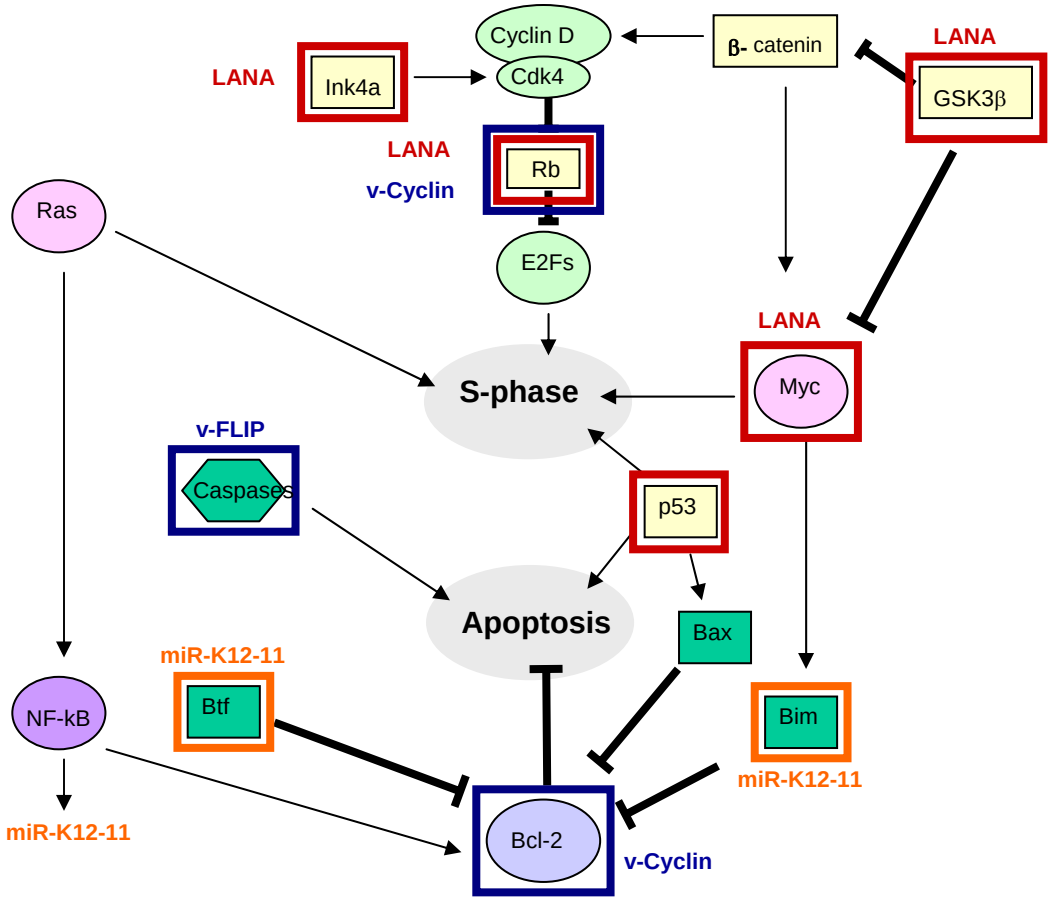

Figure 5-2. The integration of cellular pathways regulating cell cycle progression and cell survival. KLAR gene products influence members of several of these pathways, protecting infected cells from apoptosis and resulting in S phase entry. Circles indicate potential oncogenes; rectangles indicate potential or known tumor suppressors. Highlighted in red are pathways dysregulated by LANA; in blue are pathways affected by other KLAR gene products; in orange are genes potentially targeted by KSHV miR-K12-11. Note that in PEL cells, p53 pathways have recently been shown to be intact (Fakhari et al. 2006); however, LANA has also been shown to interact with an EC5S ubiquitin complex to target p53 degradation (Cai et al. 2006a).

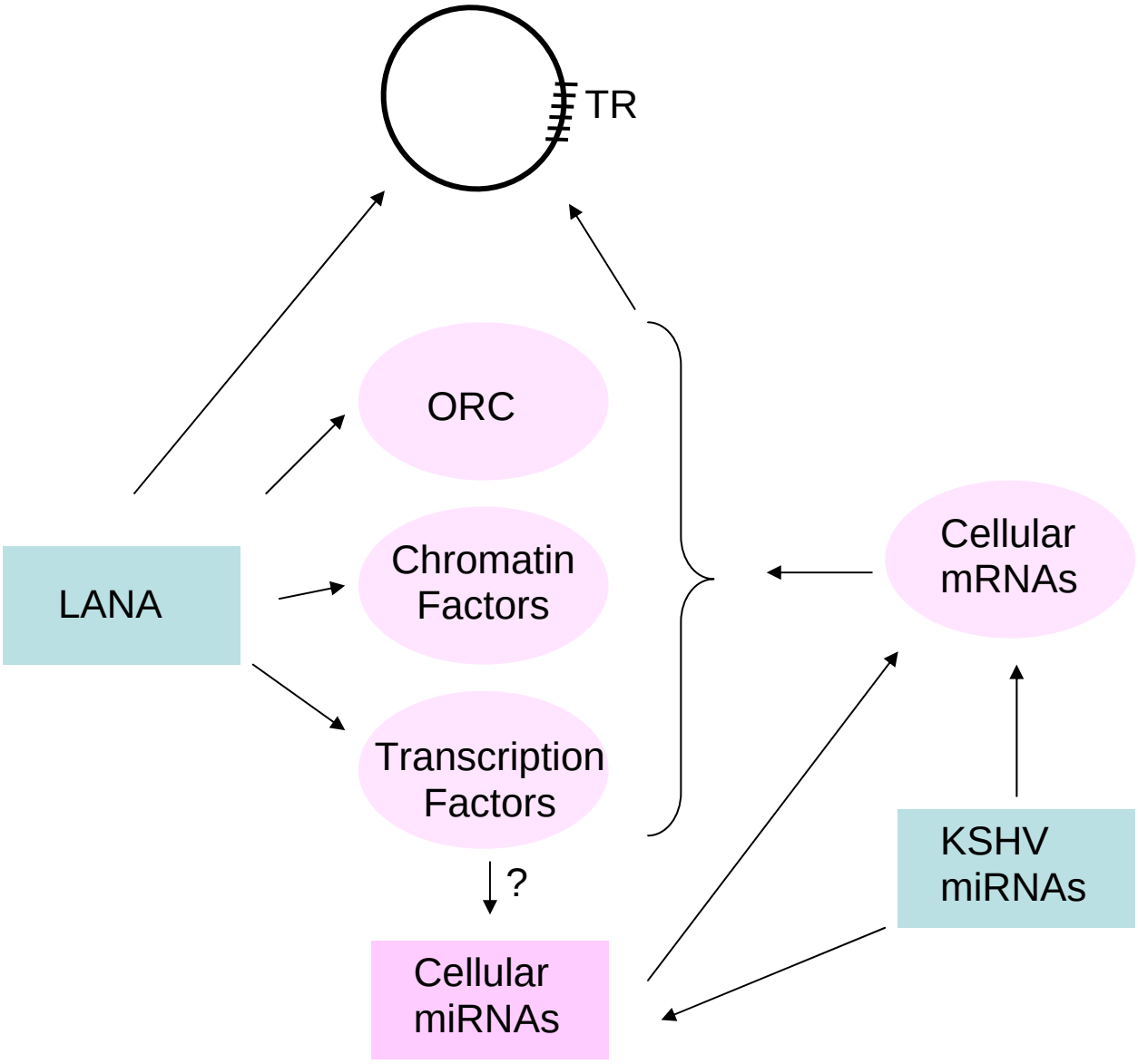

Figure 5-3. Contributions of LANA and KSHV miRNAs to KSHV episome establishment and maintenance. LANA interacts with ORC for latent DNA replication and cellular chromatin and transcription factors to stabilize episomes and modulate the host environment. KSHV miRNAs target cellular genes. Potentially, the regulation of KSHV miRNAs on cellular gene expression further contributes to the establishment and maintenance of latent viral episomes.

APPENDIX
PROTOCOLS

Hirt Extraction Protocol

- Pellet appropriate amount of cells (8 or 9 x10^6 at least for BJAB) in 15ml conical by centrifuging 1100rpm 5min. Decant media.

- Resuspend pellet in 630 µl buffer. (10mM Tris-HCl (pH7.5), 10mM EDTA, 100mM NaCl.) Transfer suspension to Expender tube.

- For 5ml of buffer:

Stock	Need
0.1M TrisHCl pH7.5	0.5ml
0.5M EDTA	0.1ml
5M NaCl	0.1ml
dH2O	4.3ml

- Lyse cells by adding 10x SDS to have a final concentration of 1% SDS (add 70 µl 10x SDS). Incubate 20min. at 37*C.

- Add 5M NaCl to have final 1M NaCl (add 175ul 5M NaCl for final 875 µl volume) and incubate overnight 4*C to precipitate salt and genomic DNA.

- Pellet salt precipitate 14,000 rpm 30min 4*C (or 27,000xg) and transfer supernatant to new tube. Centrifuge again 10min and combine supernatants that contain the plasmid/episomal DNA.

- Perform one phenol:chloroform extraction on supernatant:

- Prepare 1:1 phenol:chloroform solution in centrifuge tube and vortex.

- Add 1 volume p/c to DNA supernatant; vortex to mix completely.

- Spin immediately 14,000rpm 5min 4*C.

- Transfer upper aqueous phase containing the DNA into 2 new ependorf tubes (otherwise volume is too large), being careful not to disturb the protein layer.

- Add 2 volumes –20*C 100% EtOH to each tube and incubate on ice 20min to precipitate DNA.

- Pellet DNA by spinning 14,000rpm 10min. 4*C; Wash 1x 70% cold EtOH and dry pellet briefly.

- Resuspend pellets in 12.5 μl TE buffer and combine corresponding suspensions to have 25 μl volume.

- Digest plasmid/episomal DNA with single cutter enzyme and run 0.8% agarose gel in TAE followed by Southern blot protocol.

Extraction Of Circular Plasmid DNA Using Spin-Columns

- Pellet 5-8 x 10^6 cells and wash 1x in 1ml PBS; transfer to ependorf and pellet.

- Resuspend in 250ul TE + RNAse buffer pH 8.0 (buffer PI from QIAGEN midi prep kit).

- Add 250ul buffer G2 (Gibco) that contains 1% SDS and 200mM NaOH; invert gently to mix and incubate 5min room temp to lyse cells.

- Precipitate cell debris and chromosomal DNA by adding 350ul CsCl solution (3M CsCl, 1M K-OAc, 0.67M Acetic Acid). Mix gently and incubate on ice 15min.

- Centrifuge 15min 14,000xg to pellet cell debris.

- Load supernatant onto spin cartridge and place in 2ml wash tube. Centrifuge 1min 14,000xg and discard flow through.

- Wash 1x with 750ul wash solution. (80mM K-OAc, 10mM Tris-HCl, 40mM EDTA, 60% EtOH).

- Centrifuge 1 min 14,000xg and discard flow through. Centrifuge 1 min again.

- Transfer spin cartridge to recovery tube and elute the DNA with 75ul 65*C TE buffer. Incubate 1 min and centrifuge 2 min 14,000xg to recover circular DNA. Follow up with agarose gel/southern blot or PCR/agarose gel.

Plasmid Retention Assays

- Transfect cells with plasmid DNA using Amaxa protocols (amaxa, inc). For BJAB, cell solution T, program O-17; 5,000 copies plasmid DNA per cell. Use 5x10^5 cells per transfection.

- Incubate overnight. Prepare for FACS by spinning 5 min 1100 rpm, resuspend in cold PBS, run through cell strainer to remove clumps, and place cells into flow tubes on ice.

- Bring to flow lab for sorting. Gate on viable populations and take only higher GFP-expressers.

- Sort cells into 50% media, 50% FBS solution.

- Remove cells from sorting-fluid by spinning and resuspend in media at 50,000 cells per ml.

- Remove aliquots each day (200 µl) for analysis and fix in 2% paraformaldehyde. Cells can be stored in this solution for 1 week prior to analysis.

- For analysis of GFP expression by flow cytometry, gate on viable populations using an untransfected control.

Propidium Iodide Staining For Cell Cycle Analysis

- Count cells (need ~1-3x10^6); wash 1x PBS and resuspend by vortexing in 0.2 ml PBS (use 14 ml conical tubes).

- Fix cells by adding 1.8 ml 70% cold ethanol (EtOH) drop wise onto cells while vortexing. Incubate 15 min RT or store at 4*C (can be stored several weeks) until staining. Perform staining at same time for multiple samples and make sure you have equal cell numbers.

- Pellet cells from fixation solution (5min 1200rpm) and wash 1x 1-2ml PBS. Transfer to ependorf tube and remove PBS. Vortex cells briefly to resuspend.

- Resuspend cells in 0.8 ml staining buffer:

- 0.1% Triton X-100 (10 µl)
- 200 µl 10mg/ml RNase A
- 200 µl 20x propidium iodide stock solution (light sensitive!)
- PBS to 10 ml

- Wrap tubes in foil and incubate 45 min at 37*C.

- Pellet cells 2 min and resuspend in 1 ml PBS for flow analysis.

- Cell Cycle Analysis:

- Control, asynchronous unstained cells fixed in EtOH
- Control, asynchronous PI-stained cells
- Synchronous cells

- Adjust voltage for FSC vs SSC for cell viability

- Adjust voltage for FL2 and place FL2 peak for G1 at 200 on the 1024 scale using voltage. Collect 20,000 viable-gated events, running at ~100 to 200 events/sec

- Use Mod-Fit to analyze histograms.

Northern Blot

- Prepare glass plates for gel:

- Rinse plates with DI water, 100% Ethanol, and DI water again

- Wipe dry with Kim wipes, make sure all dust is gone.
- Also wash spacers and comb
- Assemble plates and spaces, place into bag, put into gel casting holder.
- 15% 8M Urea Denaturing Acrylamide gel, 75ml(for EMSA plates)
- 35 g Urea, Ultrapure
- 7.5 ml 10x TBE
- 28 ml 40% Acrylamide/Bis (19:1)
- Dissolve Urea, can add a little heat but if it gets warm, you have to let it cool down before attempting polymerization
- 5~10 ml DEPC H2O (to 75 ml volume)
- 300 µl 10% APS
- 30 µl TEMED
- Mix for a bit, then pour into plates (can just pour from beaker)
- Don't forget the comb
- Let polymerize for 1 hr
- Can wrap plates after polymerization in paper towels soaked in 0.5x TBE, then covered in saran wrap, then can leave o/n at RT (not in fridge! Urea will precipitate)

Pre-running the gel:

- Use 0.5x TBE buffer (will need about 1.5L)
- Run the gel at constant 65 mA for 45 min to 1 hr (to warm gel)
- Load and run the gel:
- Need to load 25 to 35 µg RNA per sample
- You want the RNA to be in <12 µl volume, then add 12 µl gel loading buffer
- If RNA is in more than 12 µl, add equal amounts of gel loading buffer
- Heat at 80°C for 5 min, move to ice

- Spin down briefly
- Rinse wells with a pipette tip
- Turn off power supply, load samples
- Run gel at 35 mA (~400V) for about 1 hr 45 min to 2 hr
- If 2 gels, double amps (but not volts!)
- (BPB runs around 12nt and cyanol around 55nt.)

Semi-dry transfer:

- Pour out buffer
- Take out plates
- Pry apart with something handy but clean (gently!)
- ***Notch upper left corner***
- Two methods to get gel off glass
- (One) place dry filter paper on gel, flip stack and move to Pyrex dish with 0.5x TBE, let get peel off glass onto wet filter paper
- (Two) place sheet of saran wrap on gel, flip, then lift one corner of the glass and use a razor blade to start the gel peeling off the glass, life glass more as gel peels off

Semi dry chamber:

- Bottom.
- Two pieces damp filter paper (with the 0.5xTBE)
- The gel (pour a bit more buffer on top)
- The membrane (Genescreen plus Hybr. Transfer membrane, Perkin Elmer)
- ***Notch same corner as gel***
- Two more pieces of damp filter paper
- Top.
- Run 400 mA for 1 or 2 hrs

- Take out membrane
- Place on dry filter paper face up
- UV crosslink (1200 J) twice

5’ end-labeling of Probe:

- 5 µl 10x PNK buffer
- 2 µl=20 pmol ANTISENSE probe DNA oligo (at 100 µM stock concentration)
- 20 µl [γ -^{32}P] ATP, 10 mCi/ml (= 200 µCi)
- 3 µl T_4 Polynucleotide Kinase, 10 U/µl
- 20 µl purelab H_2O
- 37°C 2 hr
- For U6 control probe
- Same as above, but use remaining 5 µl of radioactivity and 40 µl water

Microspin G-25 column (use Roche quickspin columns):

- Resuspend the resin in the column by shaking gently
- Place column into supplied 1.5 ml tube transfer to 15 ml conical
- Spin 5 min 2500 rpm
- Place into fresh 1.5 ml tube back into 15 ml conical
- Load radioactivity
- Spin 5 min 2500 rpm
- Discard column using forceps
- Take out 1.5 ml tube with forceps
- Measure 1 µL in scintillation counter (75,000,000 to 300,000,000 cpm)

Pre-Hybridization: Ambion ULTRAhyb-oligo

- Heat hybridization buffer in 42^{o}C water bath to dissolve any precipitated material, swirl bottle often. Take out 30 ml per gel, place into 50 ml conical at 37^{o}C in hybridization oven
- Use long tubes, 15 ml buffer per tube
- Pre-hybridization 30min to 1 hr 37^{o}C

Hybridization:

- Pour out pre-hybridization solution
- Add fresh 15 ml buffer
- Add probe (try to pipette into liquid and not let it hit the membrane)
- Hybridization o/n 37^{o}C

Wash buffer, 2xSSC / 0.1%SDS:

- 50 ml 20x SSC
- 445 ml DEPC H_2O
- 5 ml 10% SDS
- Pre heat 4 x 50 ml @ 37°C per membrane

Wash:

- Pour out hybridization buffer in radioactive liquid waste.
- Turn off temperature in hybridization oven (set temp to 22°C).
- Add 50 ml 37°C wash buffer, gently rock tube for 1 min (time it!)
- Pour out into liquid waste, add 50 ml 37°C wash buffer, rotate for 30 min in hybridization oven (temp set @22°C will get down to around 28^{o}C)
- Repeat washes with 50 ml wash buffer, 30 minutes
- Repeat wash with 50 ml wash buffer, 10 min
- Take out membrane, wrap in saran wrap
- Into screen, o/n is best, can do 4 hr
- Measure!

REAGENTS and SOLUTIONS

- **Gel Loading buffer:**
- 8M urea (60 g/mol) 0.5 mM EDTA
- 0.09%(w/v) Bromophenol Blue
- 0.09% (w/v) Xylene Cyanol FF
- **Wash buffer, 2xSSC / 0.1%SDS:**
- 50 ml 20x SSC
- 445 ml DEPC H_2O
- 5 ml 10% SDS
- Pre heat @ 37°C
- **Transfer membrane**
- GeneScreen Plus Hybr. Transfer Membrane
- Perking Elmer; NEF1017001PK
- **Hybridization solution**
- Ambion ULTRAhyb-oligo
- #AM8663

LIST OF REFERENCES

Abbott AL, Alvarez-Saavedra E, Miska EA, Lau NC, Bartel DP, et al. (2005) The let-7 MicroRNA family members mir-48, mir-84, and mir-241 function together to regulate developmental timing in Caenorhabditis elegans. Dev Cell 9: 403-414.

Adams JM, Cory S (2007) The Bcl-2 apoptotic switch in cancer development and therapy. Oncogene 26: 1324-1337.

Adang LA, Parsons CH, Kedes DH (2006) Asynchronous progression through the lytic cascade and variations in intracellular viral loads revealed by high-throughput single-cell analysis of Kaposi's sarcoma-associated herpesvirus infection. J Virol 80: 10073-10082.

Alexandru G, Zachariae W, Schleiffer A, Nasmyth K (1999) Sister chromatid separation and chromosome re-duplication are regulated by different mechanisms in response to spindle damage. EMBO J 18(10): 2707-2721.

Aluigi MG, Albini A, Carlone S, Repetto L, De Marchi R, et al. (1996) KSHV sequences in biopsies and cultured spindle cells of epidemic, iatrogenic and Mediterranean forms of Kaposi's sarcoma. Res Virol 147: 267-275.

Ambros V (2004) The functions of animal microRNAs. Nature 431: 350-355.

An FQ, Compitello N, Horwitz E, Sramkoski M, Knudsen ES, et al. (2005) The latency-associated nuclear antigen of Kaposi's sarcoma-associated herpesvirus modulates cellular gene expression and protects lymphoid cells from p16 INK4A-induced cell cycle arrest. J Biol Chem 280: 3862-3874.

An FQ, Folarin HM, Compitello N, Roth J, Gerson SL, et al. (2006) Long-term-infected telomerase-immortalized endothelial cells: a model for Kaposi's sarcoma-associated herpesvirus latency in vitro and in vivo. J Virol 80: 4833-4846.

Arad U (1998) Modified Hirt procedure for rapid purification of extrachromosomal DNA from mammalian cells. Biotechniques 24: 760-762.

Arasteh K, Hannah A (2000) The role of vascular endothelial growth factor (VEGF) in AIDS-related Kaposi's sarcoma. Oncologist 5: 28-31.

Arvanitakis L, Geras-Raaka E, Varma A, Gershengorn MC, Cesarman E (1997) Human herpesvirus KSHV encodes a constitutively active G-protein-coupled receptor linked to cell proliferation. Nature 385: 347-350.

Arvanitakis L, Mesri EA, Nador RG, Said JW, Asch AS, et al. (1996) Establishment and characterization of a primary effusion (body cavity-based) lymphoma cell line (BC-3) harboring Kaposi's sarcoma-associated herpesvirus (KSHV/HHV-8) in the absence of Epstein-Barr virus. Blood 88: 2648-2654.

AuCoin DP, Colletti KS, Xu Y, Cei SA, Pari GS (2002) Kaposi's sarcoma-associated herpesvirus (human herpesvirus 8) contains two functional lytic origins of DNA replication. J Virol 76: 7890-7896.

AuCoin DP, Colletti KS, Cei SA, Papouskova I, Tarrant M, et al. (2004) Amplification of the Kaposi's sarcoma-associated herpesvirus/human herpesvirus 8 lytic origin of DNA replication is dependent upon a cis-acting AT-rich region and an ORF50 response element and the trans-acting factors ORF50 (K-Rta) and K8 (K-bZIP). Virology 318: 542-555.

Bachman KE, Rountree MR, Baylin SB (2001) Dnmt3a and Dnmt3b are transcriptional repressors that exhibit unique localization properties to heterochromatin. J Biol Chem 276: 32282-32287.

Bagga S, Bracht J, Hunter S, Massirer K, Holtz J, et al. (2005) Regulation by let-7 and lin-4 miRNAs results in target mRNA degradation. Cell 122: 553-563.

Ballestas ME, Kaye KM (2001) Kaposi's sarcoma-associated herpesvirus latency-associated nuclear antigen 1 mediates episome persistence through cis-acting terminal repeat (TR) sequence and specifically binds TR DNA. J Virol 75: 3250-3258.

Ballestas ME, Chatis PA, Kaye KM (1999) Efficient persistence of extrachromosomal KSHV DNA mediated by latency- associated nuclear antigen. Science 284: 641-644.

Barbera AJ, Ballestas ME, Kaye KM (2004) The Kaposi's sarcoma-associated herpesvirus latency-associated nuclear antigen 1 N terminus is essential for chromosome association, DNA replication, and episome persistence. J Virol 78: 294-301.

Barbera AJ, Chodaparambil JV, Kelley-Clarke B, Joukov V, Walter JC, et al. (2006) The nucleosomal surface as a docking station for Kaposi's sarcoma herpesvirus LANA. Science 311: 856-861.

Bartel DP (2004) MicroRNAs: genomics, biogenesis, mechanism, and function. Cell 116: 281-297.

Bartel DP, Chen CZ (2004) Micromanagers of gene expression: the potentially widespread influence of metazoan microRNAs. Nat Rev Genet 5: 396-400.

Bechtel JT, Liang Y, Hvidding J, Ganem D (2003) Host range of Kaposi's sarcoma-associated herpesvirus in cultured cells. J Virol 77: 6474-6481.

Becker PB, Horz W (2002) ATP-dependent nucleosome remodeling. Ann Rev Biochem 71: 247-273.

Bertin J, Armstrong RC, Ottilie S, Martin DA, Wang Y, et al. (1997) Death effector domain-containing herpesvirus and poxvirus proteins inhibit both Fas- and TNFR1-induced apoptosis. Proc Natl Acad Sci U S A 94: 1172-1176.

Bieleski L, Talbot SJ (2001) Kaposi's sarcoma-associated herpesvirus vCyclin open reading frame contains an internal ribosome entry site. J Virol 75: 1864-1869.

Bieleski L, Hindley C, Talbot SJ (2004) A polypyrimidine tract facilitates the expression of Kaposi's sarcoma-associated herpesvirus vFLIP through an internal ribosome entry site. J Gen Virol 85: 615-620.

Bochkarev A, Barwell JA, Pfuetzner RA, Bochkareva E, Frappier L, et al. (1996) Crystal structure of the DNA-binding domain of the Epstein-Barr virus origin-binding protein, EBNA1, bound to DNA. Cell 84: 791-800.

Boshoff C, Weiss RA (1997) Aetiology of Kaposi's sarcoma: current understanding and implications for therapy. Mol Med Today 3: 488-494.

Boshoff C, Chang Y (2001) Kaposi's sarcoma-associated herpesvirus: a new DNA tumor virus. Ann Rev Med 52: 453-470.

Boshoff C, Weiss R (2002) AIDS-related malignancies. Nat Rev 2: 373-382.

Boshoff C, Schulz TF, Kennedy MM, Graham AK, Fisher C, et al. (1995) Kaposi's sarcoma-associated herpesvirus infects endothelial and spindle cells. Nat Med 1: 1274-1278.

Brennecke J, Stark A, Russell RB, Cohen SM (2005) Principles of microRNA-target recognition. PLoS Biol 3: e85.

Broxmeyer HE, Sehra S, Cooper S, Toney LM, Kusam S, et al. (2007) Aberrant Regulation of Hematopoiesis by T cells in BAZF-Deficient Mice. Mol Cell Biol. In press.

Burgler C, Macdonald PM (2005) Prediction and verification of microRNA targets by MovingTargets, a highly adaptable prediction method. BMC Genomics 6: 88.

Cai QL, Knight JS, Verma SC, Zald P, Robertson ES (2006a) EC5S ubiquitin complex is recruited by KSHV latent antigen LANA for degradation of the VHL and p53 tumor suppressors. PLoS Pathog 2: e116.

Cai X, Hagedorn CH, Cullen BR (2004) Human microRNAs are processed from capped, polyadenylated transcripts that can also function as mRNAs. RNA 10: 1957-1966.

Cai X, Lu S, Zhang Z, Gonzalez CM, Damania B, et al. (2005) Kaposi's sarcoma-associated herpesvirus expresses an array of viral microRNAs in latently infected cells. Proc Natl Acad Sci U S A 102: 5570-5575.

Cai X, Schafer A, Lu S, Bilello JP, Desrosiers RC, et al. (2006b) Epstein-Barr virus microRNAs are evolutionarily conserved and differentially expressed. PLoS Pathog 2: e23.

Calin GA, Croce CM (2006) MicroRNA signatures in human cancers. Nat Rev 6: 857-866.

Calin GA, Dumitru CD, Shimizu M, Bichi R, Zupo S, et al. (2002) Frequent deletions and down-regulation of micro- RNA genes miR15 and miR16 at 13q14 in chronic lymphocytic leukemia. Proc Natl Acad Sci U S A 99: 15524-15529.

Calin GA, Ferracin M, Cimmino A, Di Leva G, Shimizu M, et al. (2005) A MicroRNA signature associated with prognosis and progression in chronic lymphocytic leukemia. New Eng J Med 353: 1793-1801.

Campbell TB, Borok M, White IE, Gudza I, Ndemera B, et al. (2003) Relationship of Kaposi sarcoma (KS)-associated herpesvirus viremia and KS disease in Zimbabwe. Clin Infect Dis 36: 1144-1151.

Carim-Todd L, Escarceller M, Estivill X, Sumoy L (2000) Cloning of the novel gene TM6SF1 reveals conservation of clusters of paralogous genes between human chromosomes 15q24-->q26 and 19p13.3-->p12. Cytogenet Cell Genet 90: 255-260.

Cereghini S, Yaniv M (1984) Assembly of transfected DNA into chromatin: structural changes in the origin-promoter-enhancer region upon replication. EMBO J 3: 1243-1253.

Cesarman E (2002a) Epstein-Barr virus (EBV) and lymphomagenesis. Front Biosci 7: e58-65.

Cesarman E (2002b) The role of Kaposi's sarcoma-associated herpesvirus (KSHV/HHV-8) in lymphoproliferative diseases. Recent Results Cancer Res 159: 27-37.

Cesarman E, Chang Y, Moore PS, Said JW, Knowles DM (1995a) Kaposi's sarcoma-associated herpesvirus-like DNA sequences in AIDS-related body-cavity-based lymphomas. New Eng J Med 332: 1186-1191.

Cesarman E, Moore PS, Rao PH, Inghirami G, Knowles DM, et al. (1995b) In vitro establishment and characterization of two acquired immunodeficiency syndrome-related lymphoma cell lines (BC-1 and BC-2) containing Kaposi's sarcoma-associated herpesvirus-like (KSHV) DNA sequences. Blood 86: 2708-2714.

Chang Ma (2001) Kaposi's Sarcom-Associated Herpesvirus. In: Howley Ka, editor. Fields Virology. 4 ed: Lippincott Williams & Wilkins. pp. 2803-2834.

Chang Y, Bosma GC, Bosma MJ (1995) Development of B cells in scid mice with immunoglobulin transgenes: implications for the control of V(D)J recombination. Immunity 2: 607-616.

Chang Y, Cesarman E, Pessin MS, Lee F, Culpepper J, et al. (1994) Identification of herpesvirus-like DNA sequences in AIDS-associated Kaposi's sarcoma. Science 266: 1865-1869.

Chatterjee M, Osborne J, Bestetti G, Chang Y, Moore PS (2002) Viral IL-6-induced cell proliferation and immune evasion of interferon activity. Science 298: 1432-1435.

Chau CM, Lieberman PM (2004) Dynamic chromatin boundaries delineate a latency control region of Epstein-Barr virus. J Virol 78: 12308-12319.

Chaudhuri B, Xu H, Todorov I, Dutta A, Yates JL (2001) Human DNA replication initiation factors, ORC and MCM, associate with oriP of Epstein-Barr virus. Proc Natl Acad Sci U S A 98: 10085-10089.

Chen CZ, Li L, Lodish HF, Bartel DP (2004) MicroRNAs modulate hematopoietic lineage differentiation. Science 3: 83-86.

Chen J, Ueda K, Sakakibara S, Okuno T, Parravicini C, et al. (2001) Activation of latent Kaposi's sarcoma-associated herpesvirus by demethylation of the promoter of the lytic transactivator. Proc Natl Acad Sci U S A 98: 4119-4124.

Chen L, Lagunoff M (2005) Establishment and maintenance of Kaposi's sarcoma-associated herpesvirus latency in B cells. J Virol 79: 14383-14391.

Chendrimada TP, Gregory RI, Kumaraswamy E, Norman J, Cooch N, et al. (2005) TRBP recruits the Dicer complex to Ago2 for microRNA processing and gene silencing. Nature 436: 740-744.

Chendrimada TP, Finn KJ, Ji X, Baillat D, Gregory RI, et al. (2007) MicroRNA silencing through RISC recruitment of eIF6. Nature 447: 823-828.

Cheng EH, Nicholas J, Bellows DS, Hayward GS, Guo HG, et al. (1997) A Bcl-2 homolog encoded by Kaposi sarcoma-associated virus, human herpesvirus 8, inhibits apoptosis but does not heterodimerize with Bax or Bak. Proc Natl Acad Sci U S A 94: 690-694.

Cheung MC, Pantanowitz L, Dezube BJ (2005) AIDS-related malignancies: emerging challenges in the era of highly active antiretroviral therapy. Oncologist 10: 412-426.

Chou YT, Wang H, Chen Y, Danielpour D, Yang YC (2006) Cited2 modulates TGF-beta-mediated upregulation of MMP9. Oncogene 25: 5547-5560.

Cimmino A, Calin GA, Fabbri M, Iorio MV, Ferracin M, et al. (2005) miR-15 and miR-16 induce apoptosis by targeting BCL2. Proc Natl Acad Sci U S A 102: 13944-13949.

Cory S, Huang DC, Adams JM (2003) The Bcl-2 family: roles in cell survival and oncogenesis. Oncogene 22: 8590-8607.

Costinean S, Zanesi N, Pekarsky Y, Tili E, Volinia S, et al. (2006) Pre-B cell proliferation and lymphoblastic leukemia/high-grade lymphoma in E(mu)-miR155 transgenic mice. Proc Natl Acad Sci U S A 103: 7024-7029.

Cotter MA, 2nd, Robertson ES (1999) The latency-associated nuclear antigen tethers the Kaposi's sarcoma- associated herpesvirus genome to host chromosomes in body cavity-based lymphoma cells. Virology 264: 254-264.

Cotter MA, 2nd, Robertson ES (2002) Molecular biology of Kaposi's sarcoma-associated herpesvirus. Front Biosci 7: d358-375.

Cotter MA, 2nd, Subramanian C, Robertson ES (2001) The Kaposi's sarcoma-associated herpesvirus latency-associated nuclear antigen binds to specific sequences at the left end of the viral genome through its carboxy-terminus. Virology 291: 241-259.

Cui C, Griffiths A, Li G, Silva LM, Kramer MF, et al. (2006) Prediction and identification of herpes simplex virus 1-encoded microRNAs. J Virol 80: 5499-5508.

Cullen BR (2006) Viruses and microRNAs. Nat Genet 38: S25-30.

Curreli F, Friedman-Kien AE, Flore O (2005) Glycyrrhizic acid alters Kaposi sarcoma-associated herpesvirus latency, triggering p53-mediated apoptosis in transformed B lymphocytes. J Clin Investigation 115: 642-652.

de Fraipont F, Nicholson AC, Feige JJ, Van Meir EG (2001) Thrombospondins and tumor angiogenesis. Trends Mol Med 7: 401-407.

Denli AM, Tops BB, Plasterk RH, Ketting RF, Hannon GJ (2004) Processing of primary microRNAs by the Microprocessor complex. Nature 432: 231-235.

Desrosiers RC, Sasseville VG, Czajak SC, Zhang X, Mansfield KG, et al. (1997) A herpesvirus of rhesus monkeys related to the human Kaposi's sarcoma-associated herpesvirus. J Virol 71: 9764-9769.

Dews M, Homayouni A, Yu D, Murphy D, Sevignani C, et al. (2006) Augmentation of tumor angiogenesis by a Myc-activated microRNA cluster. Nat Genet 38: 1060-1065.

Dey A, Chitsaz F, Abbasi A, Misteli T, Ozato K (2003) The double bromodomain protein Brd4 binds to acetylated chromatin during interphase and mitosis. Proc Natl Acad Sci U S A 100: 8758-8763.

Dey A, Ellenberg J, Farina A, Coleman AE, Maruyama T, et al. (2000) A bromodomain protein, MCAP, associates with mitotic chromosomes and affects G(2)-to-M transition. Mol Cell Biol 20: 6537-6549.

Dittmer D, Lagunoff M, Renne R, Staskus K, Haase A, et al. (1998) A cluster of latently expressed genes in Kaposi's sarcoma-associated herpesvirus. J Virol 72: 8309-8315.

Dupin N, Diss TL, Kellam P, Tulliez M, Du MQ, et al. (2000) HHV-8 is associated with a plasmablastic variant of Castleman disease that is linked to HHV-8-positive plasmablastic lymphoma. Blood 95: 1406-1412.

Dupin N, Fisher C, Kellam P, Ariad S, Tulliez M, et al. (1999) Distribution of human herpesvirus-8 latently infected cells in Kaposi's sarcoma, multicentric Castleman's disease, and primary effusion lymphoma. Proc Natl Acad Sci U S A 96: 4546-4551.

Dutta A, Bell SP (1997) Initiation of DNA replication in eukaryotic cells. Ann Rev Cell Devel Biol 13: 293-332.

Eis PS, Tam W, Sun L, Chadburn A, Li Z, et al. (2005) Accumulation of miR-155 and BIC RNA in human B cell lymphomas. Proc Natl Acad Sci U S A 102: 3627-3632.

Enright AJ, John B, Gaul U, Tuschl T, Sander C, et al. (2003) MicroRNA targets in Drosophila. Genome Biol 5: R1.

Fais F, Gaidano G, Capello D, Gloghini A, Ghiotto F, et al. (1999) Immunoglobulin V region gene use and structure suggest antigen selection in AIDS-related primary effusion lymphomas. Leukemia 13: 1093-1099.

Fakhari FD, Dittmer DP (2002) Charting latency transcripts in Kaposi's sarcoma-associated herpesvirus by whole-genome real-time quantitative PCR. J Virol 76: 6213-6223.

Fakhari FD, Jeong JH, Kanan Y, Dittmer DP (2006) The latency-associated nuclear antigen of Kaposi sarcoma-associated herpesvirus induces B cell hyperplasia and lymphoma. J Clin Investigation 116: 735-742.

Falk KI, Szekely L, Aleman A, Ernberg I (1998) Specific methylation patterns in two control regions of Epstein-Barr virus latency: the LMP-1-coding upstream regulatory region and an origin of DNA replication (oriP). J Virol 72: 2969-2974.

Farh KK, Grimson A, Jan C, Lewis BP, Johnston WK, et al. (2005) The widespread impact of mammalian MicroRNAs on mRNA repression and evolution. Science 310: 1817-1821.

Friborg J, Jr., Kong W, Hottiger MO, Nabel GJ (1999) p53 inhibition by the LANA protein of KSHV protects against cell death. Nature 402: 889-894.

Fujimuro M, Wu FY, ApRhys C, Kajumbula H, Young DB, et al. (2003) A novel viral mechanism for dysregulation of beta-catenin in Kaposi's sarcoma-associated herpesvirus latency. Nat Med 9: 300-306.

Fuks F, Hurd PJ, Wolf D, Nan X, Bird AP, et al. (2003) The methyl-CpG-binding protein MeCP2 links DNA methylation to histone methylation. J Biol Chem 278: 4035-4040.

Garber AC, Hu J, Renne R (2002) Latency-associated nuclear antigen (LANA) cooperatively binds to two sites within the terminal repeat, and both sites contribute to the ability of LANA to suppress transcription and to facilitate DNA replication. J Biol Chem 277: 27401-27411.

Garber AC, Shu MA, Hu J, Renne R (2001) DNA binding and modulation of gene expression by the latency-associated nuclear antigen of Kaposi's sarcoma-associated herpesvirus. J Virol 75: 7882-7892.

Georgantas RW, 3rd, Hildreth R, Morisot S, Alder J, Liu CG, et al. (2007) CD34+ hematopoietic stem-progenitor cell microRNA expression and function: a circuit diagram of differentiation control. Proc Natl Acad Sci U S A 104: 2750-2755.

Giraldo G, Beth E, Haguenau F (1972) Herpes-type virus particles in tissue culture of Kaposi's sarcoma from different geographic regions. J Natl Cancer Inst 49: 1509-1526.

Godden-Kent D, Talbot SJ, Boshoff C, Chang Y, Moore P, et al. (1997) The cyclin encoded by Kaposi's sarcoma-associated herpesvirus stimulates cdk6 to phosphorylate the retinoblastoma protein and histone H1. J Virol 71: 4193-4198.

Godfrey A, Anderson J, Papanastasiou A, Takeuchi Y, Boshoff C (2005) Inhibiting primary effusion lymphoma by lentiviral vectors encoding short hairpin RNA. Blood 105: 2510-2518.

Grace Goll M, Bestor TH (2005) Eukaryotic cytosine methyltransferases. Ann Rev Biochem 74: 481-514.

Gregory RI, Chendrimada TP, Cooch N, Shiekhattar R (2005) Human RISC couples microRNA biogenesis and posttranscriptional gene silencing. Cell 123: 631-640.

Greiner DL, Hesselton RA, Shultz LD (1998) SCID mouse models of human stem cell engraftment. Stem Cells 16: 166-177.

Grossmann C, Podgrabinska S, Skobe M, Ganem D (2006) Activation of NF-kappaB by the latent vFLIP gene of Kaposi's sarcoma-associated herpesvirus is required for the spindle shape of virus-infected endothelial cells and contributes to their proinflammatory phenotype. J Virol 80: 7179-7185.

Grundhoff A, Ganem D (2001) Mechanisms governing expression of the v-FLIP gene of Kaposi's sarcoma-associated herpesvirus. J Virol 75: 1857-1863.

Grundhoff A, Ganem D (2003) The latency-associated nuclear antigen of Kaposi's sarcoma-associated herpesvirus permits replication of terminal repeat-containing plasmids. J Virol 77: 2779-2783.

Grundhoff A, Ganem D (2004) Inefficient establishment of KSHV latency suggests an additional role for continued lytic replication in Kaposi sarcoma pathogenesis. J Clin Investigation 113(1): 124-136.

Grundhoff A, Sullivan CS, Ganem D (2006) A combined computational and microarray-based approach identifies novel microRNAs encoded by human gamma-herpesviruses. RNA 12: 733-750.

Gupta A, Gartner JJ, Sethupathy P, Hatzigeorgiou AG, Fraser NW (2006) Anti-apoptotic function of a microRNA encoded by the HSV-1 latency-associated transcript. Nature 442: 82-85.

Haasch D, Chen YW, Reilly RM, Chiou XG, Koterski S, et al. (2002) T cell activation induces a noncoding RNA transcript sensitive to inhibition by immunosuppressant drugs and encoded by the proto-oncogene, BIC. Cell Immun 217: 78-86.

Hakimi MA, Bochar DA, Schmiesing JA, Dong Y, Barak OG, et al. (2002) A chromatin remodelling complex that loads cohesin onto human chromosomes. Nature 418: 994-998.

Hammerschmidt W, Sugden B (2004) Epstein-Barr virus sustains Burkitt's lymphomas and Hodgkin's disease. Trends Mol Med 10: 331-336.

Han J, Lee Y, Yeom KH, Nam JW, Heo I, et al. (2006) Molecular basis for the recognition of primary microRNAs by the Drosha-DGCR8 complex. Cell 125: 887-901.

Harrison S, Fisenne K, Hearing J (1994) Sequence requirements of the Epstein-Barr virus latent origin of DNA replication. J Virol 68: 1913-1925.

He L, Thomson JM, Hemann MT, Hernando-Monge E, Mu D, et al. (2005) A microRNA polycistron as a potential human oncogene. Nature 435: 828-833.

Hebner C, Lasanen J, Battle S, Aiyar A (2003) The spacing between adjacent binding sites in the family of repeats affects the functions of Epstein-Barr nuclear antigen 1 in transcription activation and stable plasmid maintenance. Virology 311: 263-274.

Hirt B (1967) Selective extraction of polyoma DNA from infected mouse cell cultures. J Mol Biol 26: 365-369.

Hu J, Renne R (2005) Characterization of the minimal replicator of Kaposi's sarcoma-associated herpesvirus latent origin. J Virol 79: 2637-2642.

Hu J, Garber AC, Renne R (2002) The latency-associated nuclear antigen of Kaposi's sarcoma-associated herpesvirus supports latent DNA replication in dividing cells. J Virol 76: 11677-11687.

Hung SC, Kang MS, Kieff E (2001) Maintenance of Epstein-Barr virus (EBV) oriP-based episomes requires EBV-encoded nuclear antigen-1 chromosome-binding domains, which can be replaced by high-mobility group-I or histone H1. Proc Natl Acad Sci U S A 98: 1865-1870.

Hutvagner G (2005) Small RNA asymmetry in RNAi: function in RISC assembly and gene regulation. FEBS 579: 5850-5857.

Hutvagner G, Simard MJ, Mello CC, Zamore PD (2004) Sequence-specific inhibition of small RNA function. PLoS Biol 2: E98.

Hwang HW, Mendell JT (2006) MicroRNAs in cell proliferation, cell death, and tumorigenesis. British J Cancer 94: 776-780.

Igarashi K, Sun J (2006) The heme-Bach1 pathway in the regulation of oxidative stress response and erythroid differentiation. Antioxid Redox Signal 8: 107-118.

Iida T, Suetake I, Tajima S, Morioka H, Ohta S, et al. (2002) PCNA clamp facilitates action of DNA cytosine methyltransferase 1 on hemimethylated DNA. Genes Cells 7: 997-1007.

Inoue M, Takahashi K, Niide O, Shibata M, Fukuzawa M, et al. (2005) LDOC1, a novel MZF-1-interacting protein, induces apoptosis. FEBS 579: 604-608.

Iorio MV, Ferracin M, Liu CG, Veronese A, Spizzo R, et al. (2005) MicroRNA gene expression deregulation in human breast cancer. Cancer Res 65: 7065-7070.

Ito S, Yanagi K (2003) Epstein-Barr virus (EBV) nuclear antigen 1 colocalizes with cellular replication foci in the absence of EBV plasmids. J Virol 77: 3824-3831.

Ivanov D, Nasmyth K (2005) A topological interaction between cohesin rings and a circular minichromosome. Cell 122: 849-860.

Jenner RG, Maillard K, Cattini N, Weiss RA, Boshoff C, et al. (2003) Kaposi's sarcoma-associated herpesvirus-infected primary effusion lymphoma has a plasma cell gene expression profile. Proc Natl Acad Sci U S A 100: 10399-10404.

Jeong JH, Orvis J, Kim JW, McMurtrey CP, Renne R, et al. (2004) Regulation and autoregulation of the promoter for the latency-associated nuclear antigen of Kaposi's sarcoma-associated herpesvirus. J Biol Chem 279: 16822-16831.

Jeong S, Stein A (1994) Micrococcal nuclease digestion of nuclei reveals extended nucleosome ladders having anomalous DNA lengths for chromatin assembled on non-replicating plasmids in transfected cells. Nucleic Acids Res 22: 370-375.

John B, Enright AJ, Aravin A, Tuschl T, Sander C, et al. (2004) Human MicroRNA targets. PLoS Biol 2: e363.

Johnson SM, Grosshans H, Shingara J, Byrom M, Jarvis R, et al. (2005) RAS is regulated by the let-7 microRNA family. Cell 120(5): 635-647.

Kanda T, Kamiya M, Maruo S, Iwakiri D, Takada K (2007) Symmetrical localization of extrachromosomally replicating viral genomes on sister chromatids. J Cell Sci120: 1529-1539.

Kaposi M (1872) Idiopathic multiple pigmented sarcoma of the skin. Arch Dertmatol Syphil 4: 265-273.

Kasof GM, Goyal L, White E (1999) Btf, a novel death-promoting transcriptional repressor that interacts with Bcl-2-related proteins. Mol Cell Biol 19: 4390-4404.

Kedes DH, Lagunoff M, Renne R, Ganem D (1997) Identification of the gene encoding the major latency-associated nuclear antigen of the Kaposi's sarcoma-associated herpesvirus. J Clin Investigation 100: 2606-2610.

Kelley-Clarke B, Ballestas ME, Komatsu T, Kaye KM (2007a) Kaposi's sarcoma herpesvirus C-terminal LANA concentrates at pericentromeric and peri-telomeric regions of a subset of mitotic chromosomes. Virology 357: 149-157.

Kelley-Clarke B, Ballestas ME, Srinivasan V, Barbera AJ, Komatsu T, et al. (2007b) Determination of Kaposi's sarcoma-associated herpesvirus C-terminal latency-associated nuclear antigen residues mediating chromosome association and DNA binding. J Virol 81: 4348-4356.

Kent JR, Zeng PY, Atanasiu D, Gardner J, Fraser NW, et al. (2004) During lytic infection herpes simplex virus type 1 is associated with histones bearing modifications that correlate with active transcription. J Virol 78: 10178-10186.

Kirchmaier AL, Sugden B (1995) Plasmid maintenance of derivatives of oriP of Epstein-Barr virus. J Virol 69: 1280-1283.

Kiriakidou M, Tan GS, Lamprinaki S, De Planell-Saguer M, Nelson PT, et al. (2007) An mRNA m(7)G Cap Binding-like Motif within Human Ago2 Represses Translation. Cell 129: 1141-1151.

Klein U, Gloghini A, Gaidano G, Chadburn A, Cesarman E, et al. (2003) Gene expression profile analysis of AIDS-related primary effusion lymphoma (PEL) suggests a plasmablastic derivation and identifies PEL-specific transcripts. Blood 101: 4115-4121.

Kluiver J, Poppema S, de Jong D, Blokzijl T, Harms G, et al. (2005) BIC and miR-155 are highly expressed in Hodgkin, primary mediastinal and diffuse large B cell lymphomas. J Pathog 207: 243-249.

Knight JS, Cotter MA, 2nd, Robertson ES (2001) The latency-associated nuclear antigen of Kaposi's sarcoma-associated herpesvirus transactivates the telomerase reverse transcriptase promoter. J Biol Chem 276: 22971-22978.

Komatsu T, Ballestas ME, Barbera AJ, Kelley-Clarke B, Kaye KM (2004) KSHV LANA1 binds DNA as an oligomer and residues N-terminal to the oligomerization domain are essential for DNA binding, replication, and episome persistence. Virology 319: 225-236.

Krek A, Grun D, Poy MN, Wolf R, Rosenberg L, et al. (2005) Combinatorial microRNA target predictions. Nat Genet 37: 495-500.

Krishnan HH, Naranatt PP, Smith MS, Zeng L, Bloomer C, et al. (2004) Concurrent expression of latent and a limited number of lytic genes with immune modulation and antiapoptotic function by Kaposi's sarcoma-associated herpesvirus early during infection of primary endothelial and fibroblast cells and subsequent decline of lytic gene expression. J Virol 78: 3601-3620.

Krithivas A, Young DB, Liao G, Greene D, Hayward SD (2000) Human herpesvirus 8 LANA interacts with proteins of the mSin3 corepressor complex and negatively regulates Epstein-Barr virus gene expression in dually infected PEL cells. J Virol 74: 9637-9645.

Krithivas A, Fujimuro M, Weidner M, Young DB, Hayward SD (2002) Protein interactions targeting the latency-associated nuclear antigen of Kaposi's sarcoma-associated herpesvirus to cell chromosomes. J Virol 76: 11596-11604.

Kubat NJ, Tran RK, McAnany P, Bloom DC (2004a) Specific histone tail modification and not DNA methylation is a determinant of herpes simplex virus type 1 latent gene expression. J Virol 78: 1139-1149.

Kubat NJ, Amelio AL, Giordani NV, Bloom DC (2004b) The herpes simplex virus type 1 latency-associated transcript (LAT) enhancer/rcr is hyperacetylated during latency independently of LAT transcription. J Virol 78: 12508-12518.

Kuehbacher A, Urbich C, Zeiher AM, Dimmeler S (2007) Role of Dicer and Drosha for Endothelial MicroRNA Expression and Angiogenesis. Circ Res. In Press.

Lagos-Quintana M, Rauhut R, Lendeckel W, Tuschl T (2001) Identification of novel genes coding for small expressed RNAs. Science 294: 853-858.

Lagos-Quintana M, Rauhut R, Yalcin A, Meyer J, Lendeckel W, et al. (2002) Identification of tissue-specific microRNAs from mouse. Curr Biol 12: 735-739.

Lagos D, Trotter MW, Vart RJ, Wang HW, Matthews NC, et al. (2007) Kaposi sarcoma herpesvirus-encoded vFLIP and vIRF1 regulate antigen presentation in lymphatic endothelial cells. Blood 109: 1550-1558.

Lagunoff M, Ganem D (1997) The structure and coding organization of the genomic termini of Kaposi's sarcoma-associated herpesvirus. Virology 236: 147-154.

Lagunoff M, Bechtel J, Venetsanakos E, Roy AM, Abbey N, et al. (2002) De novo infection and serial transmission of Kaposi's sarcoma-associated herpesvirus in cultured endothelial cells. J Virol 76: 2440-2448.

Lai EC (2004) Predicting and validating microRNA targets. Genome Biol 5: 115.

Lan K, Kuppers DA, Verma SC, Robertson ES (2004) Kaposi's sarcoma-associated herpesvirus-encoded latency-associated nuclear antigen inhibits lytic replication by targeting Rta: a potential mechanism for virus-mediated control of latency. J Virol 78: 6585-6594.

Lan K, Kuppers DA, Verma SC, Sharma N, Murakami M, et al. (2005) Induction of Kaposi's sarcoma-associated herpesvirus latency-associated nuclear antigen by the lytic transactivator RTA: a novel mechanism for establishment of latency. J Virol 79: 7453-7465.

Larregina AT, Morelli AE, Dewey RA, Castro MG, Fontana A, et al. (1998) FasL induces Fas/Apo1-mediated apoptosis in human embryonic kidney 293 cells routinely used to generate E1-deleted adenoviral vectors. Gene Therapy 5: 563-568.

Lau NC, Lim LP, Weinstein EG, Bartel DP (2001) An abundant class of tiny RNAs with probable regulatory roles in Caenorhabditis elegans. Science 294: 858-862.

Lawler J (2002) Thrombospondin-1 as an endogenous inhibitor of angiogenesis and tumor growth. J Cell Mol Med 6: 1-12.

Lawrie CH, Soneji S, Marafioti T, Cooper CD, Palazzo S, et al. (2007) Microrna expression distinguishes between germinal center B cell-like and activated B cell-like subtypes of diffuse large B cell lymphoma. Int J Cancer. In Press.

Lee R, Feinbaum R, Ambros V (2004) A short history of a short RNA. Cell 116: S89-92.

Lee RC, Feinbaum RL, Ambros V (1993) The C. elegans heterochronic gene lin-4 encodes small RNAs with antisense complementarity to lin-14. Cell 75: 843-854.

Lee Y, Ahn C, Han J, Choi H, Kim J, et al. (2003) The nuclear RNase III Drosha initiates microRNA processing. Nature 425: 415-419.

Lee YS, Dutta A (2007) The tumor suppressor microRNA let-7 represses the HMGA2 oncogene. Genes Develop 21: 1025-1030.

Leger-Ravet MB, Peuchmaur M, Devergne O, Audouin J, Raphael M, et al. (1991) Interleukin-6 gene expression in Castleman's disease. Blood 78: 2923-2930.

Leight ER, Sugden B (2000) EBNA-1: a protein pivotal to latent infection by Epstein-Barr virus. Rev Med Virol 10: 83-100.

Leight ER, Sugden B (2001) Establishment of an oriP replicon is dependent upon an infrequent, epigenetic event. Mol Cell Biol 21: 4149-4161.

Lewis BP, Burge CB, Bartel DP (2005) Conserved seed pairing, often flanked by adenosines, indicates that thousands of human genes are microRNA targets. Cell 120: 15-20.

Lewis BP, Shih IH, Jones-Rhoades MW, Bartel DP, Burge CB (2003) Prediction of mammalian microRNA targets. Cell 115: 787-798.

Li M, Lee H, Yoon DW, Albrecht JC, Fleckenstein B, et al. (1997) Kaposi's sarcoma-associated herpesvirus encodes a functional cyclin. J Virol 71: 1984-1991.

Liebowitz D, Kieff E (1993) Epstein-Barr virus. In: Roizman B, Whitley RJ, Lopez C, editors. The human herpesviruses. New York: Raven Press. pp. 107-172.

Lim C, Choi C, Choe J (2004) Mitotic chromosome-binding activity of latency-associated nuclear antigen 1 is required for DNA replication from terminal repeat sequence of Kaposi's sarcoma-associated herpesvirus. J Virol 78: 7248-7256.

Lim C, Sohn H, Gwack Y, Choe J (2000) Latency-associated nuclear antigen of Kaposi's sarcoma-associated herpesvirus (human herpesvirus-8) binds ATF4/CREB2 and inhibits its transcriptional activation activity. J Gen Virol 81: 2645-2652.

Lim C, Sohn H, Lee D, Gwack Y, Choe J (2002) Functional dissection of latency-associated nuclear antigen 1 of Kaposi's sarcoma-associated herpesvirus involved in latent DNA replication and transcription of terminal repeats of the viral genome. J Virol 76: 10320-10331.

Lim C, Lee D, Seo T, Choi C, Choe J (2003a) Latency-associated nuclear antigen of Kaposi's sarcoma-associated herpesvirus functionally interacts with heterochromatin protein 1. J Biol Chem 278: 7397-7405.

Lim LP, Glasner ME, Yekta S, Burge CB, Bartel DP (2003b) Vertebrate microRNA genes. Science 299: 1540.

Lin CL, Li H, Wang Y, Zhu FX, Kudchodkar S, et al. (2003) Kaposi's sarcoma-associated herpesvirus lytic origin (ori-Lyt)-dependent DNA replication: identification of the ori-Lyt and association of K8 bZip protein with the origin. J Virol 77: 5578-5588.

Lu F, Zhou J, Wiedmer A, Madden K, Yuan Y, et al. (2003) Chromatin remodeling of the Kaposi's sarcoma-associated herpesvirus ORF50 promoter correlates with reactivation from latency. J Virol 77: 11425-11435.

Lu S, Cullen BR (2004) Adenovirus VA1 noncoding RNA can inhibit small interfering RNA and MicroRNA biogenesis. J Virol 78: 12868-12876.

Lukac DM, Renne R, Kirshner JR, Ganem D (1998) Reactivation of Kaposi's sarcoma-associated herpesvirus infection from latency by expression of the ORF 50 transactivator, a homolog of the EBV R protein. Virology 252: 304-312.

Lukac DM, Garibyan L, Kirshner JR, Palmeri D, Ganem D (2001) DNA binding by Kaposi's sarcoma-associated herpesvirus lytic switch protein is necessary for transcriptional activation of two viral delayed early promoters. J Virol 75: 6786-6799.

Lund E, Guttinger S, Calado A, Dahlberg JE, Kutay U (2004) Nuclear export of microRNA precursors. Science 303: 95-98.

Lupton S, Levine AJ (1985) Mapping genetic elements of Epstein-Barr virus that facilitate extrachromosomal persistence of Epstein-Barr virus-derived plasmids in human cells. Mol Cell Biol 5: 2533-2542.

Manders PM, Hunter PJ, Telaranta AI, Carr JM, Marshall JL, et al. (2005) BCL6b mediates the enhanced magnitude of the secondary response of memory CD8+ T lymphocytes. Proc Natl Acad Sci U S A 102: 7418-7425.

Marechal V, Dehee A, Chikhi-Brachet R, Piolot T, Coppey-Moisan M, et al. (1999) Mapping EBNA-1 domains involved in binding to metaphase chromosomes. J Virol 73: 4385-4392.

Marinissen MJ, Tanos T, Bolos M, de Sagarra MR, Coso OA, et al. (2006) Inhibition of heme oxygenase-1 interferes with the transforming activity of the Kaposi sarcoma herpesvirus-encoded G protein-coupled receptor. J Biol Chem 281: 11332-11346.

Martin JN, Ganem DE, Osmond DH, Page-Shafer KA, Macrae D, et al. (1998) Sexual transmission and the natural history of human herpesvirus 8 infection. New Eng J Med 338: 948-954.

Martin MM, Lee EJ, Buckenberger JA, Schmittgen TD, Elton TS (2006) MicroRNA-155 regulates human angiotensin II type 1 receptor expression in fibroblasts. J Biol Chem 281: 18277-18284.

Matolcsy A, Nador RG, Cesarman E, Knowles DM (1998) Immunoglobulin VH gene mutational analysis suggests that primary effusion lymphomas derive from different stages of B cell maturation. American J Pathol 153: 1609-1614.

Matranga C, Tomari Y, Shin C, Bartel DP, Zamore PD (2005) Passenger-strand cleavage facilitates assembly of siRNA into Ago2-containing RNAi enzyme complexes. Cell 123: 607-620.

Mattsson K, Kiss C, Platt GM, Simpson GR, Kashuba E, et al. (2002) Latent nuclear antigen of Kaposi's sarcoma herpesvirus/human herpesvirus-8 induces and relocates RING3 to nuclear heterochromatin regions. J Gen Virol 83: 179-188.

Mayr C, Hemann MT, Bartel DP (2007) Disrupting the pairing between let-7 and Hmga2 enhances oncogenic transformation. Science 315: 1576-1579.

McAllister SC, Hansen SG, Ruhl RA, Raggo CM, DeFilippis VR, et al. (2004) Kaposi sarcoma-associated herpesvirus (KSHV) induces heme oxygenase-1 expression and activity in KSHV-infected endothelial cells. Blood 103: 3465-3473.

McCormick C, Ganem D (2005) The kaposin B protein of KSHV activates the p38/MK2 pathway and stabilizes cytokine mRNAs. Science 307: 739-741.

Meister G, Landthaler M, Dorsett Y, Tuschl T (2004) Sequence-specific inhibition of microRNA- and siRNA-induced RNA silencing. RNA 10: 544-550.

Mello JA, Almouzni G (2001) The ins and outs of nucleosome assembly. Curr Op Genet Dev 11: 136-141.

Miller G, Heston L, Grogan E, Gradoville L, Rigsby M, et al. (1997) Selective switch between latency and lytic replication of Kaposi's sarcoma herpesvirus and Epstein-Barr virus in dually infected body cavity lymphoma cells. J Virol 71: 314-324.

Mizutani K, Koike D, Suetsugu S, Takenawa T (2005) WAVE3 functions as a negative regulator of LDOC1. J Biochem 138: 639-646.

Moore PSaC, Y. (2001) Kaposi's Sarcoma-Associated Herpesvirus; Knipe DMaH, P. M., editor. Philadelphia: Lippincott Williams & Wilkins.

Muralidhar S, Pumfery AM, Hassani M, Sadaie MR, Kishishita M, et al. (1998) Identification of kaposin (open reading frame K12) as a human herpesvirus 8 (Kaposi's sarcoma-associated herpesvirus) transforming gene. J Virol 72: 4980-4988.

Nador RG, Cesarman E, Chadburn A, Dawson DB, Ansari MQ, et al. (1996) Primary effusion lymphoma: a distinct clinicopathologic entity associated with the Kaposi's sarcoma-associated herpes virus. Blood 88: 645-656.

Nan X, Ng HH, Johnson CA, Laherty CD, Turner BM, et al. (1998) Transcriptional repression by the methyl-CpG-binding protein MeCP2 involves a histone deacetylase complex. Nature 393: 386-389.

Naranatt PP, Krishnan HH, Svojanovsky SR, Bloomer C, Mathur S, et al. (2004) Host gene induction and transcriptional reprogramming in Kaposi's sarcoma-associated herpesvirus (KSHV/HHV-8)-infected endothelial, fibroblast, and B cells: insights into modulation events early during infection. Cancer Res 64: 72-84.

Nasmyth K (2001) Disseminating the genome: joining, resolving, and separating sister chromatids during mitosis and meiosis. Ann Rev Genet 35: 673-745.

Nasmyth K (2005) How do so few control so many? Cell 120: 739-746.

Nasmyth K, Peters JM, Uhlmann F (2000) Splitting the chromosome: cutting the ties that bind sister chromatids. Science 288: 1379-1385.

Neipel F, Albrecht JC, Fleckenstein B (1997) Cell-homologous genes in the Kaposi's sarcoma-associated rhadinovirus human herpesvirus 8: determinants of its pathogenicity? J Virol 71: 4187-4192.

Nicholas J (2007) Human herpesvirus 8-encoded proteins with potential roles in virus-associated neoplasia. Front Biosci 12: 265-281.

Nishitani H, Lygerou Z (2002) Control of DNA replication licensing in a cell cycle. Genes Cells 7: 523-534.

Nottrott S, Simard MJ, Richter JD (2006) Human let-7a miRNA blocks protein production on actively translating polyribosomes. Nat Struct Mol Biol 13: 1108-1114.

O'Connell RM, Taganov KD, Boldin MP, Cheng G, Baltimore D (2007) MicroRNA-155 is induced during the macrophage inflammatory response. Proc Natl Acad Sci U S A 104: 1604-1609.

Ohsaki E, Ueda K, Sakakibara S, Do E, Yada K, et al. (2004) Poly(ADP-ribose) polymerase 1 binds to Kaposi's sarcoma-associated herpesvirus (KSHV) terminal repeat sequence and modulates KSHV replication in latency. J Virol 78: 9936-9946.

Ojala PM, Yamamoto K, Castanos-Velez E, Biberfeld P, Korsmeyer SJ, et al. (2000) The apoptotic v-cyclin-CDK6 complex phosphorylates and inactivates Bcl-2. Nat Cell Biol 2: 819-825.

Okabe S, Fukuda T, Ishibashi K, Kojima S, Okada S, et al. (1998) BAZF, a novel Bcl6 homolog, functions as a transcriptional repressor. Mol Cell Biol 18: 4235-4244.

Okano M, Bell DW, Haber DA, Li E (1999) DNA methyltransferases Dnmt3a and Dnmt3b are essential for de novo methylation and mammalian development. Cell 99: 247-257.

Oksenhendler E, Duarte M, Soulier J, Cacoub P, Welker Y, et al. (1996) Multicentric Castleman's disease in HIV infection: a clinical and pathological study of 20 patients. AIDS 10: 61-67.

Ottinger M, Christalla T, Nathan K, Brinkmann MM, Viejo-Borbolla A, et al. (2006) Kaposi's sarcoma-associated herpesvirus LANA-1 interacts with the short variant of BRD4 and releases cells from a BRD4- and BRD2/RING3-induced G1 cell cycle arrest. J Virol 80: 10772-10786.

Parker JS, Barford D (2006) Argonaute: A scaffold for the function of short regulatory RNAs. Trends Biochem Sci 31: 622-630.

Pasquinelli AE, Reinhart BJ, Slack F, Martindale MQ, Kuroda MI, et al. (2000) Conservation of the sequence and temporal expression of let-7 heterochronic regulatory RNA. Nature 408: 86-89.

Pellegrini M, Bouillet P, Robati M, Belz GT, Davey GM, et al. (2004) Loss of Bim increases T cell production and function in interleukin 7 receptor-deficient mice. J Exper Med 200: 1189-1195.

Petre CE, Sin SH, Dittmer DP (2007) Functional p53 signaling in Kaposi's sarcoma-associated herpesvirus lymphomas: implications for therapy. J Virol 81: 1912-1922.

Pfeffer S, Zavolan M, Grasser FA, Chien M, Russo JJ, et al. (2004) Identification of virus-encoded microRNAs. Science 304: 734-736.

Pfeffer S, Sewer A, Lagos-Quintana M, Sheridan R, Sander C, et al. (2005) Identification of microRNAs of the herpesvirus family. Nat Methods 2: 269-276.

Piirsoo M, Ustav E, Mandel T, Stenlund A, Ustav M (1996) Cis and trans requirements for stable episomal maintenance of the BPV-1 replicator. EMBO J 15: 1-11.

Pillai RS, Bhattacharyya SN, Artus CG, Zoller T, Cougot N, et al. (2005) Inhibition of translational initiation by Let-7 MicroRNA in human cells. Science 309: 1573-1576.

Piolot T, Tramier M, Coppey M, Nicolas JC, Marechal V (2001) Close but distinct regions of human herpesvirus 8 latency-associated nuclear antigen 1 are responsible for nuclear targeting and binding to human mitotic chromosomes. J Virol 75: 3948-3959.

Platt GM, Simpson GR, Mittnacht S, Schulz TF (1999) Latent nuclear antigen of Kaposi's sarcoma-associated herpesvirus interacts with RING3, a homolog of the drosophila female sterile homeotic (fsh) gene. J Virol 73: 9789-9795.

Raab-Traub N (1989) The human DNA tumor viruses: human papilloma virus and Epstein-Barr virus. Cancer Treat Res 47: 285-302.

Radkov SA, Kellam P, Boshoff C (2000) The latent nuclear antigen of Kaposi sarcoma-associated herpesvirus targets the retinoblastoma-E2F pathway and with the oncogene Hras transforms primary rat cells. Nat Med 6: 1121-1127.

Rand TA, Petersen S, Du F, Wang X (2005) Argonaute2 cleaves the anti-guide strand of siRNA during RISC activation. Cell 123: 621-629.

Rangaswami H, Bulbule A, Kundu GC (2006) Osteopontin: role in cell signaling and cancer progression. Trends Cell Biol 16: 79-87.

Rawlins DR, Milman G, Hayward SD, Hayward GS (1985) Sequence-specific DNA binding of the Epstein-Barr virus nuclear antigen (EBNA-1) to clustered sites in the plasmid maintenance region. Cell 42: 859-868.

Rehmsmeier M, Steffen P, Hochsmann M, Giegerich R (2004) Fast and effective prediction of microRNA/target duplexes. RNA 10: 1507-1517.

Reinhart BJ, Slack FJ, Basson M, Pasquinelli AE, Bettinger JC, et al. (2000) The 21-nucleotide let-7 RNA regulates developmental timing in Caenorhabditis elegans. Nature 403: 901-906.

Reisman D, Yates J, Sugden B (1985) A putative origin of replication of plasmids derived from Epstein-Barr virus is composed of two cis-acting components. Mol Cell Biol 5: 1822-1832.

Renne R, Barry C, Dittmer D, Compitello N, Brown PO, et al. (2001) Modulation of cellular and viral gene expression by the latency-associated nuclear antigen of Kaposi's sarcoma-associated herpesvirus. J Virol 75: 458-468.

Renne R, Zhong W, Herndier B, McGrath M, Abbey N, et al. (1996) Lytic growth of Kaposi's sarcoma-associated herpesvirus (human herpesvirus 8) in culture. Nat Med 2: 342-346.

Robertson KD, Ambinder RF (1997) Methylation of the Epstein-Barr virus genome in normal lymphocytes. Blood 90: 4480-4484.

Robertson KD, Manns A, Swinnen LJ, Zong JC, Gulley ML, et al. (1996) CpG methylation of the major Epstein-Barr virus latency promoter in Burkitt's lymphoma and Hodgkin's disease. Blood 88: 3129-3136.

Rodriguez A, Griffiths-Jones S, Ashurst JL, Bradley A (2004) Identification of mammalian microRNA host genes and transcription units. Genome Res 14: 1902-1910.

Rodriguez A, Vigorito E, Clare S, Warren MV, Couttet P, et al. (2007) Requirement of bic/microRNA-155 for normal immune function. Science 316: 608-611.

Rollo EE, Hempson SJ, Bansal A, Tsao E, Habib I, et al. (2005) The cytokine osteopontin modulates the severity of rotavirus diarrhea. J Virol 79: 3509-3516.

Ruby JG, Jan C, Player C, Axtell MJ, Lee W, et al. (2006) Large-scale sequencing reveals 21U-RNAs and additional microRNAs and endogenous siRNAs in C. elegans. Cell 127: 1193-1207.

Russo JJ, Bohenzky RA, Chien MC, Chen J, Yan M, et al. (1996) Nucleotide sequence of the Kaposi sarcoma-associated herpesvirus (HHV8). Proc Natl Acad Sci U S A 93: 14862-14867.

Sadler R, Wu L, Forghani B, Renne R, Zhong W, et al. (1999) A complex translational program generates multiple novel proteins from the latently expressed kaposin (K12) locus of Kaposi's sarcoma- associated herpesvirus. J Virol 73: 5722-5730.

Sakakibara S, Ueda K, Nishimura K, Do E, Ohsaki E, et al. (2004) Accumulation of heterochromatin components on the terminal repeat sequence of Kaposi's sarcoma-associated herpesvirus mediated by the latency-associated nuclear antigen. J Virol 78: 7299-7310.

Samols MA, Hu J, Skalsky RL, Renne R (2005) Cloning and identification of a microRNA cluster within the latency-associated region of Kaposi's sarcoma-associated herpesvirus. J Virol 79: 9301-9305.

Samols MA, Skalsky, R.L., Maldonado, A.M., Riva, A., Lopez, M.C., Baker, H.V., and R. Renne (2007) Identification of cellular genes targeted by KSHV-encoded microRNAs. PLoS Pathog 3: e65.

Samols MA, Renne, R. (2006) Virus-encided microRNAs: a new chapter in virus-host cell interaction. Future Virology 1: 233-242.

Sarid R, Sato T, Bohenzky RA, Russo JJ, Chang Y (1997) Kaposi's sarcoma-associated herpesvirus encodes a functional bcl-2 homologue. Nat Med 3: 293-298.

Sarid R, Flore O, Bohenzky RA, Chang Y, Moore PS (1998) Transcription mapping of the Kaposi's sarcoma-associated herpesvirus (human herpesvirus 8) genome in a body cavity-based lymphoma cell line (BC-1). J Virol 72: 1005-1012.

Sasaki T, Gilbert DM (2007) The many faces of the origin recognition complex. Curr Op Cell Biol 19: 337-343.

Schafer A, Cai X, Bilello JP, Desrosiers RC, Cullen BR (2007) Cloning and analysis of microRNAs encoded by the primate gamma-herpesvirus rhesus monkey rhadinovirus. Virology 364: 21-27.

Schulz TF (1998) Kaposi's sarcoma-associated herpesvirus (human herpesvirus-8). J Gen Virol 79: 1573-1591.

Schwam DR, Luciano RL, Mahajan SS, Wong L, Wilson AC (2000) Carboxy terminus of human herpesvirus 8 latency-associated nuclear antigen mediates dimerization, transcriptional repression, and targeting to nuclear bodies. J Virol 74: 8532-8540.

Schwartz EJ, Dorfman RF, Kohler S (2003) Human herpesvirus-8 latent nuclear antigen-1 expression in endemic Kaposi sarcoma: an immunohistochemical study of 16 cases. The American J Surg Pathol 27: 1546-1550.

Sears J, Kolman J, Wahl GM, Aiyar A (2003) Metaphase chromosome tethering is necessary for the DNA synthesis and maintenance of oriP plasmids but is insufficient for transcription activation by Epstein-Barr nuclear antigen 1. J Virol 77: 11767-11780.

Shamay M, Krithivas A, Zhang J, Hayward SD (2006) Recruitment of the de novo DNA methyltransferase Dnmt3a by Kaposi's sarcoma-associated herpesvirus LANA. Proc Natl Acad Sci U S A 103: 14554-14559.

Shaw JE, Levinger LF, Carter CW, Jr. (1979) Nucleosomal structure of Epstein-Barr virus DNA in transformed cell lines. J Virol 29: 657-665.

Shibahara K, Stillman B (1999) Replication-dependent marking of DNA by PCNA facilitates CAF-1-coupled inheritance of chromatin. Cell 96: 575-585.

Shinohara H, Fukushi M, Higuchi M, Oie M, Hoshi O, et al. (2002) Chromosome binding site of latency-associated nuclear antigen of Kaposi's sarcoma-associated herpesvirus is essential for persistent episome maintenance and is functionally replaced by histone H1. J Virol 76: 12917-12924.

Si H, Verma SC, Robertson ES (2006) Proteomic analysis of the Kaposi's sarcoma-associated herpesvirus terminal repeat element binding proteins. J Virol 80: 9017-9030.

Silla T, Haal I, Geimanen J, Janikson K, Abroi A, et al. (2005) Episomal maintenance of plasmids with hybrid origins in mouse cells. J Virol 79: 15277-15288.

Slack FJ, Basson M, Liu Z, Ambros V, Horvitz HR, et al. (2000) The lin-41 RBCC gene acts in the C. elegans heterochronic pathway between the let-7 regulatory RNA and the LIN-29 transcription factor. Mol Cell 5: 659-669.

Song MJ, Li X, Brown HJ, Sun R (2002) Characterization of interactions between RTA and the promoter of polyadenylated nuclear RNA in Kaposi's sarcoma-associated herpesvirus/human herpesvirus 8. J Virol 76: 5000-5013.

Sood P, Krek A, Zavolan M, Macino G, Rajewsky N (2006) Cell-type-specific signatures of microRNAs on target mRNA expression. Proc Natl Acad Sci U S A 103: 2746-2751.

Soulier J, Grollet L, Oksenhendler E, Cacoub P, Cazals-Hatem D, et al. (1995) Kaposi's sarcoma-associated herpesvirus-like DNA sequences in multicentric Castleman's disease. Blood 86: 1276-1280.

Stark A, Brennecke J, Russell RB, Cohen SM (2003) Identification of Drosophila MicroRNA targets. PLoS Biol 1: E60.

Staskus KA, Sun R, Miller G, Racz P, Jaslowski A, et al. (1999) Cellular tropism and viral interleukin-6 expression distinguish human herpesvirus 8 involvement in Kaposi's sarcoma, primary effusion lymphoma, and multicentric Castleman's disease. J Virol 73: 4181-4187.

Staskus KA, Zhong W, Gebhard K, Herndier B, Wang H, et al. (1997) Kaposi's sarcoma-associated herpesvirus gene expression in endothelial (spindle) tumor cells. J Virol 71: 715-719.

Stedman W, Deng Z, Lu F, Lieberman PM (2004) ORC, MCM, and histone hyperacetylation at the Kaposi's sarcoma-associated herpesvirus latent replication origin. J Virol 78: 12566-12575.

Sullivan CS, Ganem D (2005) MicroRNAs and viral infection. Mol Cell 20: 3-7.

Sullivan CS, Grundhoff AT, Tevethia S, Pipas JM, Ganem D (2005) SV40-encoded microRNAs regulate viral gene expression and reduce susceptibility to cytotoxic T cells. Nature 435: 682-686.

Sun R, Lin SF, Gradoville L, Yuan Y, Zhu F, et al. (1998) A viral gene that activates lytic cycle expression of Kaposi's sarcoma- associated herpesvirus. Proc Natl Acad Sci U S A 95: 10866-10871.

Szekely L, Kiss C, Mattsson K, Kashuba E, Pokrovskaja K, et al. (1999) Human herpesvirus-8-encoded LNA-1 accumulates in heterochromatin- associated nuclear bodies. J Gen Virol 80: 2889-2900.

Takada K, Ono Y (1989) Synchronous and sequential activation of latently infected Epstein-Barr virus genomes. J Virol 63: 445-449.

Takeda DY, Dutta A (2005) DNA replication and progression through S phase. Oncogene 24: 2827-2843.

Talbot SJ, Weiss RA, Kellam P, Boshoff C (1999) Transcriptional analysis of human herpesvirus-8 open reading frames 71, 72, 73, K14, and 74 in a primary effusion lymphoma cell line. Virology 257: 84-94.

Tam W, Dahlberg JE (2006) miR-155/BIC as an oncogenic microRNA. Genes Chrom Cancer 45: 211-212.

Tam W, Ben-Yehuda D, Hayward WS (1997) bic, a novel gene activated by proviral insertions in avian leukosis virus-induced lymphomas, is likely to function through its noncoding RNA. Mol Cell Biol 17: 1490-1502.

Tam W, Hughes SH, Hayward WS, Besmer P (2002) Avian bic, a gene isolated from a common retroviral site in avian leukosis virus-induced lymphomas that encodes a noncoding RNA, cooperates with c-myc in lymphomagenesis and erythroleukemogenesis. J Virol 76: 4275-4286.

Tao Q, Robertson KD, Manns A, Hildesheim A, Ambinder RF (1998) The Epstein-Barr virus major latent promoter Qp is constitutively active, hypomethylated, and methylation sensitive. J Virol 72: 7075-7083.

Tao Q, Swinnen LJ, Yang J, Srivastava G, Robertson KD, et al. (1999) Methylation status of the Epstein-Barr virus major latent promoter C in iatrogenic B cell lymphoproliferative disease. Application of PCR-based analysis. American J Pathol 155: 619-625.

Taraboletti G, Benelli R, Borsotti P, Rusnati M, Presta M, et al. (1999) Thrombospondin-1 inhibits Kaposi's sarcoma (KS) cell and HIV-1 Tat-induced angiogenesis and is poorly expressed in KS lesions. J Pathog 188: 76-81.

Thai TH, Calado DP, Casola S, Ansel KM, Xiao C, et al. (2007) Regulation of the germinal center response by microRNA-155. Science 316: 604-608.

van den Berg A, Kroesen BJ, Kooistra K, de Jong D, Briggs J, et al. (2003) High expression of B-cell receptor inducible gene BIC in all subtypes of Hodgkin lymphoma. Genes Chrom Cancer 37: 20-28.

Vatolin S, Navaratne K, Weil RJ (2006) A novel method to detect functional microRNA targets. J Mol Biol 358: 983-996.

Verma SC, Choudhuri T, Robertson ES (2007) The minimal replicator element of the Kaposi's sarcoma-associated herpesvirus terminal repeat supports replication in a semiconservative and cell-cycle-dependent manner. J Virol 81: 3402-3413.

Verma SC, Choudhuri T, Kaul R, Robertson ES (2006) Latency-associated nuclear antigen (LANA) of Kaposi's sarcoma-associated herpesvirus interacts with origin recognition complexes at the LANA binding sequence within the terminal repeats. J Virol 80: 2243-2256.

Viejo-Borbolla A, Ottinger M, Bruning E, Burger A, Konig R, et al. (2005) Brd2/RING3 interacts with a chromatin-binding domain in the Kaposi's Sarcoma-associated herpesvirus latency-associated nuclear antigen 1 (LANA-1) that is required for multiple functions of LANA-1. J Virol 79: 13618-13629.

Volinia S, Calin GA, Liu CG, Ambs S, Cimmino A, et al. (2006) A microRNA expression signature of human solid tumors defines cancer gene targets. Proc Natl Acad Sci U S A 103: 2257-2261.

Voorhoeve PM, le Sage C, Schrier M, Gillis AJ, Stoop H, et al. (2006) A genetic screen implicates miRNA-372 and miRNA-373 as oncogenes in testicular germ cell tumors. Cell 124: 1169-1181.

Wang H, Ach RA, Curry B (2007) Direct and sensitive miRNA profiling from low-input total RNA. RNA 13: 151-159.

Watanabe T, Sugaya M, Atkins AM, Aquilino EA, Yang A, et al. (2003) Kaposi's sarcoma-associated herpesvirus latency-associated nuclear antigen prolongs the life span of primary human umbilical vein endothelial cells. J Virol 77: 6188-6196.

Wightman B, Ha I, Ruvkun G (1993) Posttranscriptional regulation of the heterochronic gene lin-14 by lin-4 mediates temporal pattern formation in C. elegans. Cell 75: 855-862.

Wong LY, Matchett GA, Wilson AC (2004) Transcriptional activation by the Kaposi's sarcoma-associated herpesvirus latency-associated nuclear antigen is facilitated by an N-terminal chromatin-binding motif. J Virol 78: 10074-10085.

Wu L, Fan J, Belasco JG (2006) MicroRNAs direct rapid deadenylation of mRNA. Proc Natl Acad Sci U S A 103: 4034-4039.

Wysokenski DA, Yates JL (1989) Multiple EBNA1-binding sites are required to form an EBNA1-dependent enhancer and to activate a minimal replicative origin within oriP of Epstein-Barr virus. J Virol 63: 2657-2666.

Xu Y, Rodriguez-Huete A, Pari GS (2006) Evaluation of the Lytic Origins of Replication of Kaposi's Sarcoma-Associated Virus/Human Herpesvirus 8 in the Context of the Viral Genome. J Virol 80: 9905-9909.

Yanaihara N, Caplen N, Bowman E, Seike M, Kumamoto K, et al. (2006) Unique microRNA molecular profiles in lung cancer diagnosis and prognosis. Cancer Cell 9: 189-198.

Yang L, Mohr I, Fouts E, Lim DA, Nohaile M, et al. (1993) The E1 protein of bovine papilloma virus 1 is an ATP-dependent DNA helicase. Proc Natl Acad Sci U S A 90: 5086-5090.

Yates J, Warren N, Reisman D, Sugden B (1984) A cis-acting element from the Epstein-Barr viral genome that permits stable replication of recombinant plasmids in latently infected cells. Proc Natl Acad Sci U S A 81: 3806-3810.

Yates JL, Guan N (1991) Epstein-Barr virus-derived plasmids replicate only once per cell cycle and are not amplified after entry into cells. J Virol 65: 483-488.

Yates JL, Warren N, Sugden B (1985) Stable replication of plasmids derived from Epstein-Barr virus in various mammalian cells. Nature 313: 812-815.

Yates JL, Camiolo SM, Ali S, Ying A (1996) Comparison of the EBNA1 proteins of Epstein-Barr virus and herpesvirus papio in sequence and function. Virology 222: 1-13.

Ye FC, Zhou FC, Yoo SM, Xie JP, Browning PJ, et al. (2004) Disruption of Kaposi's sarcoma-associated herpesvirus latent nuclear antigen leads to abortive episome persistence. J Virol 78: 11121-11129.

Yekta S, Shih IH, Bartel DP (2004) MicroRNA-directed cleavage of HOXB8 mRNA. Science 304: 594-596.

Yi R, Qin Y, Macara IG, Cullen BR (2003) Exportin-5 mediates the nuclear export of pre-microRNAs and short hairpin RNAs. Genes Develop 17: 3011-3016.

You J, Croyle JL, Nishimura A, Ozato K, Howley PM (2004) Interaction of the bovine papillomavirus E2 protein with Brd4 tethers the viral DNA to host mitotic chromosomes. Cell 117: 349-360.

You J, Srinivasan V, Denis GV, Harrington WJ, Jr., Ballestas ME, et al. (2006) Kaposi's sarcoma-associated herpesvirus latency-associated nuclear antigen interacts with bromodomain protein Brd4 on host mitotic chromosomes. J Virol 80: 8909-8919.

Zeng Y, Cullen BR (2005) Efficient processing of primary microRNA hairpins by Drosha requires flanking nonstructured RNA sequences. J Biol Chem 280: 27595-27603.

Zeng Y, Yi R, Cullen BR (2003) MicroRNAs and small interfering RNAs can inhibit mRNA expression by similar mechanisms. Proc Natl Acad Sci U S A 100: 9779-9784.

Zhang J, Xu F, Hashimshony T, Keshet I, Cedar H (2002) Establishment of transcriptional competence in early and late S phase. Nature 420: 198-202.

Zhang Z, Shibahara K, Stillman B (2000) PCNA connects DNA replication to epigenetic inheritance in yeast. Nature 408: 221-225.

Zhou J, Chau CM, Deng Z, Shiekhattar R, Spindler MP, et al. (2005) Cell cycle regulation of chromatin at an origin of DNA replication. EMBO J 24: 1406-1417.

Ziegler JL, Newton R, Katongole-Mbidde E, Mbulataiye S, De Cock K, et al. (1997) Risk factors for Kaposi's sarcoma in HIV-positive subjects in Uganda. AIDS 11: 1619-1626.

BIOGRAPHICAL SKETCH

Rebecca Lynn Skalsky was born in Duluth, Minnesota. The eldest of two daughters in a military family, she grew up mostly in Geilenkirchen, Germany and Anchorage, Alaska, graduating as valedictorian from East Anchorage High School in 1998. She earned her B.S. in biology, with a concentration in microbiology, in addition to a certificate in foreign language studies in German, from Michigan Technological University in 2002.

Upon graduating in May 2002, she entered the Ph.D. program at Case Western Reserve University in Cleveland, Ohio. She completed 2 full years at Case before transferring with her dissertation advisor and lab to the University of Florida (UF) in Gainesville, Florida. At UF, she entered the Interdisciplinary Program in Biomedical Sciences and continued her studies on episomal maintenance and viral microRNAs of Kaposi's sarcoma-associated herpesvirus. She will earn her Ph.D. in medical sciences, with a concentration in immunology and microbiology.

Upon completion of her Ph.D. program, Rebecca will be moving with her family to Raleigh, North Carolina to explore post-doctoral opportunities. Rebecca has been married to Nathan Skalsky, an IBM engineer, for 2.5 years. Their first child will be born in December 2007.